Characterisation of Exhaust Gaseous and Particle Emissions from a DI Diesel Engine with Retrofitting of a Diesel Oxidation Catalyst

WONG, CHI PIU

M. PHIL.

The Hong Kong Polytechnic University

2003

THE HONG KONG POLYTECHNIC UNIVERSITY
DEPARTMENT OF MECHANICAL ENGINEERING

Characterisation of Exhaust Gaseous and Particle Emissions from a DI Diesel Engine with Retrofitting of a Diesel Oxidation Catalyst

By

Wong, Chi Piu

A thesis submitted in partial fulfillment of the requirements of
The Hong Kong Polytechnic University
for the degree of Master of Philosophy

Department of Mechanical Engineering
The Hong Kong Polytechnic University

May 2003

Certificate of Originality

I hereby declare that this thesis is my own work and that, to the best of my knowledge and belief, it reproduces no material previously published or written nor material which has been accepted for the award of any other degree or diploma in any other University or Institute, except where due acknowledgement and reference have been made in the text of the thesis.

_____ (Signed)

WING CHI PU (Name of Student)

Abstract

The combined effects of diesel oxidation catalyst (DOC) and ultra low sulphur diesel (ULSD) fuel on the characteristics of diesel exhaust gaseous and particle emissions under a diesel engine dynamometer test bed using a steady-state mode cycle of the standard Economic Commission for Europe Regulation 49 test modes for different engine loads from 10% to 100% of full engine load at a maximum torque of constant speed and idle to fast engine acceleration conditions have been investigated by using the developed gaseous and particle emission measurement systems. In the absence of a standard diesel exhaust particle sampling measurement system, a mini-dilution tunnel sampling (MDTS) and an ejector diluter sampling (EDS) measurement systems have been evaluated to ascertain the most reliable measurement system that can minimise the particle transformations (i.e. nucleation, condensation and coagulation) which affect the exhaust particle number and size distributions during the dilution process. Comparing the particle number and volume concentrations, the MDTS measurement system measures a lower level in the nuclei mode but a higher level in the accumulation mode than EDS measurement system. The measured results also show that the MDTS measurement system shifts the particle count median diameter (CMD) to larger particle number and volume concentration for all engine load conditions. It is mainly because the mini-tunnel dilution leads to particle transformations of nucleation and condensation simultaneously when the exhaust particle emission is cooled and diluted. However, the effect of coagulation on the total number concentration has shown to be negligible. On the other hand, the EDS measurement system can minimise the particle transformations that affect the exhaust particle number and size distributions during the heated dilution process.

A fresh DOC can substantially reduce the nuclei mode particle number concentration from 17% to 50%, the total particle number concentration from 15% to 49% and the total particle mass concentration from 24% to 75%, and slightly increase the accumulation mode particle concentration from 1% to 7% when the diesel engine load increases from 10% to 100% of full engine load at a maximum torque of constant speed. Amongst this significant reduction of nuclei mode particle number concentration, 14% to 35% reduction is mainly attributed to the oxidation process that taken place, and the other 3% to 15% reduction comes from the dominant particle thermophoresis and electrostatic deposition mechanism inside the catalyst. However, the alteration level of particle CMD is not pronounced for different engine load conditions. Between the nucleation and accumulation particle modes, it is shown that the used catalyst increases 60% of the particle number concentration in accumulation particle mode (i.e. 650 nm) after 30 operation hours.

It is also found that the installation of used DOC can reduce the gaseous emissions from 10% to 97% for CO emission and 4% to 14% for HC, but there is no effect on the NOx when the diesel engine load increases from 10% to 100% of full engine load at a maximum torque of constant speed. In the fast engine acceleration test, it is shown that there is no significant reduction of gaseous emissions in CO and HC at the initial stage until the oxidation process of catalyst had taken place for about 200 seconds.

Acknowledgements

I wish to express my deep gratitude to my Chief Supervisor, Dr. T.L. Chan for his guidance, useful comments, and encouragement in the course of my research. I would also like to express my sincere appreciation to my Second Supervisor, Prof. C.W. Leung for his counsel, support and encouragement throughout the research programme.

I am also appreciative to Dr. C.S. Cheung for his valuable lectures regarding the measurement and control diesel exhaust emission technology and helpful suggestions during this study.

I would like to acknowledge the Thermodynamics Laboratory Technician, Dr. C. S. Tse, who helps to maintain the reliability and quality of instruments and provides technical support throughout the project. I also wish to thank Ir. K. K. Lo and the technicians in the Project Laboratory for their assistance in solving the technical problems.

Finally, I wish to express my gratitude to my family members and girlfriend, Bianca Choi for their understanding, love, encouragement and patience.

Table of Contents

List of Publications

1. Wong C.P., Chan T.L., Leung C.W. and Cheung C.S., "Performance of diesel oxidation catalyst for a light duty vehicle under Hong Kong driving conditions". *Proc. of 6th Int. Conf. on Urban Transport and the Environment for 21st Century*, Cambridge, UK, pp. 393-401, July 26-28 (2000).

2. Chan T.L., Dong G., Cheung C.S., Leung C.W., Wong C.P. and Hung W.T. "Monte Carlo simulation of nitrogen oxides dispersion from a vehicular exhaust plume and its sensitivity studies". *Atmospheric Environment*, Vol.35, No.35, pp.6117-6127 (2001).

List of Figures and Tables

Figures:

Tables:

Nomenclature

A_i	Inner surface area of the catalyst channel, m^2
B_e	Bias error
BARO	Barometric pressure, Pa
C_c	Cunningham slip correction factor
CMD	Count median diameter, nm
D_{AB}	Diffusion coefficient for a particle of a given size
D_h	Hydraulic diameter of the channel, mm
D_p	Diameter of particle, nm
DCO	CO volume concentration in exhaust gas, ppm (dry basis)
DCO_2	CO_2 volume concentration in exhaust gas, ppm (dry basis)
DHC	HC volume concentration in exhaust gas, ppm (dry basis)
DKNOx	NO volume concentration in exhaust gas, ppm (dry basis)
E_a	Activation energy or Arrhenius activation energy, Nm/kg
E_b	Brownian diffusion particle deposition efficiency, %
E_e	Electrostatic particle attraction efficiency, %
E_g	Gravitational particle settling efficiency, %
E_i	Impaction particle deposition efficiency, %

E_t	Thermophoresis particle deposition efficiency, %
E_T	Total particle deposition efficiency, %
$(f/a)_m$	Measured dry fuel air ratio
$(f/a)_{stoich}$	Stoichiometric fuel-air ratio
h	Height of the catalyst channel, m
H	Specific humidity, g H_2O/g of dry air
h_m	Average mass transfer coefficient in the catalyst channel, W/m^2K
k	Boltzmann constant, 1.38×10^{-16} dyn·cm/K
K	Water-gas equilibrium constant, 3.5
K_t	Dimensional thermophoretic constant, 0.55
K_w	Wet to dry correction factor
L	Length of the catalyst channel, m
m_T	Total particle mass concentration, mg/m^3
M_{air}	Molecular weight of air, 28.96 kg/kmol
M_C	Molecular weight of carbon, 12.01 kg/kmol
M_H	Molecular weight of hydrogen, 1 kg/kmol
M_{H_2O}	Molecular weight of water, 18.02 kg/kmol
M_{NO_2}	Molecular weight of nitrogen dioxide, 46 kg/kmol
N(t)	Number of particles at the residence time

N_d	Particle number concentration at particular particle diameter (d), #/cm^3
P	Pressure, Pa
P_v	Partial vapour pressure, Pa
Pr	Prandtl number
Q	Average volume flow rate through the catalyst channel, m^3/s
R	Specific gas constant for air, 297 J/kgK
Re	Reynolds number
RH	Relative humidity, %
S	Standard deviation of measured data
tS_x	Random error
Sh_L	Averaged Sherwood number over the length of the tube, 2.98
St_k	Stoke number of the particle
t	95th percentile point for the two-tailed student t distribution
T	Absolute temperature of the exhaust gas, K
U	Average free stream velocity inside the channel, mm/s
U_T	Total uncertainty of the measured data, %
V_e	Terminal electrostatic velocity, m/s
V_s	Terminal settling velocity of the particle, m/s
w	Wall thickness of the catalyst channel, m

W_f	Mass flow rate of diesel fuel, g/hr
WHC	HC volume concentration in exhaust gas, ppm (wet basis)
$\overline{X}$	Average value of the measured data
Y	Water-vapour volume concentration of intake air (g H_2O/g dry air)
Z	Electrical mobility of the particle, cm^2/Volt· s
ϕ	Equivalence ratio = $(f/a)_m/(f/a)_{stoich}$

Greek letters

χ_i	concentration of gaseous emissions, i = CO, HC & NOx
α	Molecular hydrogen/carbon ratio of the fuel = 1.805
ρ	Particle density
ρ_e	Exhaust gas density
μ	Viscosity of exhaust gas
λ	Mean free path of the particle
σ_g	Geometric standard deviation

Subscripts

DB	Dry bulb
d	Particle diameter, range from 15 to 670nm
i	Inlet of diesel oxidation catalyst
o	Outlet of diesel oxidation catalyst

Chapter 1 Introduction

1.1 Background and Description of the Problems

Urban pollution has been the subject of growing public concern for more than a decade in Hong Kong. In the White Paper of the Hong Kong government [1] and at a recent environmental meeting [2], and Policy Address of the Chief Executive in 1999 [3], it has been identified that motor vehicles emissions are the major source of urban air pollution. This is attributed to the fact that roads are dominated by motor vehicles in Hong Kong, in which taxis, light buses, public buses and goods vehicles (or trucks) operate with diesel engine extensively. Their exhaust emissions normally affect the ambient air and its composition is an important factor affecting the urban air quality.

In Hong Kong, motor vehicles are dominated by diesel and petrol engines. Compared with petrol engines, diesel engines generate far less carbon monoxide and hydrocarbons, but give rise to a greater amount of nitrogen oxides and particulate matter. From previous investigations, researchers have estimated that the particulate emissions from diesel engine per traveled distance is over 10 times higher than the particulate emissions from petrol engine of equivalent power running on unleaded

petrol, and over hundredfold higher than that of petrol engine equipped with three-way catalytic converter [4]. According to the statistical data from the Environmental Protection Department of the HKSAR Government, over 50% of respirable suspended particulates in the ambient air is caused by diesel vehicle emissions [5]. Consequently, diesel vehicle emissions have become the major concern related to the air pollution problem in Hong Kong.

Typically, diesel exhaust emission contains a complex mixture of gas such as carbon monoxide (CO), carbon dioxide (CO_2), hydrocarbons (HC), nitrogen oxides (NOx), sulphur dioxide (SO_2), formaldehyde and particulate matter (PM) [6]. Diesel engines normally generate more particulate matters than gasoline and compressed natural gas engines [7]. Various pollutants can cause different adverse health effects on human body, for example, CO tends to block the hemoglobin oxygen carrying capacity and therefore reduces the oxygen supply to the tissue and cause headaches, dizziness and nausea. Particulate matter emitted from the diesel engine contains a large amount of fine (diameter < 2.5 μm) and ultra-fine (diameter < 0.1 μm) particles. It has been identified as not only inducing respiratory health problems but is also probably carcinogenic to humans, potential of autoimmune disorders [8], alteration in ability of blood coagulated and increased cardiovascular disorders [9]. Many epidemiological/health studies have suggested that there is a strong correlation

between mortality and size of particles ranging from fine particles (i.e. $PM_{2.5}$) to even smaller particles, ultrafine particles and nano-sized particles for those smaller than 100 and 50 nm diameter, respectively [10-12]. There are numerous diesel vehicles running in the urban area and emitting particulates into the ambient air everyday. These ultra-fine particles have been found to suspend and exist on or near the roadway [13-16]. They are easy for people to inhale and are able to pass through the nasal chamber and bronchia to reach the alveoli and deposited there [17]. On the other hand, the automotive emissions are also considered to be the reason for visibility reduction in Hong Kong [18]. Thus, a great deal of attention has been focused on the exhaust emissions from the diesel vehicles recently.

The Government of the HKSAR has implemented a series of policy measures to improve the urban air quality, these include introducing stringent practicable emissions and diesel fuel standard (i.e. ultra low sulphur diesel, ULSD) and requiring commercial light-duty and heavy-duty diesel vehicles to retrofit a low-cost trap/diesel oxidation catalyst (DOC), and passive particulate trap in different phases, respectively [19]. Since 2001, policy has been implemented to subsidise the vehicle owners of pre-Euro light-duty diesel vehicles to install the low-cost particulate trap or DOC. More than 80% of the light diesel fleet, or 24,000 light-duty diesel vehicles have already been fitted with these devices. In addition, the bus companies have

retrofitted about 2,000 older buses of pre-Euro or Euro I engine models with diesel oxidation catalytic converter. Basically, the diesel oxidation catalytic converter uses the oxidation process to reduce the amount of CO, HC and particulate emissions by mass in the exhaust gas from the vehicle. The usage of high quality ULSD fuel can abate particulate emission, sulphur dioxide and also enable the use of advanced control technologies [20-21]. By using the DOC and ULSD fuel, the exhaust gas is likely to be cleaner and the air pollution will seem to be improved. However, this may not reflect the full picture because the most important parameter related to the particulate emission is the size and number of particles emitted from the vehicle. The particle number and size directly affect the air pollution problem and the human health of the people. If the DOC can reduce the total mass of particulate matters but generates more ultra-fine particles, then it will totally defeat the original objective of retrofitting the DOCs to the light-duty and heavy-duty vehicles. Therefore, it is necessary to have a better understanding of the combined effects of DOC and ULSD fuel on the characteristics of diesel exhaust gaseous and particle emissions from different diesel engine load and idle to fast engine acceleration conditions combined effects of performance of DOC in reducing the particulate emission in terms of the size and number of particles.

According to the present vehicle emission regulations, the diesel vehicular particulate emission standards and control are usually based on the total mass of particulate emission and smoke level, at which the measurement procedures are well established [11,22-23]. However, mass-based methods are at the edge of detectability of particulate emission by modern low emission diesel engines and the diesel aftertreatment devices with reduced particle mass concentration and smoke level may significantly increase emission of larger number of ultra-fine particles [24]. The emission standard and regulation normally use the mass rates but it cannot reflect the true measure of the particulate concentration. Recently, many researchers have shifted their interest from measuring the mass concentration of particles to the size and number concentration of particles emitted from motor vehicles. The present investigation is intended to have a better understanding of the combined effects on the DOC and ULSD fuel on the characteristics of the exhaust particle size concentration and distribution from a diesel engine. Before conducting any study, it is essential to establish a highly reliable and repeatable particle emission measurement system. Since the 1980s, the dilution tunnel measurement system has been widely used to measure the exhaust particle emission from diesel vehicles. Along with the emission measurement technology evolving in the last two decades, some researchers have changed from the conventional mini-dilution tunnel sampling

measurement system to an ejector diluter sampling measurement system for determining the characteristics of particle emission. In order to obtain highly accurate and reliable results of the exhaust particle size distribution and concentration from the DOC, the particle emission sampling measurement system must be used carefully. Hence, two particle emission sampling measurement systems (i.e. a mini-dilution tunnel and ejector diluter) will be established, and their particle results will be compared and evaluated with each other to determine the most reliable and repeatable particle emission sampling measurement system for subsequent experiments.

1.2 Objectives and Scope of Study

Although the measurement system for determining diesel exhaust gaseous and particulate (by mass) emissions have been established for more than two decades, along with researchers become more interesting in diesel exhaust particle number and size concentration, conventional measurement technique is not able to provide a reliable information in these aspects. Over the past decade, researchers normally used two different types of particle emission sampling measurement system, namely mini-dilution tunnel and ejector diluter, to determine the exhaust particle emission from a diesel engine. They did not have any thorough comparison on the

characteristics of both particle emission measurement systems. Hence, a detailed experimental investigation is required to study the characterisation of diesel exhaust particle size distribution and concentration using these two measurement systems.

Although considerable research groups have published on the characterisation of exhaust gaseous and particle emissions from a diesel engine/vehicle, but there is still a paucity of information on the combined effects of DOC and ULSD fuel on the characteristics of gaseous and particle emissions for different diesel engine load conditions. Hence, the following target objectives were discerned to allow accomplishment of specific research aims:

(i) To establish a conventional mini-dilution tunnel and ejector diluter sampling measurement systems and evaluate the characteristics of exhaust particle emission in terms of the particle number and volume concentration, particle CMD and particle transformation processes for different diesel engine load conditions.

(ii) To investigate the combined effects of DOC and ULSD (i.e. 0.005% by weight S or 50 ppm S) fuel on the characteristics of diesel gaseous and particle emissions for different diesel engine load and engine acceleration conditions.

(iii) To identify the characteristics of diesel particle deposition and oxidation from fresh and used catalyst of DOC for different engine load conditions.

1.3 Outline of Thesis

This thesis consists of seven chapters which describe the development of two particle measurement systems for diesel exhaust gaseous and particle emissions, the performance study of a DOC in terms of gaseous and particle emissions under a diesel engine dynamometer test bed using a steady-state mode cycle of the standard Economic Commission for Europe Regulation 49 test modes for different engine loads from 10% to 100% of full engine load at a maximum torque of constant speed and idle to fast engine acceleration conditions, and the characterisation study of particle deposition in a DOC.

A description of each Chapter is provided as follows:

Chapter 1 describes the need for this investigation of diesel exhaust gaseous and particle emissions, as well as diesel aftertreatment device and provides background information on air pollution issue in Hong Kong and global trend in this field. The major objectives of this research programme are also mentioned in this chapter.

Chapter 2 presents a literature survey on the emission formation, measurement of diesel exhaust pollutants and the development of diesel aftertreatment device. The chapter provides the necessary technical information of diesel exhaust emission for this research programme.

Chapter 3 presents our preliminary study on the on-road performance of DOC for a light-duty vehicle under the Hong Kong driving conditions. Detailed information about the experiment and results are also provided [25].

Chapter 4 describes a comprehensive experimental work on studying the performance of a diesel oxidation catalyst on exhaust gaseous and particle emissions. The detailed description of conventional mini-dilution tunnel and state-of-the-art ejector dilutor particle measurement systems and the SAE standard gaseous measurement system were presented. The engine test bed, testing procedures, data handling and uncertainty of the experiment were also mentioned.

Chapter 5 discusses the study of particle deposition efficiency on catalyst surface against particle diameter and chemical kinetic analysis of a DOC on exhaust gaseous emission for different gaseous temperatures. The essential equations for the calculation are also listed.

Chapter 6 presents the characteristics of particle emission measured from the two developed particle measurement systems. The particle number and volume distributions obtained from the two particle measurement systems were compared to determine the most reliable and repeatable particle emission measurement system. On the other hand, the characteristics of DOC performance in the gaseous and particle emissions were also reported. Both results were presented under three engine conditions: 10%, 50% and 100% of full engine load at a maximum torque of constant speed (i.e. 2200 rpm), and a fast engine acceleration and idle testing conditions. The characteristics of diesel particle deposition and oxidation for the catalyst were also discussed.

Finally, Chapter 7 presents the conclusion of the research programme and offers some recommendations for future work.

Chapter 2 Literature Review

2.1 Combustion and Pollutants Formation in a Diesel Engine

2.1.1 Combustion in diesel engine

Diesel engine is a compression ignition engine with a diffusion flame [26]. Near the end of the compression stroke, liquid fuel is injected as one or more fuel jets. The injector receives fuel at very high pressures in order to produce rapid injection. The fuel jets entrain air and break up into fine fuel droplets, this provides rapid mixing which is essential if the combustion is to occur sufficiently fast. The air is warmed up due to the compression heating and its temperature is higher than the injected fuel. It will enhance the evaporation of fuel droplets. The enthalpy of evaporation is supplied by the air surrounding the droplets, so this air will be cooled by evaporation. The fuel droplets will not ignite spontaneously the moment evaporation begins. Even if the vapour is hot enough for ignition, sufficient air must be entrained to generate a favourable air/fuel mixture ratio for combustion to proceed at a significant rate. The fuel spray can be imagined as a core of droplets and fuel vapour surrounding by an area comprising wholly evaporated droplets with significant air around them. Further from the centre of the spray, the evaporation will be completed and an air/fuel vapour mixture will exist.

Before the combustion starts, the fuel spray may consist of a vapour core on the wall and possibly along its surface. The spray boundary will be pure air, and a discrete area just inside this boundary will be too weak to burn significantly whatever the combustion temperature is. The fuel/air ratio will become richer towards the spray core, passing through the stoichiometric value towards the centre. Ignition will be started once the fuel is completely evaporated and the temperature is sufficiently high for compression ignition. In all diesel applications, the overall air-fuel ratio is lean of stoichiometric, varying from 1.25 to 5.0:1 excess air ratio. Once the ignition begins, the heat transfer to the adjacent area of the spray will increase rapidly, thus combustion will rapidly cover a major part of the spray [27]. Once the premixed mixture is burnt, the combustion will slow down. The second phase of burning will occur, which is called the diffusion burning period.

Towards the end of combustion, the cylinder pressure is decreasing when the piston moves down the bore. The combustion rate will slow down due to the temperature and pressure dependence of chemical kinetic effects as the chemical reactions slow down, so that the reaction rates rather than the air/fuel mixing process dominate.

2.1.2 Formation of diesel pollutants

Diesel engine generates a series of pollutants (i.e. HC, CO, NOx and PM) during the combustion process. The formation processes of those pollutants have been investigated for more than two decades [28] and the formation information of those pollutants will be reviewed in the following section.

Hydrocarbons (HC)

Hydrocarbons always present in the diesel engine exhaust and contribute to photochemical smog and the potential toxic or carcinogenic effects. There are several possible sources of HC in the diesel combustion process. Greeves et al. [29] suggested that the major source of HC emission arises from some vapourised fuel at the edge of the spray which is mixed with increasing quantities of air such that it is too weak to burn when the temperature becomes high enough for ignition. In addition, some HC could remain at the very rich region in the core of the fuel spray due to the late injection process, but only a very small amount of HC will be involved. Towards the end of the injection process, when the injector is closing, the fuel spray will become weaker resulting in little penetration of oxygen rich area and poor atomisation. Because of the decreasing cylinder pressure and temperature, the oxidation reactions may be slow and incomplete, and therefore cause HC emission.

Carbon Monoxide (CO)

Carbon monoxide is an intermediate product in the combustion of hydrocarbons fuels. If sufficient oxygen is available, oxidation from CO to CO_2 will occur, but the reaction may be incomplete due to a short residence time or a low gas temperature. Sufficient oxygen will not be available in all areas of the engine combustion chamber, the local mixture strength being quite rich. Unless these areas receive oxygen later in the engine cycle, and before the temperature is dropped substantially, CO will be formed and remain unoxidised. Although CO may be formed in other areas during combustion reactions, the availability of temperature and oxygen (due to over-all lean mixture strength of the diesel fuel) will be high enough for complete combustion. Fortunately, the total amount of CO formed is substantially less than that of petrol engines due to oxygen availability.

Nitrogen Oxides (NOx)

Nitric oxide (NO) is formed during combustion due to the co-existence of the nitrogen and oxygen in air at very high temperature. When additional oxygen is available, the reaction will proceed to nitrogen dioxide (NO_2) but little NO_2 is actually formed in diesel engine. Several simple reactions have been proposed for the NO formation, the most widely accepted being the Zeldovich chain reaction [30]:

$$O_2 \rightarrow 2O \quad (2.1)$$

$$O + N_2 \rightarrow NO + N \quad (2.2)$$

$$N + O_2 \rightarrow NO + O \quad (2.3)$$

$$N + OH \rightarrow NO + H \quad (2.4)$$

The reaction is activated by atomic oxygen formed by dissociation of oxygen at high temperature encountered during combustion. It follows that the NO concentration is a function of local oxygen concentration and temperature, but the reaction rates are significant only at high temperature. NO can be formed in all regions of the spray, but the temperature and local oxygen concentration dependence will result in a major variation of NO concentration throughout the combustion chamber. From previous investigations, the researchers suggested that a major amount of NO could be formed in the central core of the spray since its temperature will become very high, but this will be subjected to the availability of oxygen [31].

Soot and Particulate Matter

Two different classes of smoke emission are emitted from diesel engines. Under cold starting, idling and possibly low engine load conditions with low compression ratio engine, a cloud of vapour often referred to as blue-white smoke is emitted. This result is mainly due to the fuel and lubricating oil being emitted

without being completely burnt. Soot, or black smoke emitted during normal operation of a warm engine is a separate problem. Black smoke is emitted at all engine loads, but the amount is usually small at low engine load condition. Normally, even when the smoke emission is very bad, the percentage of the total fuel input remaining burnt is small. Broome et al. [32] reported that a smoke reading of 72 HSU can be occurred with 99% complete combustion. Thus, the black smoke is not simply an incomplete combustion phenomenon.

The mechanism of soot formation is complex and not fully understood but possible methods have been proposed by previous researchers [32-33] and in recent literature review [34]. Essentially the process can be divided into three phases: nucleation or the formation of precursors, the growth of these nuclei into soot particles and their coagulation into large particles. In diesel engine, fuel is unmixed before the start of combustion and is likely to suffer the combined effects of lack of oxygen and high temperature later in the cycle. However, it is the fuel injected after combustion has started that is least likely to receive sufficient oxygen and hence most exhaust soot will result from the second phase of burning (diffusion burning). Any soot formed during the initial rapid combustion period is likely to be burnt up, with the availability of oxygen being high. The exception will be soot formed on the

engine combustion chamber walls, hence this is likely to be a second source of soot formation in high-speed direct injection engine.

All the above discussions are concerned with visual smoke emission alone, but smoke particles carry a variety of diesel particulates. These particulates included the invisible fine particles and ultra-fine particles in the exhaust gas. They cause many adverse health effects and may be carcinogenic to human beings.

2.2 Diesel Emissions Measurement Technique

2.2.1 Measurement of diesel exhaust gaseous emissions

In the early 1980s, a constant volume sampling (CVS) system had been regulated for measuring vehicular exhaust emissions in emission testing centre [35]. This system has also widely been used in both laboratory or chassis dynamometer emissions measurement in order to produce a reproducible experiments. The system is able to determine exhaust emissions from petrol or diesel vehicles. A decade later, the Society of Automotive Engineers (SAE, USA) had also established a regulated measurement system to determine the vehicle exhaust emissions [36]. The two regulated measurement systems are similar and both are composed of a dilution tunnel, an air intake filter, a blower and a series of sampling equipment. In the CVS

system, the exhaust gases are diluted with filtered ambient air to maintain a constant total flow rate (exhaust + air) under all running conditions. The system can also provide a constant flow for the measuring equipment. A sampling probe is located at the downstream of the tunnel to collect a representative portion of the exhaust for subsequent analysis. The exhaust samples are stored in a sampling bag. The sampling bag is then taken to perform the gaseous concentration analysis as fast as possible. Instead of using sampling bag to collect the samples, another measurement system is also introduced in which the exhaust samples are directly drawn into the gas analysers to prevent any gaseous reaction or transformation occurred inside the sampling bag.

2.2.2 Measurement of diesel exhaust particle emission

Diesel exhaust particulates are typically composed of three modes: nuclei, accumulation and coarse particles. Particles in the nuclei mode cover the particle diameter ranges from 5 to 50 nm. Nuclei mode particles consists primarily of carbonaceous nuclei, metallic compounds, soluble organic fraction (SOF) and sulphur compounds, some of which are formed during the dilution and cooling processes [37,38]. Although the nuclei mode contributes only about 1 to 20% of total particulate mass, it is responsible for almost 90% of total particle number. The

particle diameter in the accumulation mode ranges from 50 to 500 nm. This mode consists mainly of agglomerates and adsorbed materials formed by coagulation of carbonaceous nuclei during the expansion stroke of the combustion process. The coarse particle mode is composed of particles larger than 1 μm in diameter, and contributes 5 to 20% of total particulate mass. Coarse particles arise from the growth of particulate matter which is deposited on the cylinder and exhaust tailpipe surface. The particle number concentrations of the nuclei and accumulation modes are readily changed during the dilution and cooling processes. As the results of the particles are not immutable, a reliable and stable dilution and sampling measurement system is undoubtedly crucial for obtaining meaningful diesel particle results.

In the absence of a standard measurement system to specifically determine diesel particle number concentrations [39,40], the conventional dilution tunnel has been widely used to measure the diesel gaseous and particulate emissions for more than two decades [36]. In the dilution tunnel, the exhaust gaseous and particles emissions undergo a process, which is similar to those emitted from the exhaust tailpipe to the atmosphere. The current measurement technique for exhaust particle emissions uses a CVS system, a scanning mobility particle sizer (SMPS) and an aerodynamic particle sizer (APS) to determine the particle size and number distribution. The configuration of the CVS system was discussed in the previous

Section 2.2.1 so here only the particle sizer instrument will be mentioned. The SMPS has been the common reference method for on-line measurement of particles below 1 micrometer in aerosol research for many years. The SMPS permits the measurement of particles in the critical size range from 15 to 670 nm with high reproducibility. Due to its technical superiority for the measurement of particle size distribution in the nanometer range, SMPS has been used increasingly for the characterisation of diesel exhaust particles. It has also been used to study the efficiency of exhaust aftertreatment devices for the reduction of particulate emissions from diesel engines.

The SAE practice has presented four types of CVS systems [41], but incompact size of the system and high fabrication cost cause CVS systems did not widely used in exhaust emission measurement. Thus, many researchers have tried to develop their own dilution tunnel to measure the engine exhaust particle emissions. Suzuki et al. [42] and Hirakouchi et al. [43] developed a mini-dilution tunnel for measuring diesel particulate emissions in steady state and transient engine operating conditions. The length of the tunnel was reduced to about 1.7 m and with an inner diameter of 84 mm. The tunnel is not only used to cool down the exhaust gas temperature, but also dilute the engine exhaust samples into an adequate concentration level for measurement. They found that a good correlation could be

established between the data collected using the mini-dilution tunnel and full flow exhaust dilution tunnel systems. Hirakouchi et al. [44] extended their experiments to use the mini-dilution tunnel to measure the regulated exhaust emissions (i.e. CO, HC, NOx and PM) and unregulated exhaust emissions (i.e. aldehydes and ketone, polycyclic aromatic hydrocarbons (PAH) and organic amines, etc.). They also found that the results from the mini-dilution tunnel and full-flow dilution tunnel are comparable with each other. Therefore, many researchers have preferred to use the mini-dilution tunnel to measure the engine exhaust emissions instead of using the full flow exhaust dilution tunnel system. However, there is one major factor which may affect the particle concentration in the CVS system, that is the water condensation in the dilution tunnel. Insufficient dilution will cause the water vapour to condense on the surface of the CVS and the sampling bag, absorbing water soluble components. Hood et al. [45] presented a basis for predicting a proper amount of dilution from well-known properties of the vehicle and test cycle which was used to prevent water condensation in the dilution tunnel. The condensation appears in the internal ductwork of the CVS so a practical method to eliminate the condensation is to raise the temperature of the system components. They stated that reducing the condensation can yield more repeatable and accurate emission measurements.

On the other hand, a new generation of particle measurement has been developed recently. Abdul-Khalek et al. [46] and Pagan [47] have developed a compressed air ejector type mini-dilution system to rapidly dilute and cool the vehicle exhaust gas. The exhaust emission samples were obtained directly from the vehicle tailpipe. The samples were then drawn into a diluter through negative pressure to make the dilution process. To measure the exhaust particles from diesel engines, they found that a long stabilisation time (i.e. 10 minutes) was required. Therefore, they suggested that the engine should be stabilised for a longer period before any measurements are made.

These two particle sampling measurement systems use different ways to conduct the dilution process. During the dilution process, the nanoparticles concentrations have revealed to be sensitive for the coagulation, condensation and nucleation processes, which can vary the nanoparticle number and size distribution. Hence, it is essential to understand the characteristics of diesel exhaust particle number and size distributions from these two dilution scenarios. Recently, Maricq et al. [48] have compared the motor vehicle exhaust particle size distributions using different dilution measurement techniques. Both ejector pump and dilution tunnel sampling measurement systems were used to analyse the steady state particle size distributions from the vehicle tailpipe. The gasoline and diesel vehicles were

conducted at constant engine speed under the chassis dynamometer. The particle size distributions from the dilution tunnel measurement obtained a bimodal mode whereas the ejector pump only revealed a peak particle number concentration in an accumulation mode a the diesel vehicle exhaust. They have also found that the particles in an accumulation mode is attributed to the desorption and/or pyrolysis of organic materials, either hydrocarbons deposits on the walls of the steel transfer hose or the silicone rubber, by hot exhaust gases, and their subsequent nucleation in the dilution tunnel. The results have also showed that if the transit time through the transfer hose were 2-5 seconds, about 1/3 of the nuclei mode particle will coagulate to form accumulation mode particles. This limits the ability of dilution tunnel system in providing an accurate particle number and size distribution measurement. Recently, Wei et al. [49] have studied the influence of the exhaust transfer line, tunnel residence time and dilution air temperature of the dilution tunnel and sulphur content of fuel on the exhaust particle size distribution. They have found that the coagulation of particles does not play a major role in the transfer line of a dilution tunnel, but rather the residence time is one of the critical factors directly influencing the particle number concentration.

2.3 Exhaust Aftertreatment Device in Diesel Engine

2.3.1 Development of diesel aftertreatment device

In modern emission control technology, there are numerous aftertreatment devices to reduce diesel exhaust emissions. These devices include DeNOx catalyst and selective catalytic reduction technique for NOx reduction, diesel particulate filter (DPF) for reducing the PM [50] and diesel oxidation catalyst (DOC) for gaseous emission reduction [51]. Although, industry has considerable aftertreatment devices to control exhaust emissions, the Government of the HKSAR has started to implement an incentive programme to encourage the owner of pre-Euro/Euro I vehicle (light-duty to heavy-duty) to retrofit a DOC on their vehicles. However, the negative effects of DOC on exhaust particle concentration and distribution for different engine load conditions are not fully understood.

A standard practice for the DOC is to utilise a noble metal supported on a flow-through ceramic or metallic monolith. The construction diagram of the diesel oxidation catalyst is shown in Figure 2.1. The monolith walls are coated with a thermally durable, high surface area catalytic component, generally platinum (Pt), palladium (Pd), rhodium (Rh) and zeolite. The DOC is normally installed along the exhaust tailpipe of the vehicle and close to the engine exhaust outlet.

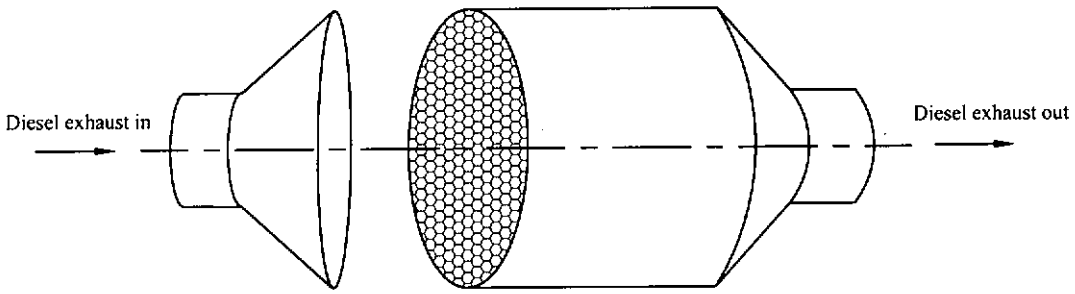

Figure 2.1 The construction diagram of the diesel oxidation catalyst.

The role of the catalyst is to provide a chemical shortcut, lower the energy requirement for chemical reactions and increase the net rate of its reaction. For example, the oxidation process of carbon monoxide requires normally about 700°C in the absence of a catalyst. The rate-limiting step is the thermal dissociation of O_2 into O atoms. The activation energy has been determined experimentally to be about 40 kcal/mole. In the presence of catalyst such as the platinum or zeolite material, the dissociation of O_2 occurs catalytically on the metal surface and the rate-limiting step becomes the reaction of adsorbed CO with adsorbed O atoms. The activation energy can be reduced to less than 20 kcal/mole and the oxidation reaction can occur at 100°C. In addition, the surface of DOC also provides numerous catalytic sites for the catalytic reaction to occur. Therefore, the presence of DOC can enhance the oxidation process of the exhaust gaseous and particle emissions, in which the CO

becomes CO_2, HC becomes H_2O and CO_2 and SOF adsorbed on the particle surface becomes H_2O and CO_2 [52-53].

During the chemical reaction, the reactants undergo the conversion process in which they must pass through the various energy barriers, namely the activation energies (E_a), before the final products are produced. Basically, the function of the catalyst is to increase the net rate of chemical reaction by reducing energy barriers or activation energies for the chemical reaction while the catalyst itself does not undergo any permanent change. For example, the hydrocarbons and oxygen are adsorbed onto the specific sites of platinum or zeolite catalyst and then are rapidly oxidised to become carbon dioxide and water. In general, platinum (Pt) and zeolite are the common materials used for the fabrication of catalysts. Since the Pt-based or zeolite-based catalyst contains numerous pores on its surface, this provides considerable catalytic sites for the reactants to perform the chemical reaction. In fact, the number of reactant molecules that can be converted into the final products within a finite time is directly related to the number of catalytic sites available. The major difference between a zeolite-based catalyst and a typical Pt-based catalyst is its pore size of substrate material. It is, therefore, common practice to maximise the number of active sites by dispersing the catalytic components onto a surface. Pt is a typical catalytic component which is commonly used to increase the number of sites for the

adsorption and catalytic reaction until zeolite-based materials have been introduced. Normally, the pore size of Pt-based catalyst is in the range of 20 to 100 Å (or $2x10^{-9}$ to 10^{-8} m), while the pore size of zeolite-based material is in the range of about 3 to 8 Å (or $3x10^{-10}$ to $8x10^{-10}$ m). Hence, the zeolite-based catalyst can provide more active sites for the reactants to carry out the chemical reaction than Pt-based catalyst [53].

2.3.2 Diesel exhaust gaseous emissions reduction

There are numerous studies on the performance of diesel oxidation catalysts for exhaust emissions reduction. Experiments based on these investigations are generally conducted in a laboratory with an engine dynamometer test bed or chassis dynamometer. The researchers use different types of engines, fuel properties, testing cycle and coating material on monolith to perform experiments. Mogi et al. [54] inspected the reduction of diesel engine emissions by using diesel oxidation catalyst on a Japanese 13-mode cycle. The experiment used various Pt loading of oxidation catalyst and low sulphur fuel (i.e. 460 ppm S) to study the oxidation activity of the catalyst. They measured the exhaust emissions of CO, HC, PM and other unregulated pollutants over the test. The results showed that the application of the DOC and low sulphur diesel fuel could abate the concentration of CO, HC and PM. The Pt loading

will also affect the reduction efficiency. Voss et al. [55] studied the performance of diesel oxidation catalysts for European bus applications. They also investigated the particulate removal performance by changing the sulphur level (110-770 ppm) under stationary engine test bed and a European ECE R49 13 mode cycle. They found that a substantial reduction of particulate matters, HC and CO could be achieved for heavy-duty diesel engine with DOC. However, NOx emissions was not affected by the catalyst. They also mentioned that even if the sulphur level in the diesel fuel is changed, the catalyst could still remove particulate emission effectively. Brown et al. [56] promoted the test on various heavy-duty engines and vehicles with and without retrofitting the diesel oxidation catalyst technology. Two urban buses, two school buses and three heavy-duty trucks were used in this study. A heavy-duty transient cycle was applied to evaluate the baseline emissions and the catalyst performance on a heavy-duty chassis dynamometer. The results indicated that a 25-45% particulate reduction could be achieved on a wide variety of heavy-duty vehicles. A significant reduction in the CO and HC emissions was also observed. The NOx emissions were found to vary within ±5% in all the tests. They claimed that it was difficult to interpret this phenomenon because the results in many of the tests were within the margin of error of the test. Tamanouchi et al. [57] have studied the effect of fuel properties and oxidation catalyst on the exhaust emissions for a

heavy-duty diesel engine and diesel passenger cars. They used two series of fuels, 90% boiling point (T90) and the polycyclic aromatic hydrocarbons (PAH) content, to test the effectiveness of the catalyst on different fuels. A transient mode test was used in which tested vehicles were run on the chassis dynamometer. They also found that the catalyst contributed to the reduction of exhaust gaseous emissions and particulate matters, however, the effect somewhat varied depending on engine type and fuel used. They concluded that the use of oxidation catalyst has turned out to be a more effective technology for decreasing the exhaust emissions than improving fuel properties such as T90 or PAH content. However, fuel quality has been improved in industrial usage and the sulphur content in the fuel has also been decreased. Therefore, when ultra low sulphur diesel fuel is used, the catalysts can have a significant effect in reducing the HC, CO and particulate matter emissions for all diesel engines [58].

2.3.3 Diesel exhaust particle emission reduction

Particle size and number distribution of diesel exhaust have increasingly become a controversial topic in the last decade. This is because the particles cause inflammation of the alveolar region of the lungs and cause breathing and heart problems in susceptible persons within days of the exposure to high levels of fine

particulate material. Some of the medical researchers hypothesize that problem is caused by the number of particle rather than its total mass [59-60]. In addition, about 90% of the diesel particulates encompass a size range from 0.0075 to 1.0 μm [61] and are considered to be potentially dangerous due to their capability to enter deep into the respiratory tract [62]. Particles smaller than 5 μm can enter the trachea and primary bronchi; and those smaller than 1 μm can reach the alveoli as shown in Figure 2.2 [63]. Therefore, most of the researchers concentrate on studying the distribution of exhaust particulate size.

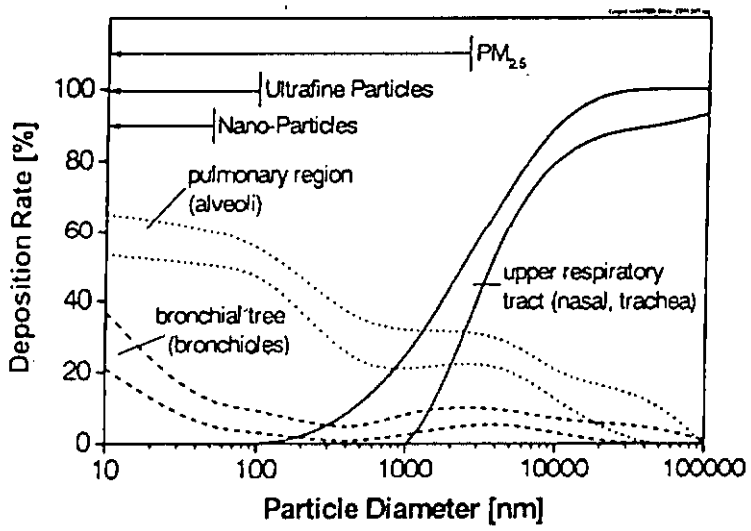

Figure 2.2 Deposition of inhaled particles in the respiratory tract [59].

Diesel engines normally generate a higher number of particulate matters than engines that run on gasoline or compressed natural gas. [7]. It is because the combustion process in a diesel engine differs from that in gasoline and compressed

natural gas engines. In gasoline and compressed natural gas engines, the air and fuel are drawn into the engine chamber for a premixed combustion in which is less chance to generate the particulate matters. In a diesel engine, the fuel is injected into the engine chamber and is then mixed with the hot compressed air for ignition process, towards the end of compression stroke. A small portion of fuel is initially burned in the premixed mode, while a larger portion of fuel is subsequently burned in the diffusion mode. The amount of particulate matters generated during the diffusion combustion depends on many factors such as engine load, engine speed, effectiveness of air-fuel mixing, amount of air available and fuel quality.

Typically, the size of the particle emitted from a diesel engine ranges from micro-scale to nano-scale. Most of the particles are smaller than 10-micron aerodynamic diameter and a significant percentage of the particles are shown in the aerodynamic diameter range, which is less than 50 nm. The size distribution of diesel particulates has shown that greater than 95% of particulates are under 10 μm in diameter, and about 90% of diesel particulates are under 2.5 μm in diameter. A large amount of SOF and soot particles were found in this smaller particle size range [38]. Rickeard et al. [64] investigated the characteristics of the exhaust particulate size distribution when different vehicle type and fuel quality were used. The test was performed on a light-duty diesel vehicle and a gasoline car and used the latest

European legislated emissions test, ECE+EUDC cycle as the test schedule. They reported that most of the particles emitted from the diesel and gasoline vehicles were very small, with median size of the order 100 nanometres (nm). The median particle size varied by only a small amount across fuel quality, vehicle and operating conditions. They also pointed out that diesel vehicle would produce 50% more particles than gasoline car in this size range. According to the above diagram showing deposition of inhaled particles, the range of particle size can penetrate the upper respiratory tract and has a deposition rate of approximately 60% the pulmonary region (alveoli). Hence, the health effect of diesel exhaust particle emissions has become a public concern.

Most of the smaller particles are SOF, which is the most harmful phase from the health standpoint [38]. However, the most of modern aftertreatment devices (i.e. diesel oxidation catalyst) have shown to reduce the SOF and particulate emissions [65-67]. Horiuchi et al. [68] found that a flow-through type oxidation catalyst can adsorb or adhere SOF on the catalyst surface at lower temperature and decompose it at higher temperature. They mentioned that oxidation catalyst could achieve a 50-60% reduction of the SOF and 40-50% reduction of the total particulate emissions from an engine. However, these previous studies of the particulate emissions were based on the mass concentration, which provides insufficient information for

understanding the characteristics of the PM emissions. Many investigations in recent years have concentrated on the number and size distribution of particles emitted from motor vehicles. Mayer et al. [69] and Luders et al. [40] have performed experiments focused on the impact of DOC on particle number emissions. Both researchers measured nanoparticles or ultra-fine particles in their investigations. They found that the application of DOC increases the number of particle emissions in the 50 nm diameter range as shown in Figure 2.3. The reason is that the DOC intensifies the aerosol formation by accelerating the oxidation reaction of SO_2 to SO_3 at a high temperature. They inferred that DOC should not be installed on a utility diesel engine, because the negative consequences far exceed the positive results. However, these experiments only used standard diesel (about 0.05% by weight S or 500 ppm S) as the testing fuel rather than ultra low sulphur diesel fuel (about 0.005% by weight S or 50 ppm S).

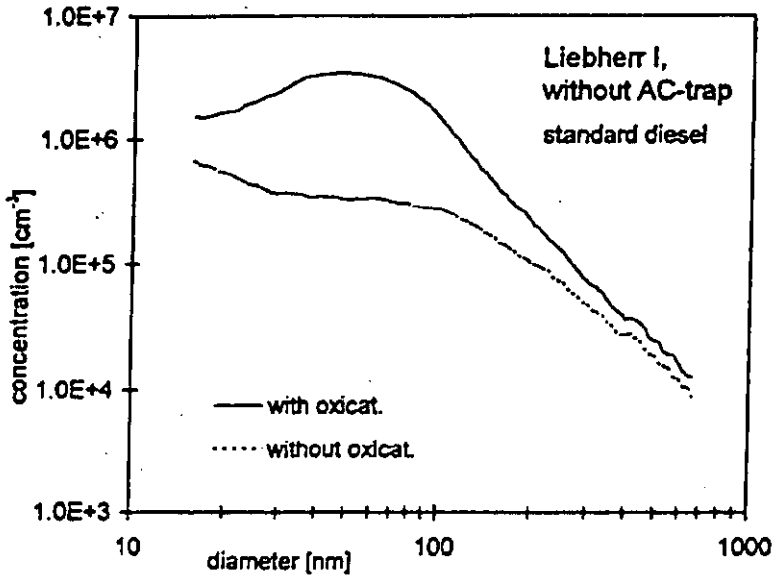

Figure 2.3 Exhaust particle size distribution from an engine with and without installing DOC [69].

Maricq et al. [70] have reported that if DOC is tested with low sulphur content fuel, the result demonstrates that DOC can reduce particle emission, whereas the use of high sulphur content fuel will have opposite result. Nevertheless, there is still a paucity of publications on the combined effect of ultra low sulphur diesel fuel and a diesel catalytic converter on particle emission. The present study is intended to characterise the combined effect of the modern DOC device and ultra low sulphur diesel fuel on the diesel exhaust particle concentration and distribution.

Chapter 3 Preliminary Study on the Performance of Diesel Oxidation Catalyst for a Light-duty Vehicle under Hong Kong Driving Conditions

3.1 Introduction

Catalytic converter has been considered as one of the immediate solutions in reducing the diesel vehicles emissions and improving the air quality. According to international experiences after installing a Diesel Oxidation Catalyst (DOC) on a diesel vehicle, the concentration of diesel exhaust emission would have a remarkable reduction. Voss et al. [55] have also proved that installing diesel oxidation catalyst on medium and heavy-duty vehicles can achieve substantial reduction of particulate, gas phase HC and CO emissions. On the other hand, Blackwood et al. [71] have found that the DOC was unable to oxidise CO to CO_2 and unburned hydrocarbons (uHCs) to CO_2 and H_2O, due to low start up engine exhaust temperature. However, those experiments were performed in the laboratory and the results can only show the behavior of the catalyst under a controllable environment. The information regarding the performance of a catalyst under on-road situation is rather limited and there is also lack of direct emission data from exhaust tailpipe of a vehicle. In addition, the testing conditions from previous studies differ from Hong Kong driving condition so it might not reflect the true characteristics. Although investigation performed in

laboratory has the advantages of being simple, reliable and easy-to-perform, the test conditions might be quite different from on-road conditions. On-road driving is random and complex, and has different patterns in different places as described by Zhao et al. [72]. Nevertheless, in order to ascertain the effectiveness of DOC in reducing exhaust gaseous pollutants and the effect on particle emissions under Hong Kong driving conditions, a preliminary investigation was carried out under local traffic conditions [25].

3.2 Diesel Exhaust Emissions Measurement System

A Euro-I standard diesel vehicle was used to perform an on-road vehicle emissions measurement. The specifications of the vehicle are shown in Table 3.1.

Fuel type	Diesel
Displacement	3660 c.c.
Gross vehicle weight	5.5 tonnes
Combustion chamber type	Direct injection (DI)
Valve mechanism	2-valve
Max. output, (kW/rpm)	72/3400
Max. torque, (Nm/rpm)	240/1800

Table 3.1 Specifications of the tested light-duty diesel vehicle.

The exhaust temperature of the catalyst inlet directly affects the performance of the catalyst so it is an important monitoring parameter in this study. In order to determine the exhaust gas temperature before entering the DOC, the catalyst was modified and a well-calibrated thermocouple was installed on the catalyst shell. A thermocouple was connected to a data logger and the instantaneous temperature variation of the exhaust gas was recorded every second. Smoke intensity of the vehicle was measured via a Hartridge Smokemeter, with results presented on a scale from 0 to 100. The sample probe of the smokemeter was inserted into the vehicle tailpipe to ensure the device can perform a proper measurement. An analog-digital convertor (ADC) was used to transmit the opacity data to a laptop computer and the data was stored every second.

For measuring the exhaust gaseous emissions, a portable exhaust gas analyser (i.e. Anapol Model EU200/4) was used to measure the instantaneous concentration of CO, CO_2, NOx, and O_2. The accuracy of the exhaust gas analyser ranges from 0.5% to 2.3% for CO, CO_2 and O_2, whereas NOx emission ranges from 1.5% to 3.5%. The sample probe of the analyser was also put deeply into the vehicle exhaust tailpipe. The analyser applies the non-dispersive infra-red (NDIR) method for determining the concentration of CO and CO_2, and adopts the electrochemical method for detecting the gas of NOx and O_2. The emission data were captured every second by using the

same laptop computer. The gas analyser was calibrated with certified standard gases before performing the on-road vehicle emissions measurement.

A series of sampling system including a water separator, a sampling pump and a sampling bag were used to collect the exhaust particle emission from the vehicle. The use of sampling bag is the common method to collect the exhaust samples from an on-road vehicle [73-74]. The particle sampling started at the beginning of each trial and ceased with the end of each driving. After each trial, the collected sample was then analysed by using a particle sizer, namely aerodynamic particle sizer (APS), to determine the particle number concentration and size distribution [75]. The APS sizes and counts particles from 0.5-30 μm in 32 particle size channels. The operation principle of APS is using a nozzle to accelerate the particle to pass through a laser beam and a sensor is used to measure the time for the particle to pass through the laser beam. The measured time is then used to correlate the particle velocity with the aerodynamic diameter of the particle. Meanwhile, the number of particle in the sample is determined by the sensor and the result is then transmitted into the computer. The arrangement of the on-road vehicle emissions measurement system is shown in Figure 3.1.

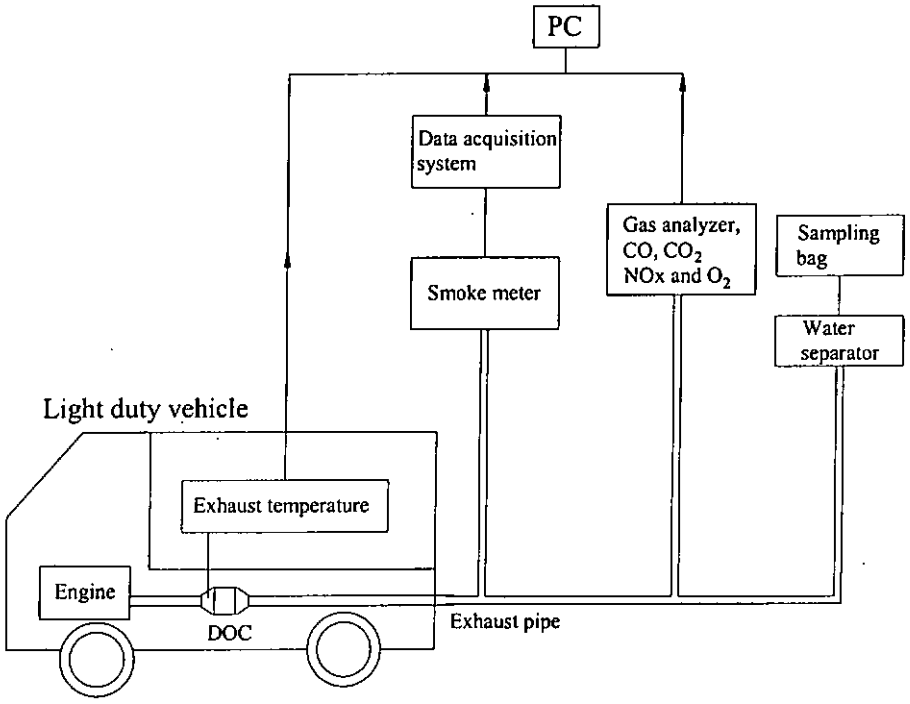

Figure 3.1 Arrangement of the on-road light-duty diesel vehicle emissions measurement system [25].

3.3 Methodology for Data Analysis

All on-road vehicle emission tests were performed on the same driving route under the uphill, downhill and flat road conditions to determine the characteristics of DOC. Four tests were performed on the same driving route. Thus, the on-road vehicle emission data is presented on average. The inclined road ratio for the uphill was 1:8, while the downhill was 1:5. The driving period for each trial was about 500 seconds. The result analysis was mainly divided into three phases as shown in Table 3.2.

Phase	Driving period	Road condition
1	30-120 seconds	Uphill
2	250-300 seconds	Downhill
3	350-500 seconds	Flat

Table 3.2 Road conditions during the test period [25].

In phase 1, the analysis was mostly focused on the performance of the catalyst during engine cold start condition. "Cold start" means that any engines start to operate when the temperature of oil, coolant and all elements of engine equals to the ambient temperature [76]. In this study, the time for this period was the first 120 seconds of driving. The remaining phases (i.e. 2 and 3) were mainly used to investigate the effectiveness of the diesel oxidation catalyst after warm-up. Parametric effects of exhaust emissions, temperature and smoke intensity were measured instantaneously in order to understand their correlation for different driving conditions on the road. The collected particles in the sampling bag were also used to study the average particle concentration and size distribution over a test period.

3.4 Preliminary Results and Discussion

3.4.1 Performance of DOC at cold start running

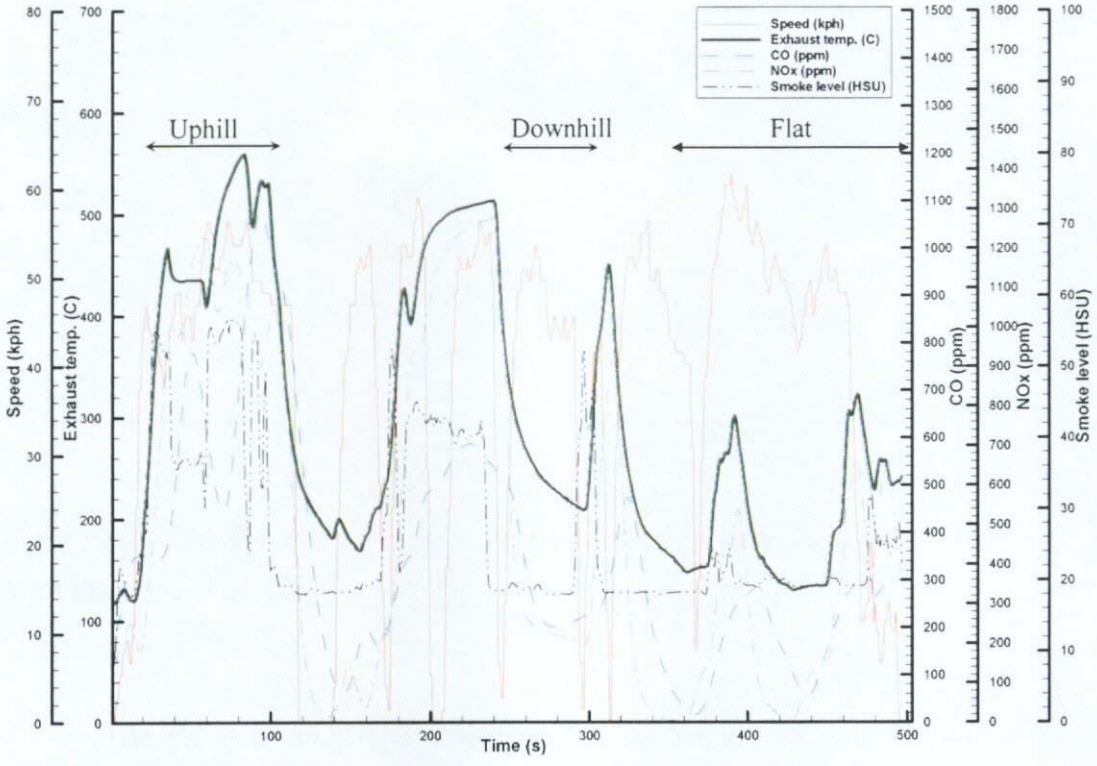

Figure 3.2 Exhaust emission characteristics of the on-road light-duty diesel vehicle without installing DOC [25].

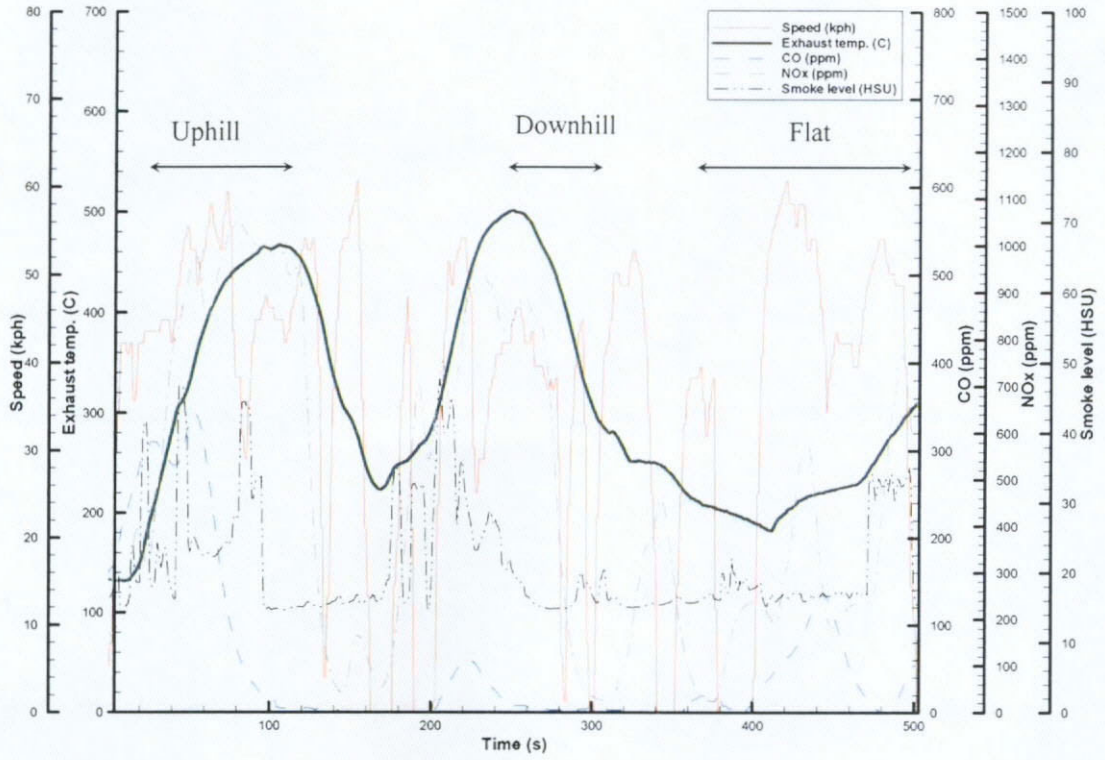

Figure 3.3 Exhaust emission characteristics of the on-road light-duty diesel vehicle with installed DOC [25].

The exhaust emissions characteristics of the vehicle without and with the installation of a DOC are shown in Figures 3.2 and 3.3, respectively. The designated vehicle was undergone three on-road driving phases: uphill, downhill and flat road conditions. Figure 3.2 shows that the highest concentration of CO and NOx emissions emitted from the vehicle without installing of a DOC appears at the first phase. This is because the engine generates more energy when the vehicle is climbing up, so the exhaust gas temperature also tends to rise. The increase in exhaust gas temperature also enhances the formation of NOx, therefore the vehicle produces a large amount of NOx during this traveling period. In Figure 3.3, the CO

concentration increases at the beginning due to the engine performance at cold start and then the DOC is not ready to perform the oxidation process effectively at such low exhaust gas temperature. Basically, cold start diesel engine will emit more CO, HC and PM than a warm start engine [77]. This result is due to the low intake air temperature which causes an inadequate final compression temperature and so delayed ignition. The combustion was exacerbated by poor fuel conditioning, heat loss from cold engine components, insufficient air movement, localised over-enrichment and incomplete fuel combustion [78]. Therefore, these phenomena raise the exhaust emissions. In addition, the increase in CO concentration makes it unable for the catalyst to completely oxidise the CO to CO_2 when the engine is cold start. The findings agree well with the results of Blackwood et al. [71] and also demonstrate that the catalyst might not function efficiently even running on road.

3.4.2 Reduction in diesel exhaust gaseous emissions

The exhaust emissions are considerably high. Table 3.3 summarises the reduction of CO and NOx after the vehicle installed the DOC. The average CO emission from the vehicle without installing the DOC in each state of a test is 709, 266 and 163 ppm, respectively. After the vehicle was installed with the DOC, the CO emission reduces significantly. The results agree with the findings from

Voss et al. [55]. Even the engine is cold start in the first part, the DOC can still oxidise a certain amount of CO. However, the percentage reduction of CO emission is smaller when compared with the subsequent driving. As the DOC is warmed up after the uphill period, it can eliminate most of the CO emission when the vehicle runs in the downhill period even the exhaust gas temperature is about 200°C. For the flat road condition, the DOC can also reduce about 80% of CO emission.

	CO			NOx		
Road condition	W/o DOC (ppm)	With DOC (ppm)	Percentage reduction (%)	W/o DOC (ppm)	With DOC (ppm)	Percentage reduction (%)
Uphill	709	152	78.6	981	915	6.7
Downhill	266	15	94.4	534	514	3.7
Flat	163	32	80.4	300	288	4.0

Table 3.3 The average exhaust emission concentration emitted from the on-road light-duty diesel vehicle [25].

The level of NOx emission is usually related to the vehicle speed. The formation rate of the NOx is dependent on the availability of oxygen and the combustion temperature. While the vehicle speed increases, it implies that the engine is required to generate more power to increase the speed. The combustion inside the engine becomes more efficient and will raise the combustion temperature. Consequently, this phenomenon encourages the formation of NOx and the emission concentration of NOx augments when the speed increases. The average emission

concentration of NOx from the vehicle without installing DOC, in each part of a test is 981, 534 and 300 ppm, respectively. Figures 3.2 and 3.3 show that the vehicle emits a large amount of NOx during uphill period and quite similar level between downhill and flat road. Usually, the DOC has no effect on the NOx emission concentration as described by Blackwood et al. [71], but the result shows that there is a reduction in NOx. The result can be attributed to the fact that DOC produces a back pressure to the engine and affects its performance. Hence, the exhaust gas temperature becomes lower and it causes lower NOx emission concentration.

3.4.3 Performance on smoke opacity level

Road condition	W/o DOC (HSU)	With DOC (HSU)	Percentage reduction (%)
Uphill	39.2	24.7	37.0
Downhill	22.8	16.6	27.2
Flat	21.3	19.8	7.1

Table 3.4 The average smoke opacity level emitted from the light-duty diesel vehicle [25].

The average smoke opacity level of the vehicle is summarised in Table 3.4. The DOC can reduce the smoke opacity level of the vehicle effectively during the uphill period. The average smoke level is 24.7 HSU, which is normally acceptable, and the reduction percentage is 37%. The reduction level seems to be high but when

compared with the abatement of the exhaust gaseous emissions, it becomes less significant. The smoke level can also be lowered in the downhill condition even the original value is not so high. The minimum reduction in smoke level appears in the flat road condition. It should be noted in Table 3.4 that under the flat road condition, the percentage reduction of smoke emission is unusually lower than that in the downhill condition. This can be explained by using the results in Figure 3.3. During the second uphill road condition, the vehicle was run at the traveling period between 200 to 250 seconds before the start of the downhill condition. The exhaust gas temperature at the inlet of DOC was raised up to about 500°C at the traveling time, 250 seconds. Therefore, the exhaust gas temperature of vehicle in downhill road condition during the traveling period of 250 to 300 seconds still remained higher than the flat road condition. Thus, the DOC is more effective in oxidising the SOF of the particulate matters at the downhill road condition than the flat road condition due to the higher exhaust gas temperature. The oxidation of SOF can be related to the smoke emission level which normally contains numerous particulate matters. Hence, the reduction of SOF can directly abate to the smoke emission level. Regardless of the road condition, it can be concluded that DOC does have a function to decrease the smoke level of a vehicle.

3.4.4 Diesel exhaust particle number and size distribution

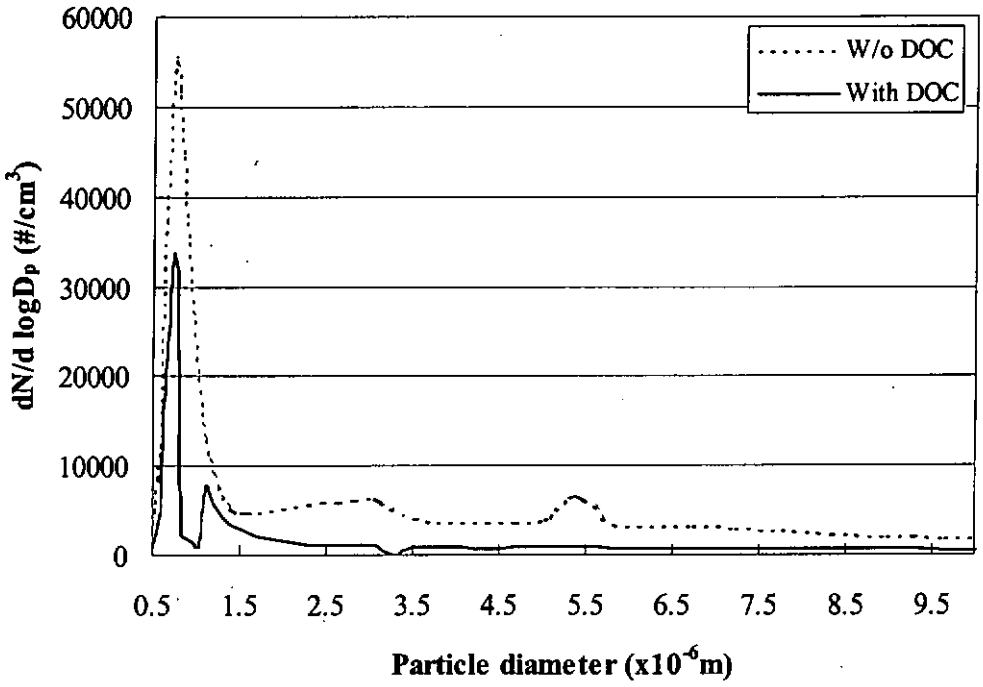

Figure 3.4 Particle number and size distribution emitted from the light-duty diesel vehicle [25].

The particle concentration and size distribution emitted from the vehicle is shown in Figure 3.4. The results showed that the vehicle produces a large amount of respirable suspended particulate (RSP), with high concentration especially at the size of 0.7 μm. These particles are harmful because they can suspend in air and is inhalable. After the vehicle installs the DOC, the particle concentration is substantially decreased. The average percent reduction in particle concentration is 67.8% for particle size ranging from 0.4 to 1 μm. The vehicle seems to produce a small amount of large particles (i.e. $PM_{2.5}$ and PM_{10}). With the application of DOC,

the average percentage reduction in particle concentration is 78.2% for those particulates. It is likely that the DOC is able to lessen the larger particulate more efficiently. However, modern low emission engines and aftertreatment devices with reduced particle mass concentrations and smoke level may significantly increase emission of larger number of ultra-fine particles [24]. Hence, it is intended to investigate the combined effects of DOC and ULSD fuel on the concentration and distributions of ultra-fine particle and nanoparticles emitted from a diesel vehicle.

Chapter 4 Experimental Investigation of Diesel Oxidation Catalyst in Exhaust Gaseous and Particle Emissions

4.1 Introduction

In order to investigate thoroughly the characteristics of a catalytic converter in removing exhaust gaseous and particle emissions, a comprehensive experiment was performed in an engine dynamometer test bed. The experiment includes several engine testing procedures, which were in compliance with a steady-state mode cycle of the standard Economic Commission for Europe Regulation 49 test modes [79]. Two particle measurement systems were established to determine exhaust particle emission emitted from diesel engine. Unlike gaseous emissions, diesel exhaust particles can readily undergo transformations such as coagulation, condensation and adsorption, and form nanoparticles by the nucleation of gaseous particles during dilution and cooling of exhaust gases. A conventional dilution tunnel and state-of-the-art ejector dilutor measurement systems were established and to compare the results were compared to find out the most stable and reliable measurement system for particle emission.

An exhaust gaseous emission measurement system was built up to measure diesel exhaust gaseous emissions such as CO, HC and NOx in accordance with the

standard practice of SAE [80]. Meanwhile, exhaust gas temperature at the inlet and outlet of the DOC, fuel consumption, engine speed and load, and ambient air condition were also recorded. The detailed descriptions of the measurement system and the experimental procedures are presented as follows.

4.2 Diesel Engine Dynamometer Test Bed and ULSD Fuel Used for Testing

A 4-stroke 2289c.c. direct injection (DI) diesel engine mounted on an engine dynamometer test bed was used to perform the present study. The specifications of the engine are presented in Appendix A1. The engine speed was controlled by using a control valve that was fixed on the engine, and the engine load can be adjusted via a hydraulic dynamometer. During the testing, the engine was directly coupled to the main shaft for transmitting the power to revolve a rotor inside the casing, through which water was circulated simultaneously to provide the hydraulic resistance and carry away the heat generated from the engine. The engine intake air passed through an air filter to remove any incoming particulate matter. The engine exhaust tailpipe was connected to the exhaust system and discharged into the atmosphere. The configuration of the diesel engine and the hydraulic dynamometer is shown in Figure 4.1. Ultra low sulphur diesel (ULSD) fuel was used throughout these experiments. The fuel properties are provided in Appendix A2.

Figure 4.1 The configuration of the direct injection (DI) diesel engine and the hydraulic dynamometer test bed.

4.3 Particle Emission Measurement System

4.3.1 Instrumentation

Particle number and size distributions of diesel exhaust were measured using a scanning mobility particle sizer (SMPS) from TSI Inc. model 3934, USA. This is composed of an electrostatic classifier model 3071A and condensation particle counter (CPC) model 3010. The electrostatic classifier is used to classify the size of the particle which is being counted. The monodisperse sample from the classifier are then transferred to the CPC in order to determine the particle number concentration in the sample. A detailed description about the SMPS particle instrument is presented

in Appendix B. In the present study, the flowrates of aerosol and sheath air were set to 0.3 litre min^{-1} and 3 litre min^{-1}, respectively. The particle sizes were measured for the range between 16 and 670 nm.

4.3.2 Mini-dilution tunnel and sampling (MDTS) measurement system

The schematic diagram of a mini-dilution tunnel and sampling (MDTS) measurement system is shown in Figure. 4.2. The mini-dilution tunnel was made of a 117 mm diameter and 1670 mm long stainless steel tubing. A partial of exhaust gases was introduced to the tunnel through a transfer line. An adjustable valve was used to control the amount of exhaust gas introduced to the tunnel, and a vortex flowmeter was installed on the transfer line to measure the volumetric flow rate of the exhaust sample. Compressed air at 23°C dry bulb and 63% relative humidity was used for the dilution. It was filtered by a set of particles and an oil filter, to remove the large particles and oil moisture. The volumetric flow rate of the compressed air was determined by a laminar flowmeter. The laminar flowmeter is a device which consists of a bundle of straws. The length of the straw is very long (i.e. 150 mm, however its bore is smaller than about 0.5 mm. It allows the fluid to flow through it, so the pressure difference across the straw can be measured by a manometer to determine its flowrate. The dilution air was then introduced into the tunnel, where it

was mixed with the exhaust gases. The diluted exhaust samples were continuously transferred through the tunnel and a sampling probe was located at 1170 mm to the downstream of the mini-dilution tunnel. The residence time of the exhaust samples inside the dilution tunnel was about 1.2 seconds. A sample was directly extracted from the dilution tunnel flow. It was then transferred to the SMPS to count the number and size distribution of the particles. The dilution ratio was determined by the ratio of the raw exhaust gas flow to the diluted exhaust flow [81]. The dilution ratio was 7 throughout the experiments. Although the exhaust sampling is not isokinetic, it is not expected to affect the measured particles for below 4 μm in diameter [82].

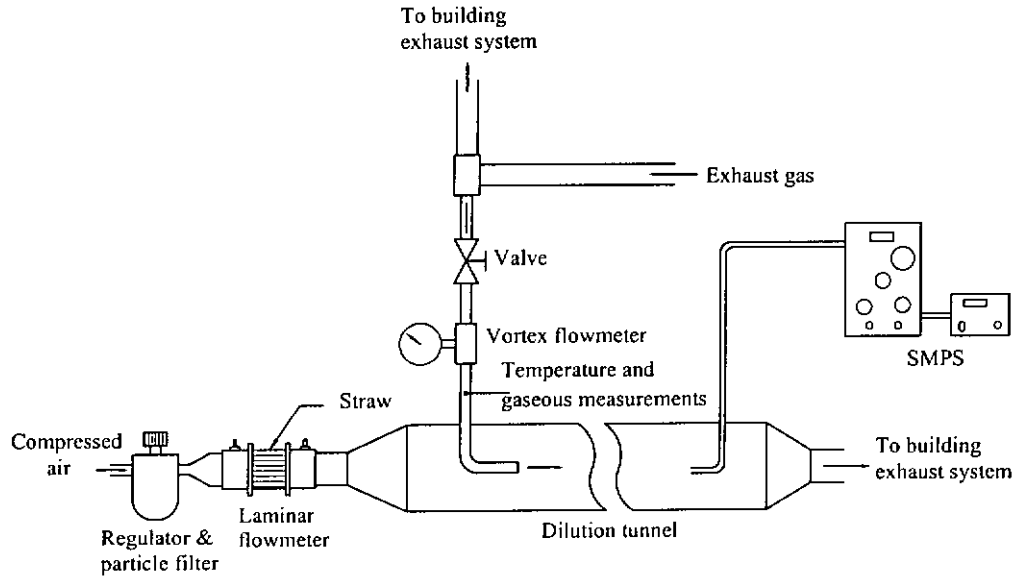

Figure 4.2 A mini-dilution tunnel and sampling (MDTS) measurement system.

In order to ensure uniformity in the mini-dilution tunnel, a multi-hole transfer line is used to distribute the exhaust samples equally into the tunnel [42, 43, 68]. The dispersion process of the exhaust samples inside the dilution tunnel is shown in Figure 4.3.

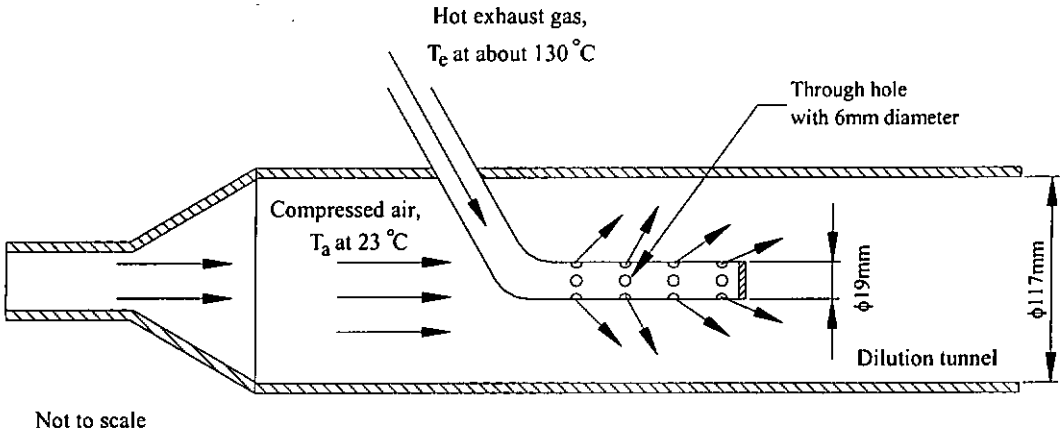

Figure 4.3 Configuration of a multi-hole transfer line and the dispersion process of the exhaust samples inside the mini-dilution tunnel.

4.3.3 Ejector diluter and sampling (EDS) measurement system

An ejector diluter from Dekati Ltd. was used to obtain the particle emissions directly from the exhaust tailpipe line. It consists of two diluters, a pressurised air heater, a temperature controller and a dryer and filters set. The schematic diagram of an ejector diluter and sampling (EDS) measurement system is shown in Figure 4.4. A L-shaped stainless steel tube- the sample probe- was inserted into the exhaust pipe. The 6.4 mm diameter sample probe was connected with a transfer line made of a 1000 mm stainless steel tube. The transfer line was insulated and heated to sustain a

surface temperature of about 200 °C, in order to prevent a thermophoretic deposition and condensation of aerosol particles on the tube wall [83]. Dry and particle-free pressurised air was introduced into the diluter through an ejector cavity. The dilution air was heated up to the exhaust gaseous temperature in the primary diluter. In general, the saturation vapour pressure of a substance is a function of its temperature. The vapour pressure of volatile components for the collected exhaust samples decreases for the heated dilution. Hence, it allows secondary dilution at room temperature of 23°C without causing any condensation of the volatile components. Therefore, the particle size was not increased by the condensation of the vapour molecules. The high flow rate of the dilution air induced a pressure drop in the ejector cavity, hence the exhaust particle sample was extracted into the diluter through the transfer line. The diluted air was mixed with the exhaust particle sample inside the ejector cavity. The dilution ratio of the primary diluter was 8. A portion of the diluted samples was then introduced into the secondary diluter for further dilution. Hence, the overall dilution ratio of EDS measurement system was 64. The total residence time was about 0.1 second for the primary and secondary ejector diluters which were connected together as obtained from Dekati Ltd., Finland.

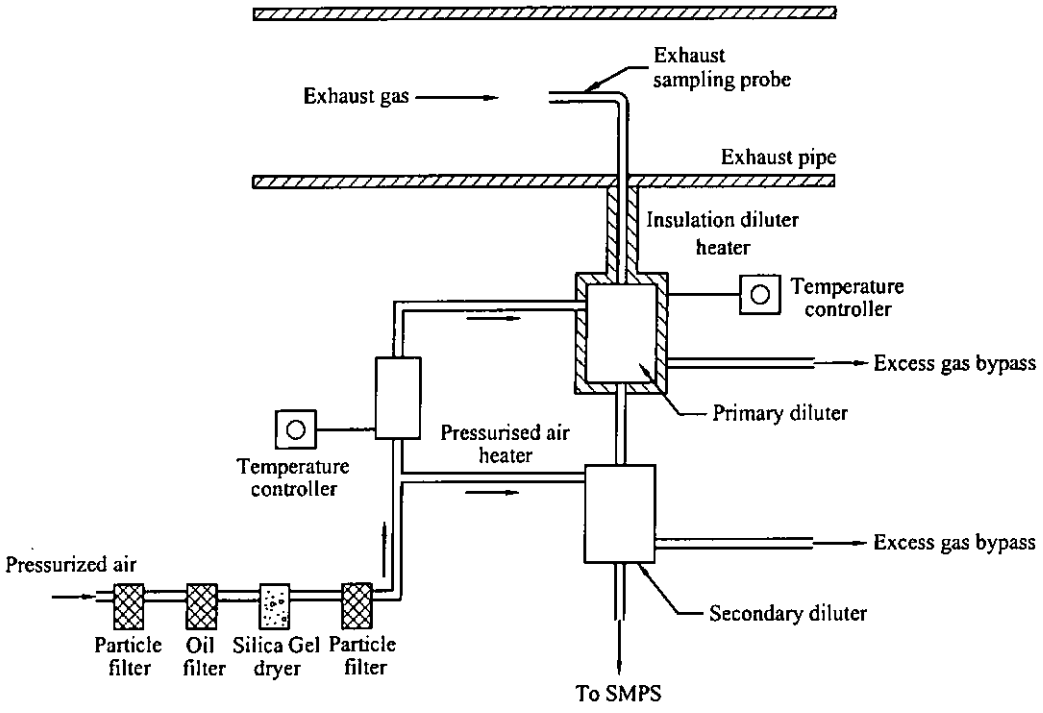

Not to scale

Figure 4.4 An ejector diluter and sampling (EDS) measurement system.

4.4 Gaseous Emissions Measurement System

4.4.1 Instrumentation

The exhaust emissions from the diesel engine will be measured by a series of gas analysers in the laboratory. Three gas analysers are used for detecting all the kinds of gases in the exhaust plume. All of the gas analysers were calibrated regularly in order to maintain high measurement accuracy.

CO and CO_2 gas analyser

A portable multi-detection gas analyser (Anapol Model EU200/4) as shown in Figure 4.5, was used to measure the concentration of oxygen, carbon dioxide and carbon monoxide in the exhaust plume. It is particularly designed for measuring exhaust gaseous emissions from diesel vehicles.

Figure 4.5 Non-dispersive infra-red CO and CO_2 gas analyser.

The sample gas is drawn into the analyser with the assistance of a membrane pump and then fed to the different sensors. In order to prevent the gaseous detectors from being damaged by contaminants in the exhaust gas, the exhaust sample is required to pass through a water separator and a series of particle filters to remove the water moisture and particulate in the exhaust gas, respectively. The analyser is

equipped with a non-dispersive infra-red (NDIR) sensor to detect the amount of CO_2 and CO and an electrochemical cell to measure the concentration of O_2. The operation principle of the analyser detecting the CO and CO_2 is presented in Appendix C.

HC gas analyser

A California Analytical Instrument (CAI) Model 300 HFID Analyser as shown in Figure 4.6 was used to determine the total hydrocarbons concentration in the exhaust sample. This instrument uses a regulated standard method (i.e. heated flame ionisation detection, HFID) for detecting the HC concentration. The transfer line of the sample gas before entering to the analyser was maintained at about 190 C. The sample gas was also maintained at an elevated temperature by the internal adjustable temperature oven which can be adjusted between 60 and 200 C until the sample gas exits the FID burner assembly. This prevents any loss of hydrocarbons concentration in the sample due to condensation. Therefore the results were recorded on wet basis. The operation principle of the HC analyser is presented in Appendix C.

Figure 4.6 Heated flame ionisation detection HC gas analyser.

NOx analyser

A California Analytical Instrument (CAI) Model 400 HCLD NO/NOx Analyser as shown in Figure 4.7 was used to continuously measure the total concentration of nitrogen oxides within the exhaust sample. The gaseous sample can be ambient air, exhaust gas from an internal combustion engine, or exhaust gas from a combustion process. The HCLD Analyser utilises the principle of chemiluminescence for analysing the NO or NOx concentration within the exhaust sample. A detailed description of the chemiluminescence technique is presented in the Appendix C. This measurement technique for determining the NOx emission is widely accepted and has been used to obtain the experimental gaseous result in Chan et al. [84]. The HCLD analyser measures the result in wet basis and is convenient for calculating the mass emission.

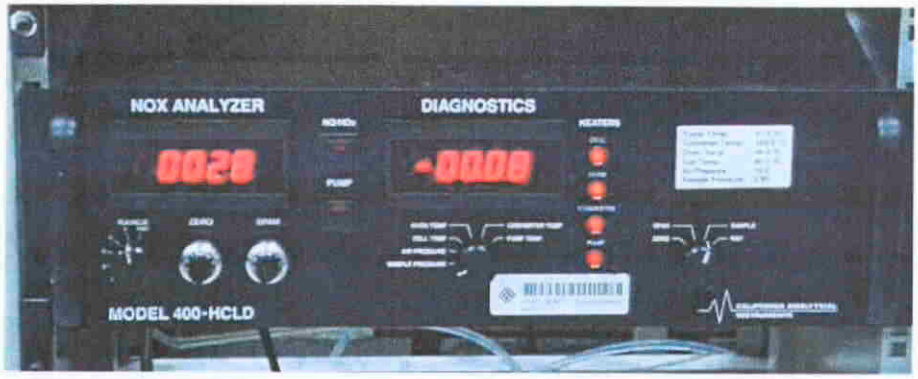

Figure 4.7 Heated chemiluminescence NOx gas analyser.

Fuel meter

A fuel meter was utilised to measure the flowrate of fuel and the fuel consumption of the diesel engine. The flow rate of fuel was used for the determination of the emission factor for various gaseous pollutants as well as for comparing the fuel consumption from different engine load conditions. The meter is of a positive displacement type, affording a very high degree of accuracy. The flow of fuel through the meter causes a centrally located piston to rotate within the measuring chamber and to displace a fixed amount of fuel from the inlet to the outlet in a continuous flow pattern. An electrical impulse is generated by a Reed-switch inside the meter housing which is then processed by the Psion II interface module. Calibration has been made on a regular basis. The connection between the fuel meter and the engine is illustrated in Figure 4.8.

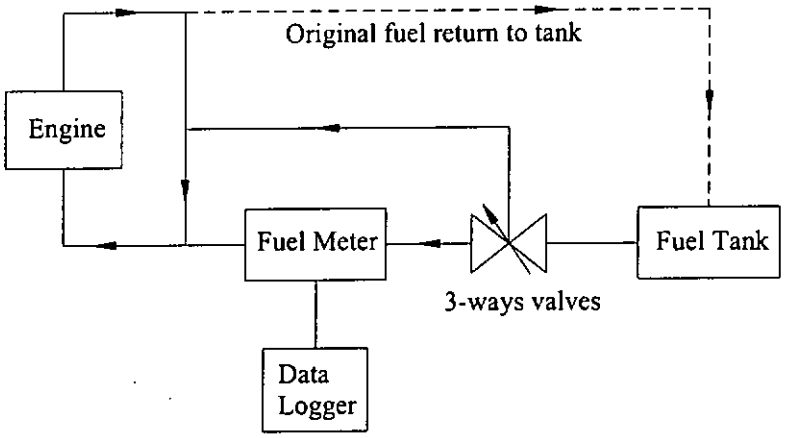

Figure 4.8 Schematic diagram of the diesel fuel measurement system.

4.4.2 Experimental measurement setup

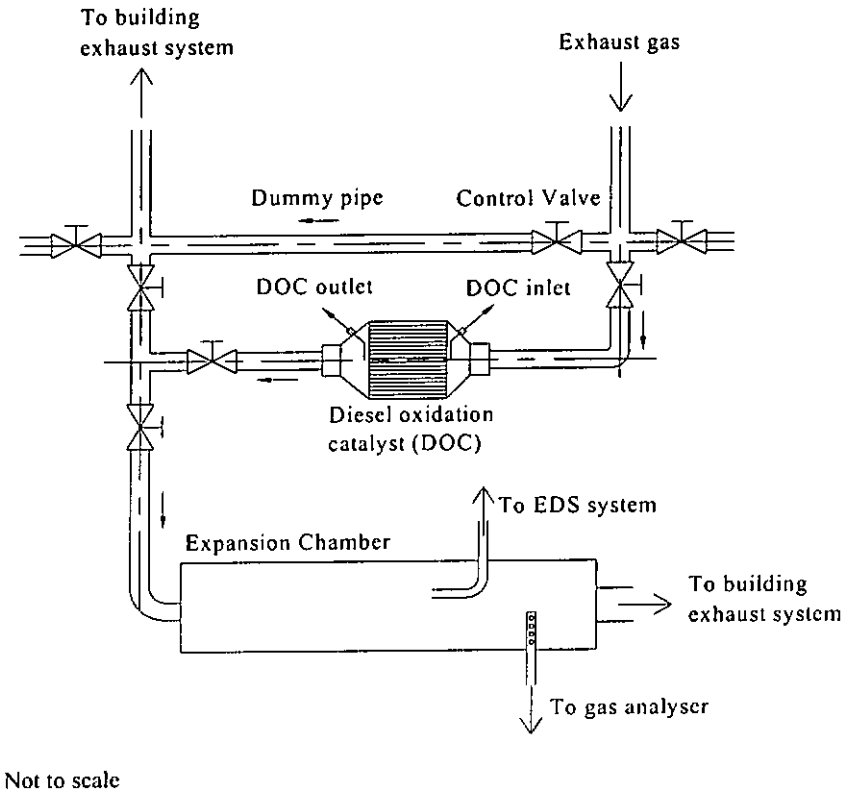

Figure 4.9 Schematic diagram of the experimental setup.

Figure 4.9 presents the experimental setup for investigating the performance of a diesel catalytic converter. The exhaust pipe of the engine test bed was modified to suit the present study. Many control valves were installed on the exhaust pipe to control the direction of the exhaust gas flow. A diesel oxidation catalyst and a dummy pipe were fixed in parallel for convenience to measure the exhaust gaseous and particle emissions emitted by the diesel engine with/without installing the DOC. The shell of the DOC had been modified for measuring the exhaust gas temperature and the back pressure at the inlet of catalyst. After the exhaust gas passes through the DOC or dummy pipe, a portion of exhaust gas will flow into an expansion chamber for sampling the exhaust emissions. The objective of the expansion chamber is to damp out any fluctuation and impulsion effects in the exhaust gas flow, which will affect the stability of sampling. The rest of the exhaust gas will flow to the building exhaust system. The sampling configuration inside the expansion chamber and the setup of the exhaust gas measurement are shown in Figure 4.10.

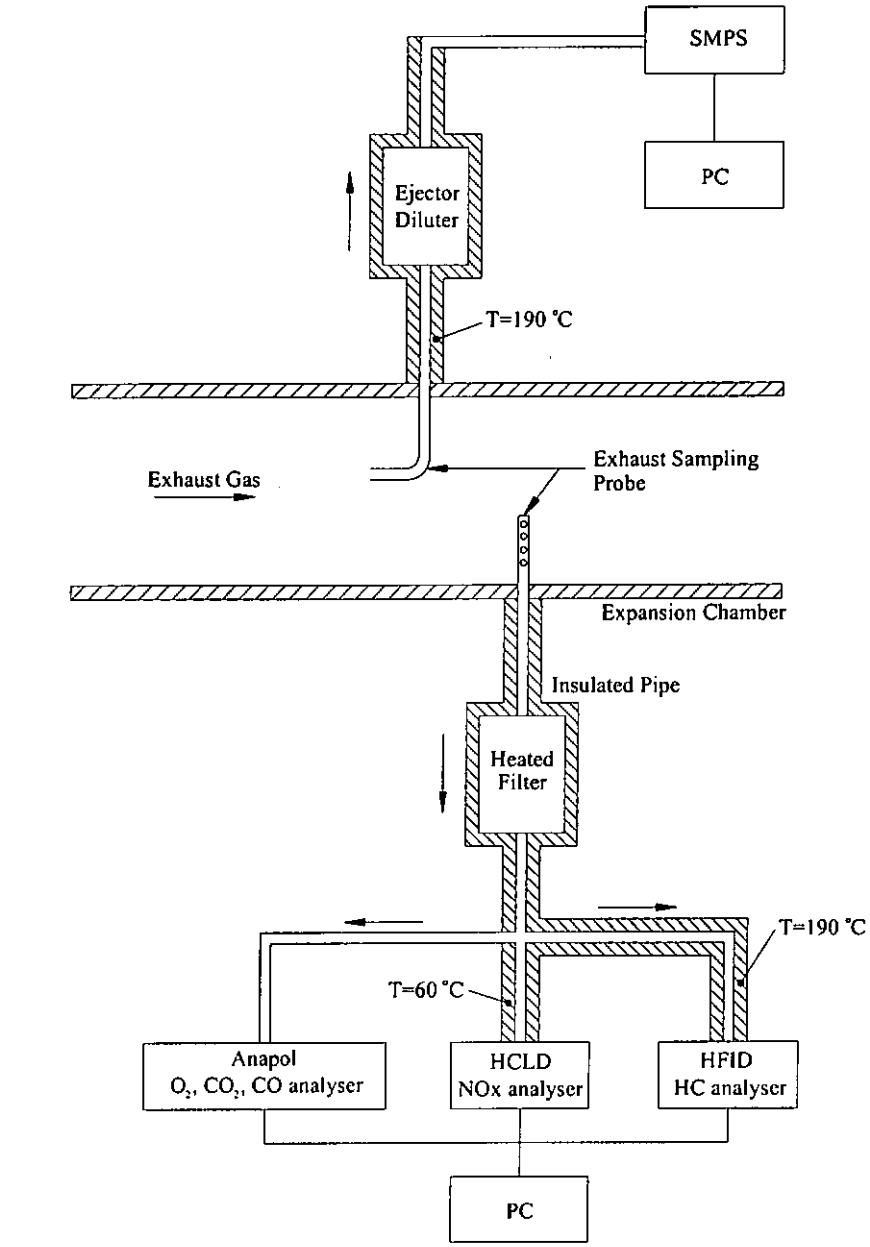

Figure 4.10 Schematic diagram of the diesel exhaust gaseous and particle emissions measurement systems.

After a portion of exhaust gas was transmitted into the expansion chamber, it will expand and flow a certain distance to reach the sampling region. There were two sampling probes located at the downstream of the chamber. For the particle

measurement, a L-shaped stainless steel sampling probe facing the direction of the gas flow was used to collect the exhaust particle sample and then passed to the particle measurement system.

The experimental setup for the exhaust gas measurement basically followed the SAE recommended practice [80]. All the sampling lines were made of stainless steel or Telfon tube for transmitting the sample to the gas analyser. Those materials can withstand the exhaust temperature and will not affect the sample integrity. A stainless steel with multi-hole sample probe was used to extract a representative sample from the engine exhaust system. According to the SAE recommended practice [80], if the total area of the sampling holes does not exceed the cross-sectional area of the probe, the multi-hole sample probe is required to insert 75% of the across of the exhaust pipe. However, the total area of the sampling holes was larger than the cross-sectional area of the probe in present experiment. Thus, the exhaust gas sampling probe only inserted 50% of the across of the exhaust pipe.

In the present study, a heated filter was used and maintained at 190°C to remove the soot in the exhaust sample and also prevent the condensation of the exhaust moisture on the filter elements. After the collected samples passed through the heated filter, they were measured by the gas analysers for determining the

gaseous emission concentrations. The transfer lines for the NOx and HC analysers were insulated and heated in accordance with the recommendation from the manufacturer to avoid the condensation of the exhaust samples on the pipe wall. The temperatures of NOx and HC analysers were kept at 60 C and 190 C, respectively. The results measured from these two instruments were wet basis value. The other gaseous concentrations (i.e. O_2, CO_2 & CO) were detected by using the Anapol gas analyser. Heating and insulation for the transfer line was not required. The results obtained from this Anapol analyser is a dry basis value because there was a water separator to remove the sample moisture. All of these gas analysers were connected to a personal computer (PC) for collecting the experimental data.

4.5 Diesel Oxidation Catalyst (DOC)

It has been proved that a flow-through diesel oxidation catalytic converter installed in a vehicle can efficiently reduce the soluble organic fraction (SOF) and total particulate matter in the exhaust, where the removal efficiency is highly dependent on the composition of the particulate being emitted [85]. In addition, it can also reduce the concentration of carbon monoxide (CO) and gaseous hydrocarbons (HC) emissions. Due to these characteristics, diesel oxidation catalyst has become a leading retrofit control strategy in both the on-road and non-road sectors throughout

the world. The name has been given as an oxidation catalyst because it transforms exhaust pollutants into harmless gases by means of oxidation. In the diesel vehicles, the catalyst oxidises CO and HC to become CO_2 and H_2O, and the liquid hydrocarbons adsorbed in the carbon particles. The liquid hydrocarbons are referred to as soluble organic fraction (SOF) and made up part of the total particulate matters. A simple diagram, as shown in Figure 4.11, is used to demonstrate the operation principle of the DOC. Oxidation catalyst is a flow-through ceramic or metallic monolith, with a surface coated with the precious metal. The platinum (Pt), palladium (Pd), rhodium (Rh) and zeolite are generally used as coating materials on the catalyst. The monolith is supported on a stainless steel canister and has two flanges on both ends of the support which is convenient for installation.

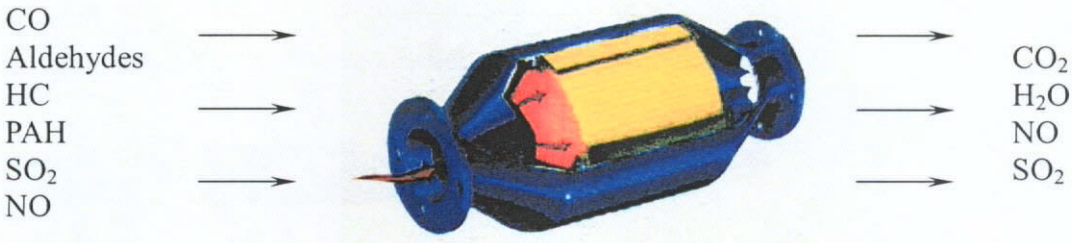

Flow through monolith
with catalytic coating

$CO+1/2O_2 \longrightarrow CO_2$
$HC+O_2 \longrightarrow CO_2+H_2O$
$PAH+O_2 \longrightarrow CO_2+H_2O$
$Aldehydes+O_2 \longrightarrow CO_2+H_2O$

Figure 4.11 The operation principle of diesel oxidation catalyst.

In the present study, two high reliable and representative diesel oxidation catalysts were used to carry out the experiment in order to prevent obtaining a bias result which cannot represent the general characteristic of the DOC. The coating material for DOC-Type A was zeolite-based, whereas the DOC-Type B was platinum-based. Two catalysts were tested independently under similar testing procedures. Figure 4.12a and b show the zeolite-based and platinum-based oxidation catalysts which were used to perform the experiment.

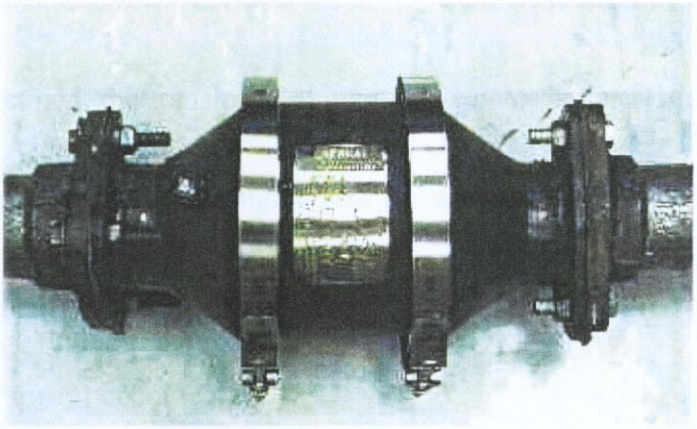

Figure 4.12a A zeolite-based diesel oxidation catalyst (DOC-Type A).

Figure 4.12b A platinum-based diesel oxidation catalyst (DOC-Type B).

4.6 Experimental Methodology

4.6.1 Testing diesel engine load modes

A diesel engine dynamometer test bed was used to perform the experimental investigation. A European driving cycle (ECE R49 13 mode cycle) was used for the testing. It consists of thirteen stabilised driving modes but only the engine modes at maximum torque speed will be used to perform the present study. The details of the testing conditions are shown in Table 4.1. Due to the limitation of the diesel engine dynamometer test bed, the transient driving cycle cannot be performed in the present study. In each measurement, the engine also allowed operation of 30 minutes in each engine condition to ensure all the engine parameters such as exhaust gas temperature, engine load and speed) become steady.

Engine load mode	Engine speed (rpm) at maximum torque	Full engine load (%)
1	2200	10
2	2200	50
3	2200	100

Table 4.1 Diesel engine load modes.

4.6.2 Measurement procedures

In the present study, the particle emission characteristics between the two particle measurement systems will be conducted first. The aim of this experiment is to determine the most reliable and accurate particle measurement system for the subsequent experiment. The engine speed was operated and stabilised at each condition for 30 minutes until the temperature of the exhaust gases and dilution air, as well as the flow meter reading, had reached a stable condition. This operation time is important for obtaining a stable result. An exhaust particle sampling measurement was then conducted to determine the particle number concentration under the selected engine mode. The time set for each exhaust particle sample with the SMPS was 120 seconds upscan and 30 seconds downscan which was suggested by manufacturer. Before collecting the next set of exhaust particle sample, it would take at least 3-5 minutes for the SMPS rod voltage to get back to zero in order to prevent interference from the previous sample that might bias the particle number concentrations. After that, three experiments were performed to characterise the DOC performance after it was installed on an engine exhaust outlet. The first part of the experiment was to examine the effectiveness of DOC in reducing the exhaust emissions. A DOC was installed on the exhaust tailpipe of the engine and paralleled with the dummy pipe. The layout of the DOC installation is presented in Figure 4.9.

At the beginning of this experiment, the control valves were adjusted to allow the exhaust gas passing through the dummy pipe only. The engine was run at the engine load mode 1 condition for ten minutes. After the ten minutes, all the engine parameters (i.e. exhaust temperature, engine load and speed) were checked to ensure those engine parameters become stable. Then, the exhaust particle and gaseous measurement were carried out to determine the baseline emission value of the diesel engine in that engine condition. Before the measurement, all the gas analysers would conduct zero and span gas calibration to eliminate measurement error. After completing the gaseous and particle emissions measurement, the control valve was adjusted again to direct the exhaust gas to pass through the DOC only. Another 30 minutes stabilised time was required for waiting a steady state engine condition and then the measurement was performed again after all the engine parameters become steady. The exhaust gaseous and particle emissions at the outlet of the DOC in that engine condition were determined. The remaining engine conditions test were conducted in the same manner. Through these experiments, the exhaust gaseous and particle emissions characteristic of a diesel engine equipped with/without DOC for different engine load conditions can be then determined.

The second part of experiment was the study of the ageing effect of DOC on the critical particle emission. The DOC was fixed on the engine test bed and the engine was run to a certain period. The particle emission measurement was carried out in every 10 hours engine operation. In the present study, only the first 40 hours particle emission from the DOC is presented because it is adequate to demonstrate the characteristic of DOC against the operation time.

The third part of experiment was to study the fast engine acceleration response of DOC in the exhaust gaseous and particle emissions. The engine was initially run at idle condition. The gaseous and particle emissions measurements began to measure the exhaust emission concentration. The engine speed and load were then adjusted in accordance with the procedures in Table 4.2. The gaseous and particle emission measurements were performed continuously to measure the baseline exhaust emissions throughout the experiment. After the baseline emission concentration was obtained, a used DOC was fixed on the tailpipe of the diesel engine dynamometer test bed. The engine ran the same testing procedures again under the situation with the DOC installed. The concentration of gaseous and particle emissions were also measured to determine the change of the exhaust emissions from the engine after installing the DOC. The results were used to study the performance of DOC against the engine speed and load.

Engine condition	Engine speed (rpm)	Engine load (%)
Idle	850	0
Idle → full load	850 → 2200	0 → 100
Full load	2200	100
Full load → idle	2200 → 850	100 → 0
Idle	850	0

Table 4.2 Fast engine acceleration testing procedures.

4.7 Experimental Data Processing

The experimental data of gaseous emission concentration obtained from those gas analysers were presented in volume basis (i.e. % or ppm). This kind of value is incomparable with the current emission regulation. It is necessary to convert the volume-based data to mass emission data (i.e. g/s). The details of data conversion are illustrated in the following section. For the particle results, the common method for presenting the particle concentration is used the particle number and size distribution. In the present study, the particle number and size distribution and concentration can be obtained from the TSI particle sizer. Hence, no data conversion is required for the experimental particle data.

4.7.1 Gaseous emissions

Humidity calculation

The properties of ambient air temperature and humidity slightly affect the exhaust gaseous emission concentration. It is necessary to convert the experimental data to compensate these effects. The dry-bulb temperature and the relative humidity of the room air were recorded during the experiment. The recorded results were used to ascertain the water-vapour volume concentration (Y) of the engine intake air. The water-vapour volume concentration was then used to calculate the wet-dry correction factor. The following calculations are based on the U.S. Environmental Protection Agency standard [86].

The saturation vapour pressure (P_{DB}) of water at the dry-bulb temperature is defined as follows:

$$P_{DB} = \exp\left[B \times (\ln T_{DB}) + \sum_{i=0}^{9} F_i T_{DB}^{i-2} \right] \quad (4.1)$$

where P_{DB} = Pressure in dry-bulb temperature (Pa)

T_{DB} = Dry-bulb temperature (K)

$B = -12.150799$

$F_0 = -8.49922 \times 10^3$

$F_1 = -7.4231865 \times 10^{3}$

$F_2 = 96.1635147$

$F_3 = 2.4917646 \times 10^{-2}$

$F_4 = -1.3160119 \times 10^{-5}$

$F_5 = -1.1460454 \times 10^{-8}$

$F_6 = 2.1701289 \times 10^{-11}$

$F_7 = -3.610258 \times 10^{-15}$

$F_8 = 3.8504519 \times 10^{-18}$

$F_9 = -1.4317 \times 10^{-21}$

The percent of relative humidity (RH) is defined by Equation 4.2. The value of RH has been recorded during the experiment so the partial vapour pressure (P_v) can be obtained by the following equation;

$$RH = \frac{P_v}{P_{DB}} \times 100 \qquad (4.2)$$

The partial vapour pressure was used to calculate the specific humidity on a dry basis of the intake air (H) and which is defined as follows:

$$H = \frac{(K)(P_v)}{BARO - P_v} \qquad (4.3)$$

where BARO = barometric pressure (Pa)

K = 0.6220 g H_2O/g dry air

Once the specific humidity (H) is found, the water vapour volume concentration on a dry basis of the engine intake air (Y) can be determined by using the Equation 4.4.

$$Y = \frac{(H)(M_{air})}{(M_{H_2O})} - \frac{P_v}{BARO - P_v} \tag{4.4}$$

where M_{air} = Molecular weight of air = 28.96 kg/kmol

M_{H_2O} = Molecular weight of water vapour = 18.02 kg/kmol

Emission calculation

After the water vapour volume concentration (Y) is determined, the wet to dry correction factor can be found and the mass emissions of the pollutants can also be calculated. The wet to dry correction factor, K_w is defined as follows [86]:

$$Kw = \frac{1}{1 + \left[\frac{\alpha\left(\frac{DCO_2}{10^2} + \frac{DCO}{10^6} + \frac{2Y}{\phi}\right)\left(\frac{DCO_2}{10^2} + \frac{DCO}{10^6} + \frac{WHC}{10^6}\right)\left(1 + \frac{\alpha}{4}\right)}{2\left(1 + \frac{\frac{DCO}{10^6}}{\left(\frac{DCO_2}{10^2}\right)K}\right)} \right]} \tag{4.5}$$

where α = atomic hydrogen/carbon ratio of the fuel = 1.805

ϕ = dry fuel-air ratio (measured)/fuel air ratio (stoichiometric)

DCO = CO volume concentration in exhaust gas, ppm (dry basis)

DCO_2 = CO_2 volume concentration in exhaust gas, % (dry basis)

WHC = HC volume concentration in exhaust gas, ppm (wet basis)

K = water-gas equilibrium constant = 3.5

Y = H_2O volume concentration of intake air (g H_2O/g dry air)

The wet basis measurement (i.e. HC and NOx emission concentration) can be converted into a dry basis as follows:

$$\text{Dry concentration} = \frac{1}{K_W} \times \text{wet concentration} \tag{4.6}$$

The stoichiometric fuel-air ratio (f/a) can be calculated as follows:

$$(f/a)_{stoich} = \frac{M_C + \alpha M_H}{138.18(1+\alpha/4)} \tag{4.7}$$

where M_C = Molecular weight of carbon, 12.01 kg/kmol

M_H = Molecular weight of hydrogen, 1 kg/kmol

The dry fuel air ratio(measured), f/a is defined as follows:

$$(f/a)_m = \frac{4.77(1+\alpha/4)(f/a)_{stoich}}{\frac{1}{\overline{X}} - \left(\frac{DCO}{2\overline{X}(10)^6}\right) - \left(\frac{DHC}{\overline{X}(10)^6}\right) + \frac{\alpha}{4}\left(1 - \frac{DCO}{\overline{X}(10)^6}\right) - \frac{0.75\alpha}{\frac{K}{\frac{DCO}{\overline{X}(10)^6}} + \left(\frac{(1-K)}{1-\frac{DHC}{\overline{X}(10)^6}}\right)}} \quad (4.8)$$

where $\overline{X} = DCO_2/10^2 + DCO/10^6 + DHC/10^6$

DHC = HC volume concentration in exhaust gas, ppm (dry basis)

For NOx emission, the dry concentration result is multiplied by a humidity correction factor to obtain a dry and humidity corrected NOx concentration. The calculation is shown as follows:

$$K_{NOx} = \frac{1}{1 + A(G-75) + B(T-85)} \quad (4.9)$$

where $A = 0.044(f/a)_m - 0.0038$

$B = -0.166(f/a)_m + 0.0053$

G = humidity of the inlet air in grams of water per pound of dry air

= (453.559/0.0648)H

T = Temperature of inlet air, °F

$$DKNO = NOx\ (dry) \times K_w \tag{4.10}$$

where DKNO = NO volume concentration in exhaust gas, in ppm (dry and humidity corrected)

K_w = wet to dry correction factor

The mass emissions of each species in grams per hour for each mode can be calculated as follows:

$$HC\ g/hr = W_{HC} = \frac{(DHC/10^4)W_f}{(DCO/10^4) + DCO_2 + (DHC/10^4)} \tag{4.11}$$

$$CO\ g/hr = W_{CO} = \frac{M_{CO}(DCO/10^4)W_f}{(M_C + \alpha M_H)[(DCO/10^4) + DCO_2 + (DHC/10^4)]} \tag{4.12}$$

$$NOx\ g/hr = W_{NOx} = \frac{M_{NO_2}(DKNO/10^4)W_f}{(M_C + \alpha M_H)[(DCO/10^4) + DCO_2 + (DHC/10^4)]} \tag{4.13}$$

where M_C = Molecular weight of carbon, 12.01 kg/kmol

M_H = Molecular weight of hydrogen, 1 kg/kmol

M_{NO_2} = Molecular weight of nitrogen dioxide, 46 kg/kmol

W_f = mass flow rate of fuel used in the engine, g/hr

4.7.2 Particle emission

The data of particle emissions are presented using the particle number concentration for specific particle diameter range (i.e. number of particles/centimeter cube) as shown in Figure 4.13. The abscissa represents the particle diameter, whereas the ordinate means the particle concentration. The unit of the ordinate uses $dN/d\ logD_p$, which is a normalised concentration result with the particle size channel. These data format can be used to compare the data collected by other researchers who used the other particle size channels.

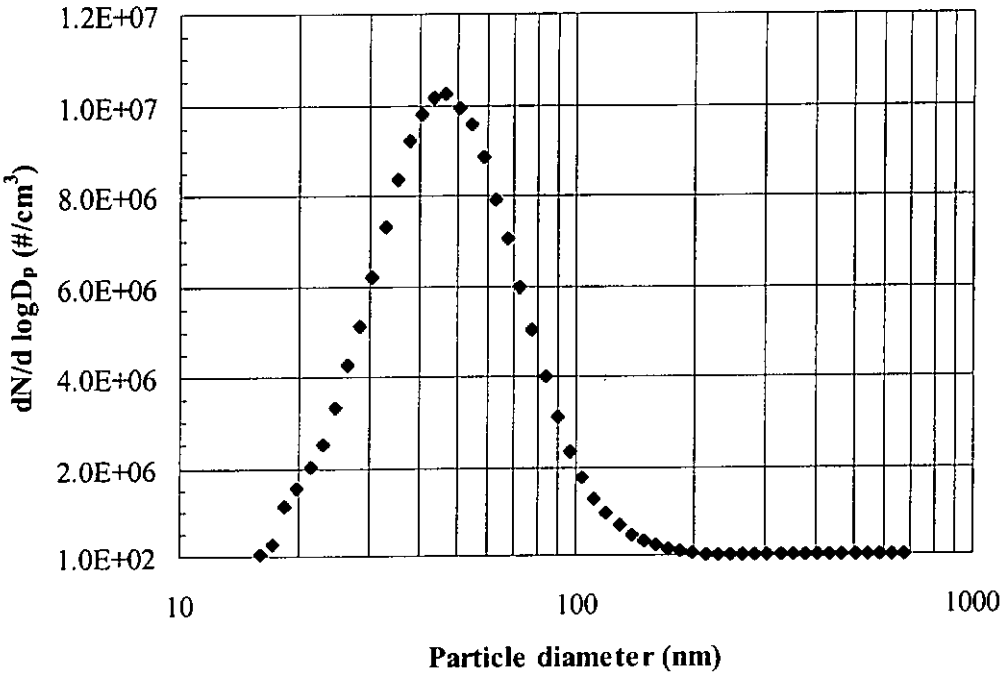

Figure 4.13 Presentation method of the particle concentration.

4.7.3 Uncertainty analysis of the gaseous and particle emissions measurement systems

Particle emission sampling measurement system

In the present study, the particle emission result of DOC investigation is mainly obtained from the scanning mobility particle sizer (SMPS) and the ejector diluter. The uncertainty of these two instruments would contribute to the total uncertainty of the particle measurement system. Consequently, tests for repeatability of particle size and concentration measurement are conducted in order to determine the sources of measurement uncertainty in various sub-systems. Normally, the SMPS and the ejector diluter are used together to measure the exhaust particle concentration, but these two components are isolated to test for the individual uncertainties. Kayes et al. [87] suggested that the SMPS initially sampled particles concentration emitted by a steady particle generation to determine the repeatability of the SMPS alone. The generator was then connected to the diluter, with the SMPS measuring the diluted particle concentration in order to evaluate the uncertainty of the diluter/SMPS combined. Finally, the data of SMPS alone and diluter/SMPS were compared to obtain the actual uncertainty of the particle measurement system. They suggested the uncertainty of the particle measurement system should be within 20%.

The total uncertainty of an instrument or system includes both the random error and the bias error. Random error (tS_x) is observed in repeated measurements which do not agree exactly because of numerous error sources. The random error can be calculated through the following equations [88]:

$$\overline{X} = \frac{1}{N}\sum_{k=1}^{N} X_k \tag{4.14}$$

$$S = \left[\frac{\sum_{k=1}^{N}(X_k - \overline{X})^2}{N-1}\right]^{1/2} \tag{4.15}$$

$$S_x = \frac{S}{\sqrt{N}} \tag{4.16}$$

where N is the number of measurements made and $\overline{X}$ is the average value of the measurements X_k.

Bias error (B_e) is the systematic error which is constant for the duration of the test of a given sample, each measurement has the same bias. The total uncertainty for 95% confidence can be defined by the following equation:

$$U_T = \sqrt{(B_e)^2 + (tS_x)^2} \tag{4.17}$$

where t is the 95th percentile point for the two-tailed student t distribution and can be obtained from the two-tailed student, t table.

Therefore, in order to determine the total uncertainty of the particle measurement system, an analysis of the random, tS_x and bias error, B_e was conducted.

Quantification of random error of particle emission measurement system

A compression ignition engine (i.e. diesel engine) was used as the steady particle generator. It is because Graskow et al. [89] stated that diesel engines have steady and consistent emissions, thus allowing a steady stream of particles with which to isolate variability in SMPS measurements. In addition, isolation of the SMPS measurement requires the use of an exhaust gas with less humidity to avoid water condensation in the passageways within the SMPS. The diesel exhaust has less humidity than the spark exhaust so diesel engine was used for determining the uncertainty of the instruments. The repeatability of the SMPS was determined by extracting samples from an undiluted exhaust plume of the diesel engine which was operated in a steady condition for one hour. This operation time is essential for the coolant and oil temperatures to reach a steady value. The results of ten consecutive sets of particle size distribution measurement are shown in Figure 4.14.

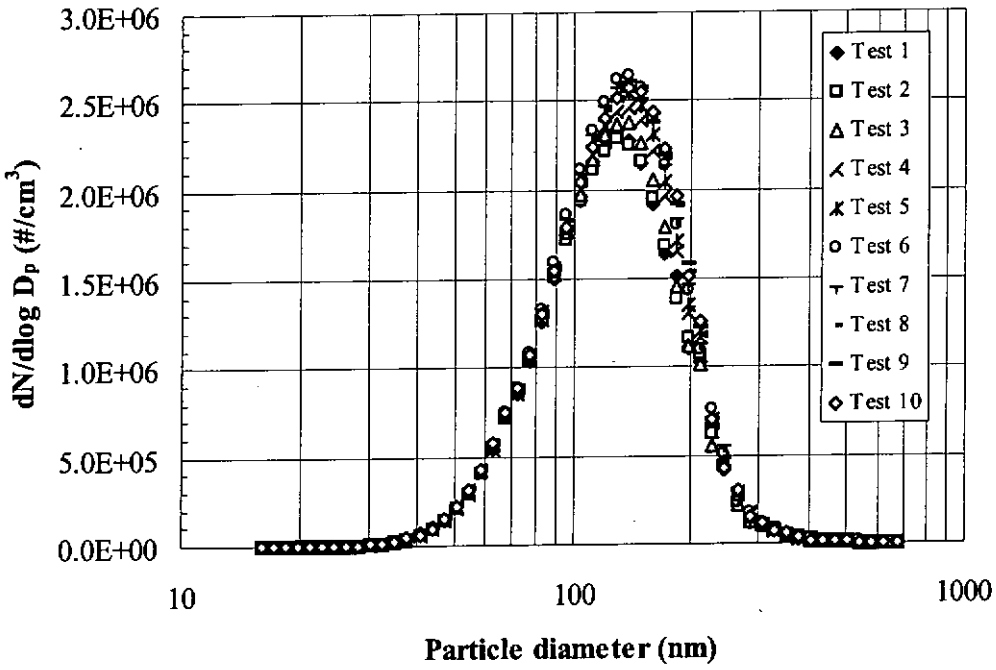

Figure 4.14 Particle size distribution measured from undiluted diesel exhaust gas in ten consecutive tests.

According to the ASME standard [88], the repeatability of the SMPS system is also equal to the random error of the system. The calculated average random error from each channel was only 5% error of the mean concentration, while the maximum random error was 10% deviated from the mean values, except at the very smaller particle sizes around 10 to 20 nm. The random error of the very smaller particles has a maximum deviation 45% from mean value. Although the particle concentration for this particle range has as much as a 45% random error, the small size range only has a small contribution to the total or integrated number concentrations. After estimating the measurement uncertainty due to the SMPS alone, the following step

can determine the uncertainty due to the combination system of ejector diluter and SMPS. The particle source from the diesel engine was run at the same condition as prior.

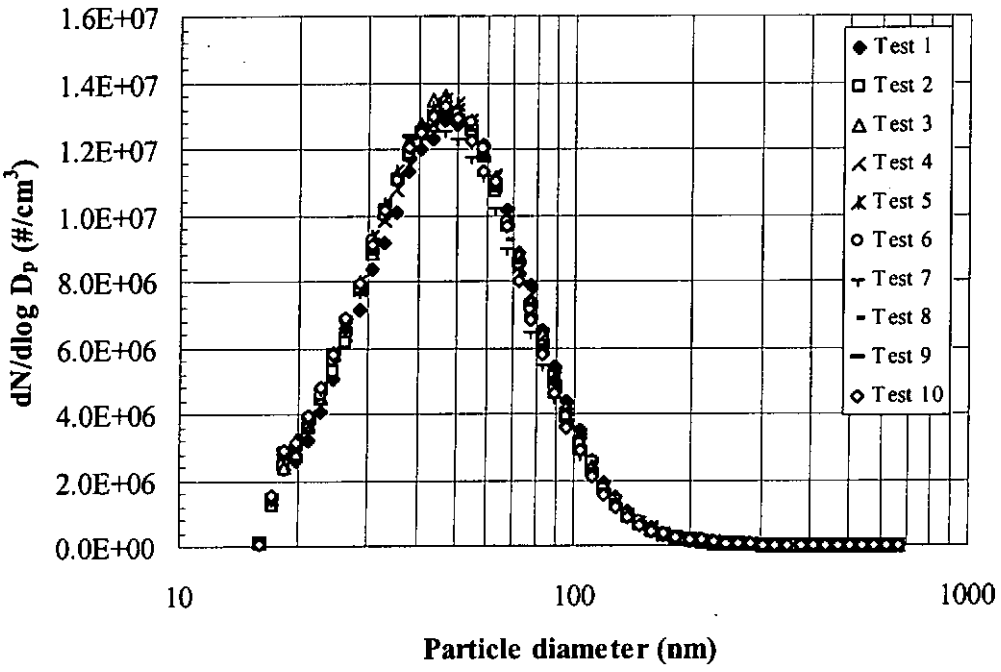

Figure 4.15 Particle size distribution measured from diluted diesel exhaust gas in ten consecutive tests.

Figure 4.15 presents the results of the ten consecutive sets of particle size distribution measured from diluted exhaust. The calculated average random error is 4% and the maximum random error is 9% from the mean concentration. The results are similar to the random error found from the SMPS alone. Since, the random error from both measurement system setups (i.e. SMPS alone, ejector diluter & SMPS) are approximately equal, the random error by virtue of the dilution process was found to

be negligible. It can be concluded that the particle measurement system is dominated by the random error of the SMPS alone. The random error of the particle measurement system is within 10%.

Determination of bias error of particle emission measurement system

Experiments were performed in order to determine the zero-offset error (i.e. bias error) of the SMPS and the combined ejector diluter and SMPS measurement systems. The zero-offset error of the SMPS was determined by providing a free particle gas stream from the ambient air to the SMPS inlet. The schematic diagram of this arrangement is shown in Figure 4.16. Two fine particle filters were installed in the SMPS inlet to remove most of the large and fine particles in the ambient air. Although, these two filters are not a high efficiency performance air (HEPA) filter, they can still remove most of the particles from the room ambient air. Normally, a HEPA filter has a 99.9% removal efficiency on particle concentration. Tests were performed to investigate the efficiency of these two filters in removing the ambient air particles. The results were presented in the Figure 4.17, which show that these filters can have 99.3% average removal efficiency from each particle size channel. So, it is believed that these two filters can have similar performance as the HEPA filter in this situation. Figure 4.18 shows the results of ten consecutive sets of

particle concentration of the filtered air. The result shows the maximum particle concentration of the filtered air, which is only 100 particle /cm^3. This concentration is only 0.01% of the diluted engine-out emissions concentration (i.e. over 1×10^6 particle/cm^3) and the influence of this offset is not significant. So, the zero-offset of the SMPS alone can be neglected.

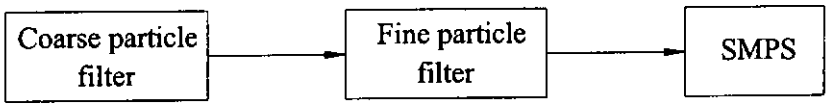

Figure 4.16 Schematic diagram of the filter arrangement to the SMPS.

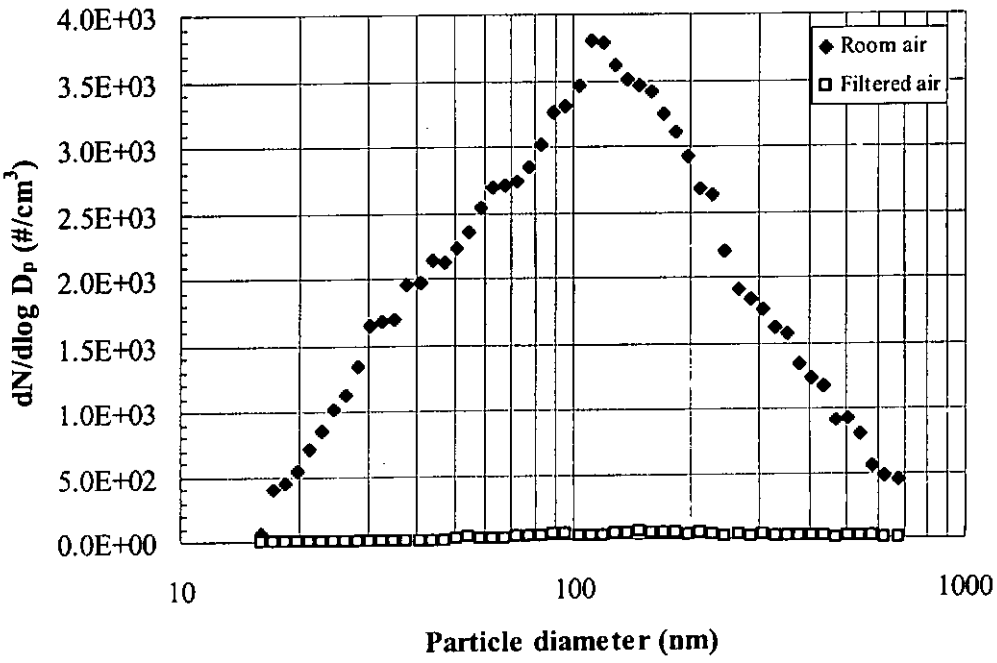

Figure 4.17 Performance of the coarse and fine particle filters in the removal of ambient air particle concentration.

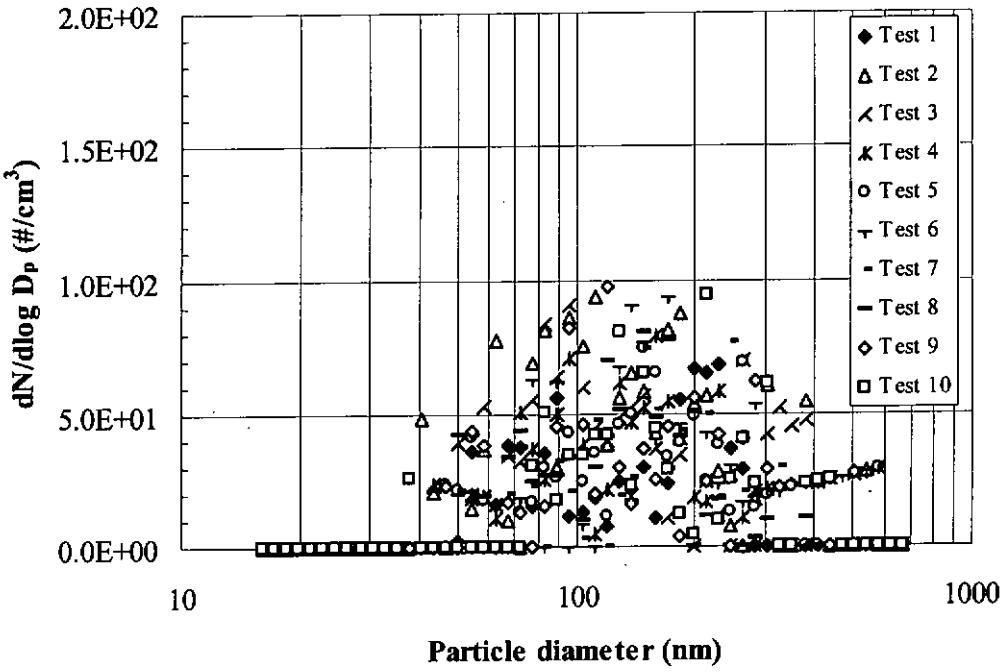

Figure 4.18 Results of ten consecutive sets of particle concentration of the filtered air measured from SMPS alone.

The zero-offset of the combined ejector diluter & SMPS system was conducted by installing the two fine particle filters to the inlet of the diluter. The schematic diagram of this arrangement is presented in Figure 4.19. Ten sets of data were also obtained and the results are shown in Figure 4.20. The results show that when the engine is not running but the filtered air is being drawn through the diluter, the air has a measured maximum particle concentration of 100 particle/cm^3, which is the same as the value found from the SMPS alone. This value can also be neglected as compared with the diluted exhaust particle concentration. So, the zero-offset error for the combined ejector diluter & SMPS system is negligible. It also states that the dilution process has no bias on the zero-offset error of the result of the SMPS alone.

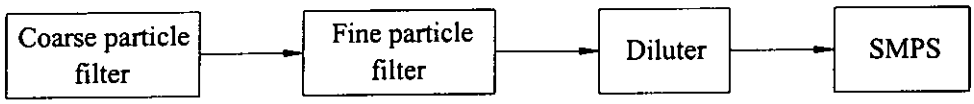

Figure 4.19 Schematic diagram of the filter arrangement with the combined ejector diluter and SMPS measurement systems.

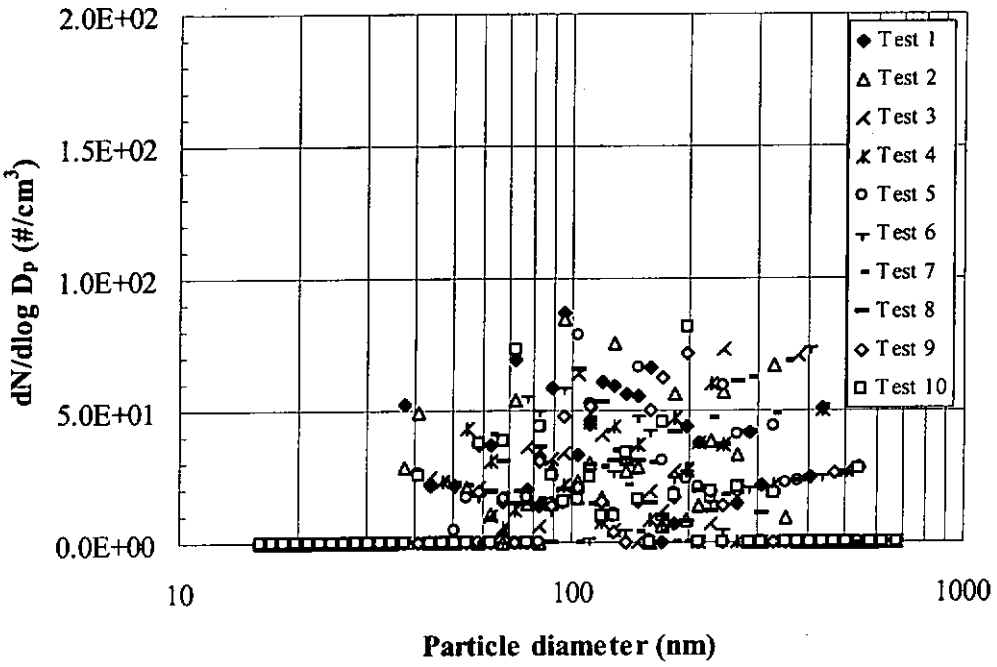

Figure 4.20 Results of ten consecutive sets of particle concentration of the filtered ambient air measured from the combined ejector diluter and SMPS measurement systems.

The other sources of the bias error in the particle measurement system can occur in the SMPS diagnostics as a result of either particle obtaining multiple charges in the Kr-85 bipolar charger or optical interference between multiple particle in the CPC. However, the SMPS software can predict and correct both of these sources of error [90]. A bias error may occur in the measurement of particle sizes.

If the flowrates of the SMPS sheath air and aerosol inlet deviate from the values input to the software, then the software will mistakenly calculate the particle mobility for particle in each channel of SMPS measurement. This problem would cause a bias in the measured particle sizes. However, these flowrates are all specified, set and calibrated to be within 0.5% of their nominal values.

Determination of the total uncertainty of particle measurement system

The total uncertainty is defined as the square-root of the sum of each error squared in Equation 4.17. The error includes the random error and the bias error of the instrument. From the previous analysis, the maximum random error and the bias error are 10% and less than 1%, respectively. Thus, the total uncertainty of the unique particle measurement system is within 10%.

Uncertainty analysis of the gaseous emission measurement system

For gaseous emission measurements, all of the instruments (i.e. Anapol, HC and NOx gas analyser) were calibrated before any measurement, in order to prevent the zero and span drift. However, these gaseous instruments still have less than 1% deviation in accordance with the user manual. This 1% variation is the bias error for those instruments. On the other hand, the random errors for these gaseous instruments were also determined by connecting the instruments to the diesel engine

dynamometer test bed. The engine was operated in a steady state condition. Then, ten consecutive sets of gaseous emissions data were measured from these analysers. An average value for each analyser was then calculated. It was found that the random errors for the HC and NOx gas analyser were only 0.5%, while the maximum random error was found from the Anapol gas analyser and which was about 1% deviated from the mean values. Hence, the total uncertainty for the gaseous measurement can be determined by using the Equation 4.17. The total uncertainty of the HC and NOx gas analysers are within 1.1% and the Anapol gas analyser (i.e. CO and CO_2) is within 1.4%, respectively.

Chapter 5 Particle Deposition and Chemical Kinetic Analysis of the Diesel Oxidation Catalyst

5.1 Introduction

This chapter discusses the study of the characteristics of the particle deposition efficiency on the catalyst surface against the particle diameter. For a diesel oxidation catalyst, it will alter the particle emission by the effect of deposition and oxidation. In addition, the DOC is able to reduce gaseous emissions from diesel engine exhaust plume. The reason for gaseous emission reduction can be attributed to the enhancement of DOC on the rate of the chemical reaction between the gaseous pollutants (i.e. CO and HC) and oxygen molecules. A chemical kinetic analysis was performed to study the characteristics of DOC on exhaust gaseous emissions under different exhaust temperatures. The DOC is assumed to be a fresh catalyst during the particle deposition and chemical kinetic analysis in the present study.

5.2 Deposition Analysis of Diesel Exhaust Particle Emission

As the exhaust gas is passing through the catalyst substrate, a certain amount of particles may be deposited on the channel surface. The deposition mechanisms include the gravitational settling, Brownian diffusion, thermophoresis, electrostatic attraction and inertial impaction [91-92]. For each deposition process, the deposition

efficiency can be calculated by applying the aerosol theory. A Pt-based catalyst (DOC-Type B) was used for performing the present study. The converter geometry of DOC is shown in Figure 5.1.

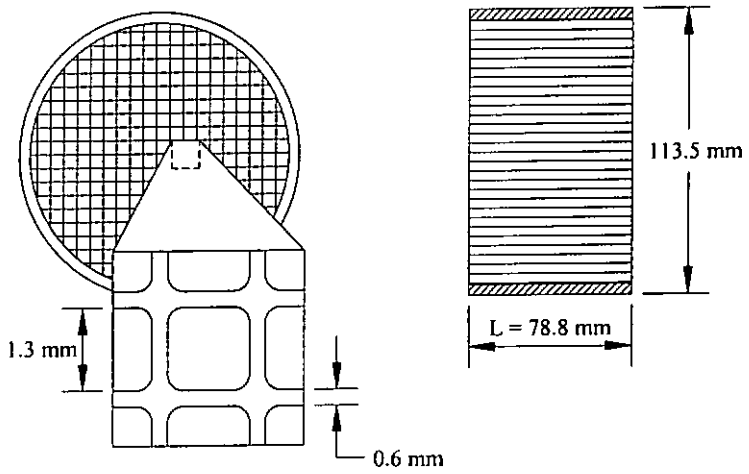

Figure 5.1 The substrate geometry of diesel oxidation catalyst.

The cell density is 64 per cm^2, and the squared channel is 1.3 mm per side. The cell wall thickness is 0.6 mm. The cylindrical monolith is 113.5 mm in diameter and 78.8 mm long. The total number of channels in the catalyst is approximately 6475. An assumption for calculating the deposition efficiency is that the exhaust flow is evenly distributed across all the cells in the monolith. In actuality, the velocity in the center of the cell is higher than the peripheral velocity of the cell. The numerical analyses of Weltens et al. [93] and Barris [94], supported by the experimental findings indicated that the velocity along the centerline of the monolith can be elevated by a factor 2 to 2.25 relative to the average flow. However, it is difficult to

determine the flow distribution across the cell. So, in order to simplify the calculation, this assumption is widely used.

The Reynolds number, Re, for a single channel within the monolith is calculated by using the above values as follows:

$$Re = \frac{\rho_e U D_h}{\mu} \tag{5.1}$$

where ρ_e is the exhaust gas density and assumed to be 0.88 to 0.67 kg/m^3 at 125 to 250°C; U is the average free stream velocity inside the channel, m/s; D_h is the hydraulic diameter of the channel, m; and μ is viscosity and assumed as 2.27×10^{-5} to 2.78×10^{-5} Pa·s at 125 to 250°C. The velocity within each channel and corresponding Re is assumed to represent an average for the entire converter. Based upon this simplified analysis, the converter operates well within the laminar flow regime at all designated testing conditions, with Re < 100.

5.2.1 Gravitational settling

For the exhaust gas flowing through the catalyst channel, the exhaust particles may settle on the substrate surface due to effect of gravity. The efficiency for this deposition is dependent on the particle size and the flow condition. The flow inside the catalyst channels is a laminar flow throughout the testing conditions. For laminar flow in a horizontal and rectangular channel, the particle deposition

efficiency due to gravitational settling is readily derived as follows:

$$E_g = \frac{V_s L}{2Uh} \tag{5.2}$$

where V_s is the terminal settling velocity of the particle, L is the length of the channel and h is the height of the channel. The terminal settling velocity of the particle is defined as follows:

$$V_s = \frac{\rho D_p^2 g}{18\mu} \tag{5.3}$$

where ρ is the particle density, D_p is the particle diameter and μ is the viscosity of exhaust gas.

5.2.2 Brownian diffusion from laminar flow

Under still air condition, aerosol particles will undergo an irregular wiggling motion, which is called Brownian motion. Small particles generally do not follow the streamlines but continuously diffuse away from them. Once the particle is collected on a surface, it would adhere to it due to van der Waal's force. The particle deposition efficiency, E_b, due to Brownian diffusion can be found by using the simple exponential equation:

$$E_b = 1 - \exp(-\frac{h_m A_i}{Q}) \quad (5.4)$$

where A_i is the inner surface area of the catalyst channel, Q is the average volume flow rate through the channel, and h_m is the average mass transfer coefficient for the tube and calculated as follows:

$$h_m = \frac{D_{AB} Sh_L}{D_h} \quad (5.5)$$

where Sh_L is the averaged Sherwood number over the length of the tube and assumed equal to 2.98 [95] and D_{AB} is the diffusion coefficient for a particle of a given size in the exhaust gas [83] and can be defined as follows:

$$D_{AB} = \frac{kTC_c}{3\pi\mu D_p} \quad (5.6)$$

where k is Boltzmann constant, T is the absolute temperature of the exhaust gas, C_c is the Cunningham slip coefficient, $C_c = [1+(2.52\lambda/D_p)]$, λ is the mean free path of particle ranges from 0.03 μm for 10 nm in diameter to 0.016 μm for 1000 nm in diameter. From Eq. 5.6, it obviously shows that the diffusion coefficient varies with the temperature and particle diameter. Thus, it is necessary to substitute the exhaust gas temperature at each engine mode and particle diameter into the equation to determine the specific value.

5.2.3 Thermophoresis deposition

When an aerosol particle subjects to a temperature gradient in the surrounding fluid, it will experience a thermophoretic force. The magnitude of the thermal force depends on the particle properties, as well as the temperature gradient. The thermal force and the aerosol particle motion are always in the direction of decreasing temperature. When a cold surface is proximate to a warm gas, thermophoresis causes particles in the exhaust plume to be deposited onto the surface. This may occur for a hot exhaust gas passing through a relative low temperature catalyst substrate surface. The particle deposition efficiency due to the thermophoresis can be defined as follows:

$$E_t = 1 - \left(\frac{T_o}{T_i}\right)^{PrK_t} \tag{5.7}$$

where Pr is the Prandtl number of the fluid, K_t is the dimensional thermophoretic constant and assumed to be 0.55 according to Talbot [96], and T_i and T_o are the inlet and outlet temperature of the catalyst in K. Although, most of the testing conditions in the present study are steady-state condition, there is still a temperature difference between the inlet and outlet of the catalyst.

5.2.4 Electrostatic attraction

Normally, diesel particles are naturally charged as a result of the combustion process [97]. Up to 85% by mass of the diesel particles are charged, depending upon the engine operating condition [98]. Larger particles, composed primarily of agglomerated carbon, are more likely to be charged than nuclei mode particles which are formed from nucleation of condensable substances as the dilution process. The charged particles can be removed by image force effects in conducting channels and by static charge electric fields in non-conducting channels. The catalyst substrate is composed of ceramic material and will be electrically non-conducting. This property will not be deteriorated by the application of the coating material of the catalyst. Under the circumstance of low relative humidity and high temperature, it is possible that islands of static charge will occur on the surface and the resulting electric fields will influence the particle motion. Liu et al. [99], investigated this effect for three types of non-conducting tubing and found that the static charge electric fields have a value of 200 V/cm. Unfortunately, there is lack of information on the electric fields in oxidation catalyst. So, in order to estimate the electrostatic deposition in the oxidation catalyst, it is assumed that the 200 V/cm field acts across the monolith channel. The particle deposition efficiency due to the electrostatic attraction can be estimated as follows:

$$E_e = \frac{V_e L}{2Uh} \tag{5.8}$$

where V_e is the terminal electrostatic velocity and given by $V_e = Z \times E_f$, where Z is the electrical mobility of the particle and E_f is equal to 200 V/cm as described by Liu et al. [100-101].

5.2.5 Inertial impaction

The inlet surface of the ceramic catalyst provides potential sites for the particle deposition due to impaction. The thickness of the ceramic wall between adjacent channels is 0.6 mm. Diesel particles possess inertia and do not follow the gas streamlines exactly. Some of the particles will impact on the 0.6 mm-wide surface surrounding the entrance to each channel. For estimating the impaction, the Stoke number is commonly used to determine the particle deposition efficiency (E_I) and the equation is shown as follows:

$$St_k = \frac{\rho_e D_p^2 U C_c}{18\mu w} \tag{5.9}$$

where ρ_e is the particle density and assumed as 0.749 to 0.570 g/cm^3 at 125 to 250°C, D_p is the particle diameter, and w is the wall thickness of the channel. Although $E_i = f(St_k)$, there is no simple relationship between the deposition efficiency and

Stokes number. However, Johnson et al. [92] depicted that below the critical Stokes number of 0.25, the impaction deposition does not occur. In the present study, the corresponding Stokes numbers for each particle size for different engine load conditions can be found and compared with this critical value.

5.2.6 Combination of the deposition effects

The total particle deposition efficiency, E_T, which accounts for N different mechanisms of particle deposition, can be calculated for a single particle diameter as follows:

$$E_T = 1 - (1 - E_1)(1 - E_2)(1 - E_3)....(1 - E_N) \quad (5.10)$$

$$= 1 - \prod_{i=15}^{670} (1 - E_d) \quad (5.11)$$

where E_d is the particle deposition efficiency for d particle diameter, d is the particle diameter, nm.

The Equations 5.10 and 5.11 assume that those deposition mechanisms are completely independent from each other but in fact some mechanisms may be completed for the same particles. Nevertheless, these equations are a fair approximation when interpreting the overall deposition efficiency.

5.3 Chemical Kinetic Analysis of Diesel Exhaust Gaseous Emissions

Basically, diesel oxidation catalyst uses a series of oxidation process to reduce the gaseous emissions from exhaust plume. The chemical kinetic analysis can be used to represent the actual reaction in the catalyst. In general, the rate of a chemical reaction is accelerated by an increase in temperature. The oxidation effect is normally represented by the Arrhenius equation [102]:

$$k = A \times \exp(-E_a/RT) \tag{5.12}$$

where k is the rate constant, A is the pre-exponential factor and always has the same units as the corresponding rate constant, E_a is the activation energy or Arrhenius activation energy, which has the same dimensions as RT, R is the universal gas constant, (J/mol K), and T is the temperature (K).

Whatever coating material is used on the catalyst substrate surface, the diesel oxidation catalyst has the same function to enhance to chemical reaction between the gaseous pollutants and oxygen. In this section, only the Pt-based catalyst oxidation reaction of CO and HC are considered. Since the DOC does not have any effect on NOx emission, the current chemical kinetic study neglects the reaction of this species. In real situation, the exhaust gas usually contains many forms of hydrocarbons, C_yH_n.

Hence, it is assumed that the total hydrocarbons inside the DOC will be oxidised into the CO_2 and H_2O, as shown in Eq.5.14. Hence, the chemical reaction of the oxidation process can be expressed by the following equations [103]:

$$CO + \frac{1}{2}O_2 \xrightarrow{RCO} CO_2 \tag{5.13}$$

$$C_yH_n + \left(1 + \frac{n}{4}\right)O_2 \xrightarrow{RHC} yCO_2 + \frac{n}{2}H_2O \tag{5.14}$$

The specific rates R_i for CO and HC can be expressed as functions of concentrations and temperature:

$$RCO = \frac{k_1 \chi_{CO} \chi_{O_2}}{F(x_s, T_s)} \tag{5.15}$$

$$RHC = \frac{k_2 \chi_{HC} \chi_{O_2}}{F(x_s, T_s)} \tag{5.16}$$

where $F(x_s, T_s) = T_s(1 + k_{a1}\chi_{CO} + k_{a2}\chi_{HC})^2(1 + k_{a3}\chi_{CO}^2\chi_{HC}^2)(1 + k_{a4}\chi_{NOx}^{0.7})$

χ_i = concentration of gaseous pollutants, i = CO, HC & NOx

Rate constant (mol s^{-1} m^{-2}),

$k_1 = 6.699 \times 10^9 \exp(-12556/T_s)$

$k_2 = 1.392 \times 10^{11} \exp(-14556/T_s)$

Adsorption constant,

$k_{a1} = 65.5 \exp(961/ T_s)$

$k_{a2} = 2080 \exp(361/ T_s)$

$k_{a3} = 3.98 \exp(11611/ T_s)$

$k_{a4} = 4.79 \exp(-3733/ T_s)$

From the above equations, the reaction rate of RCO and RHC can be obtained by substituting the catalyst substrate temperature (T_s) and measured results of O_2, CO and HC concentrations from each designated engine load condition. The experimental data of these gaseous emissions will be converted to mole fraction before any calculation. The calculated reaction rate can be plotted against the substrate temperature to illustrate the effect of temperature on its performance in Chapter 6.

Chapter 6 Presentation and Discussion of Diesel Exhaust Gaseous and Particle Emissions Investigation Results

6.1 Introduction

The characteristics of particle emission measured from the two developed particle measurement systems were presented in this chapter. The present study uses the particle number and volume distribution to compare the results obtained from these two particle measurement systems to determine the most reliable and stable particle emission measurement system. On the other hand, the characteristics of DOC performance in the gaseous and particle emissions were also reported. The gaseous and particle emissions were measured by using the state-of-the-art gaseous (i.e. SAE standard practice) and particle emission measurement system (i.e. SMPS and ejector dilutor). Both results were presented at the three engine conditions: 10%, 50% and 100% of full engine load at maximum torque speed (i.e. 2200 rpm) and a fast engine acceleration and idle testing condition. The particle deposition and oxidation characteristic of the catalyst were also discussed.

6.2 Comparison of Particle Emission Measurement System

6.2.1 Comparison of particle number and volume distributions between the MDTS and EDS measurement systems

The exhaust particle number and volume distributions based on the MDTS and EDS measurement systems for different engine load conditions are shown in Figures 6.1 to 6.6. For the nuclei mode particles below 50 nm in diameter, the results indicate that the particle number concentrations obtained from the EDS measurement system are higher than those from the MDTS measurement system for the three designated engine load modes as shown in Figures 6.1, 6.3 and 6.5. The discrepancy in particle numbers becomes significant when the engine load increases from 10% to 100% of full engine load. The particle number concentrations obtained from the EDS measurement system are higher than the MDTS measurement system for the three designated engine load modes: 10%, 50% and 100% of full engine load by a factor of about 2, 3 and 25, respectively. Compared with the MDTS measurement system, more than 8 times the particle number concentration is obtained from the EDS measurement system when the engine load is increased from 50% to 100% of full engine load.

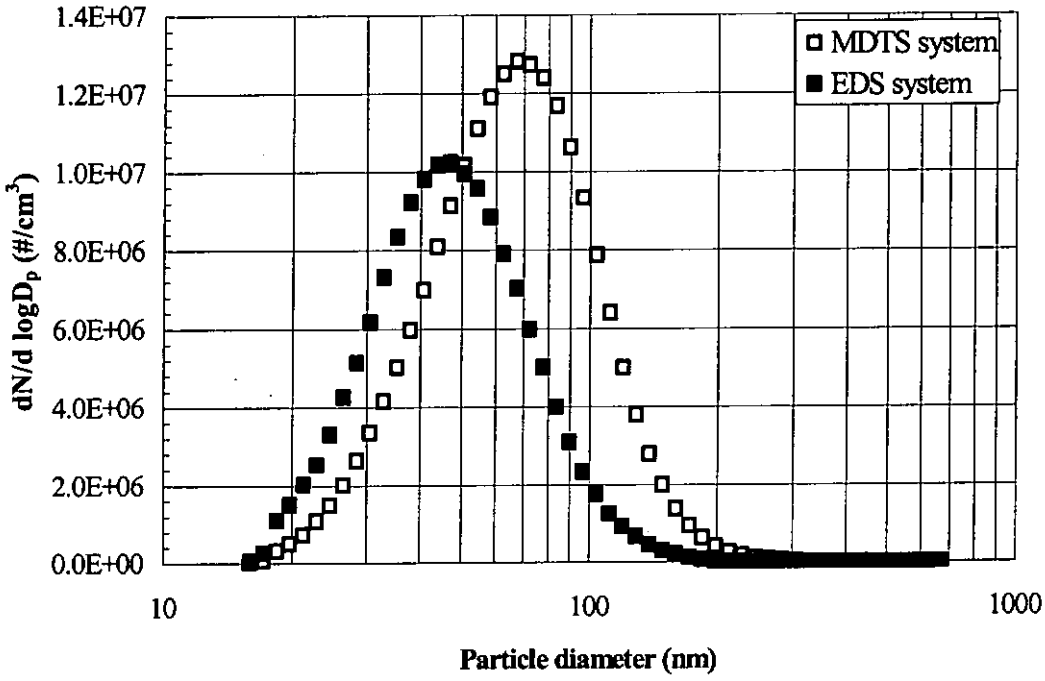

Figure 6.1 Comparison of diesel particle number size distributions from EDS and MDTS measurement systems at 10% of full engine load (Engine mode 1).

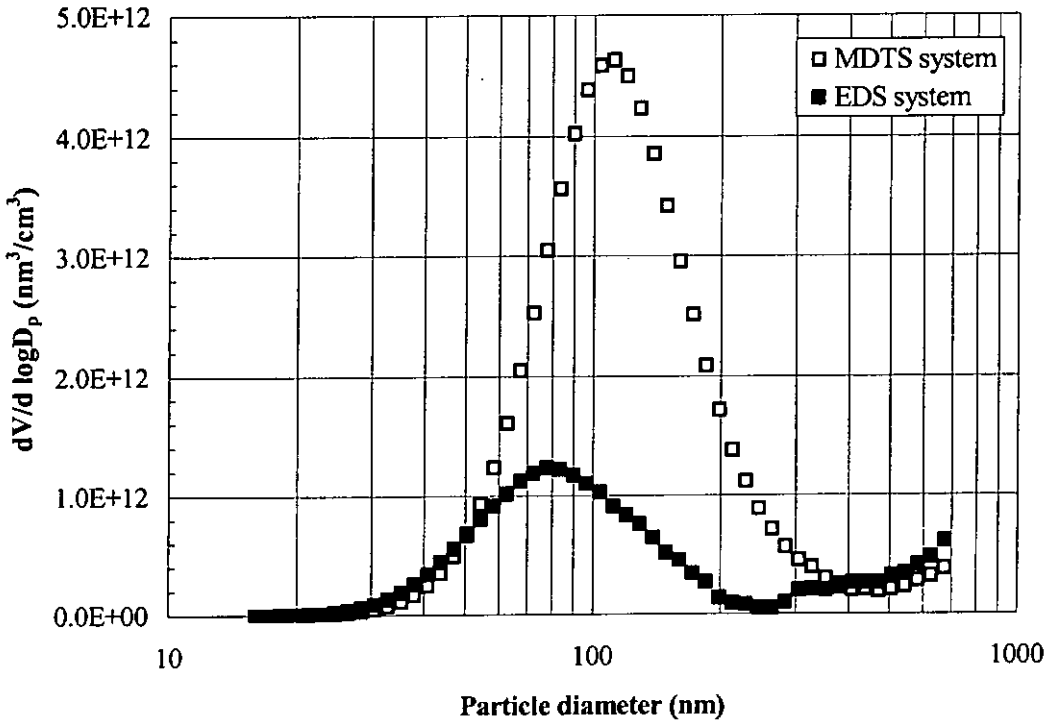

Figure 6.2 Comparison of diesel particle volume distributions from EDS and MDTS measurement systems at 10% of full engine load (Engine mode 1).

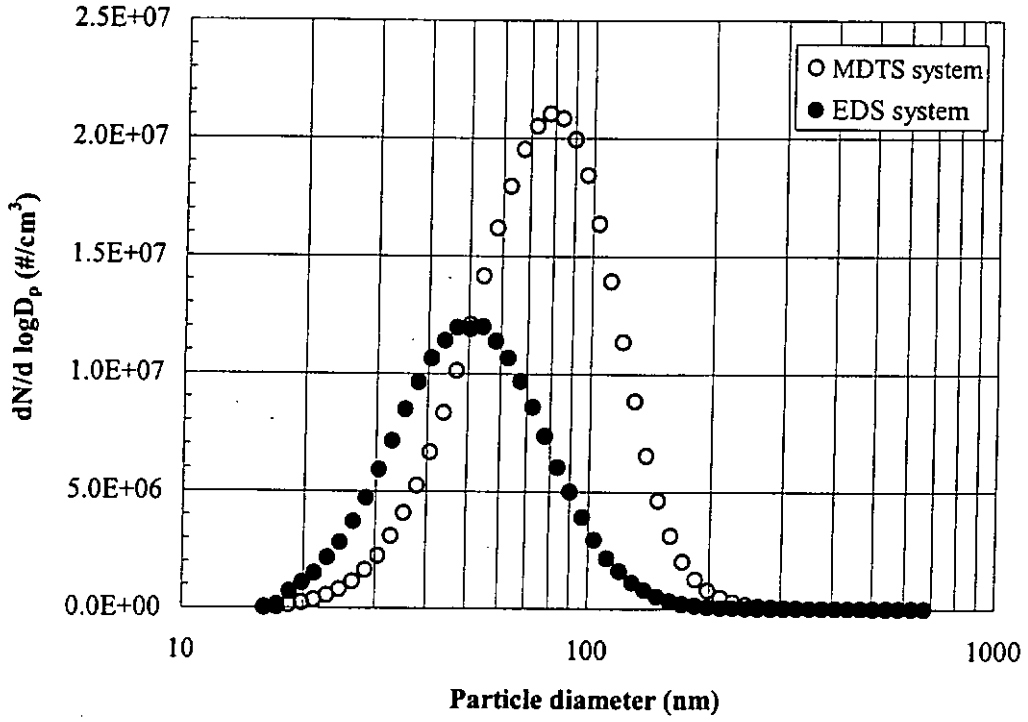

Figure 6.3 Comparison of diesel particle number size distributions from EDS and MDTS measurement systems at 50% of full engine load (Engine mode2).

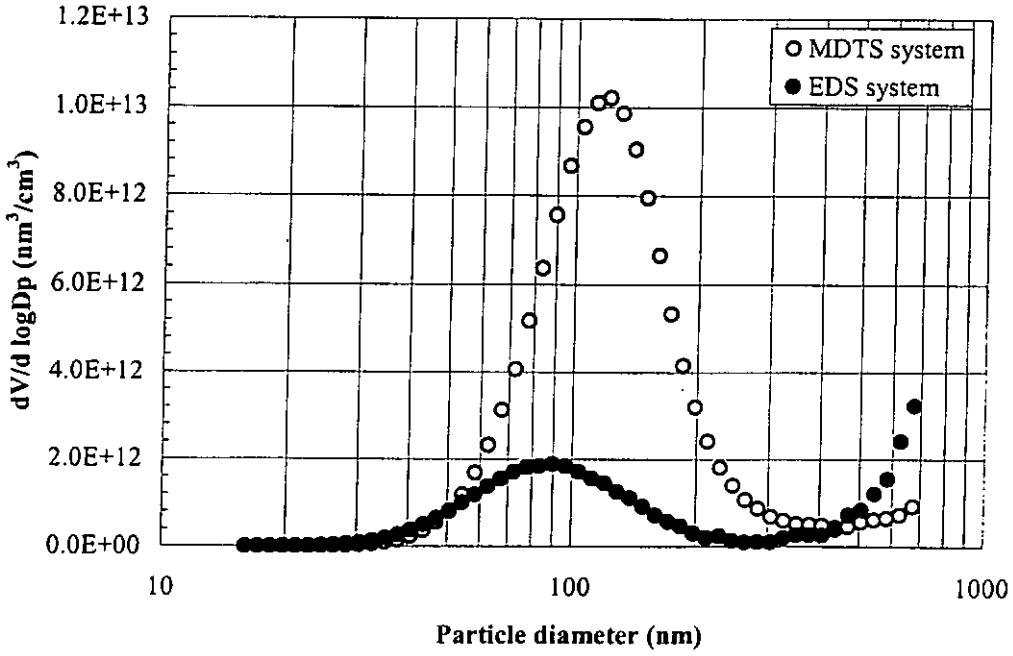

Figure 6.4 Comparison of diesel particle volume distributions from EDS and MDTS measurement systems at 50% of full engine load (Engine mode 2).

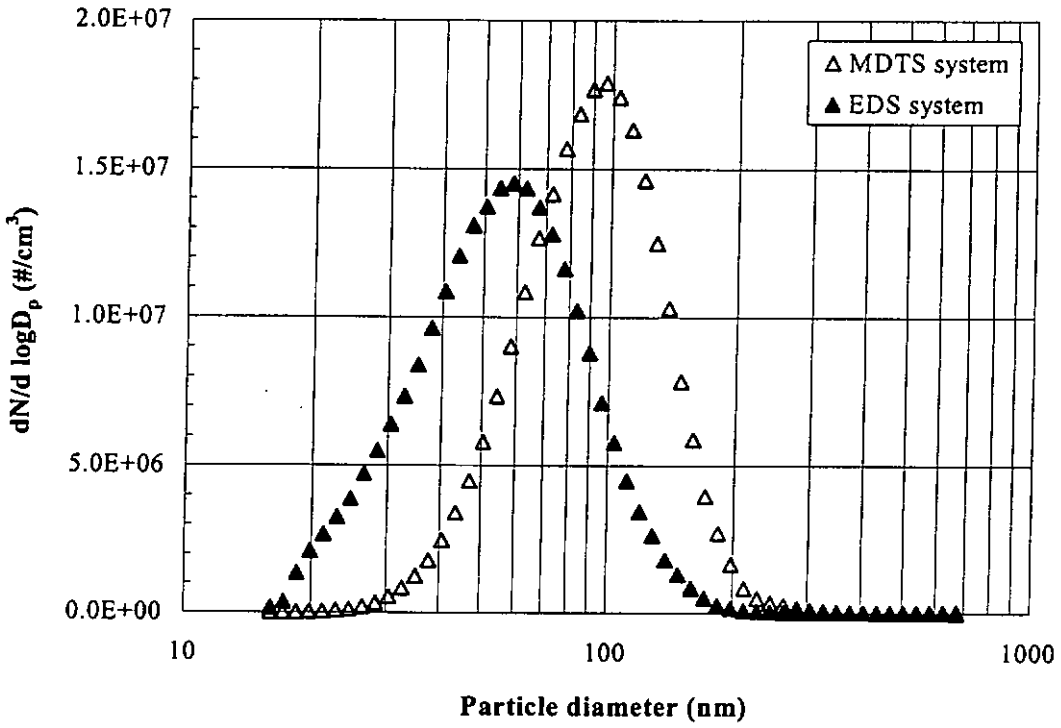

Figure 6.5 Comparison of diesel particle number size distributions from EDS and MDTS measurement systems at 100% of full engine load (Engine mode 3).

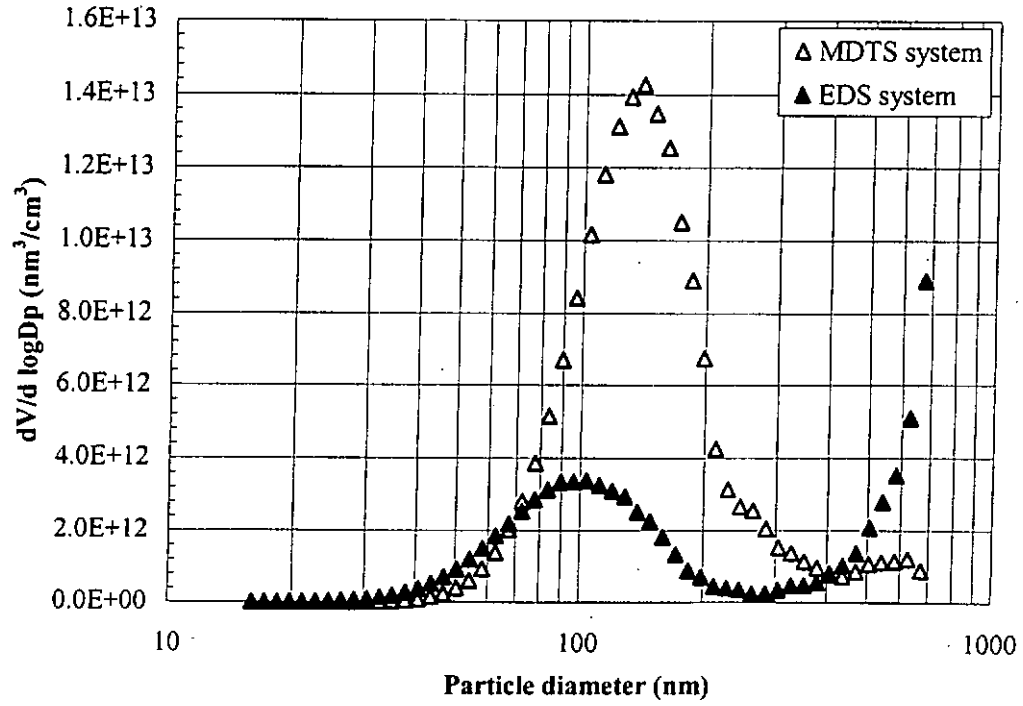

Figure 6.6 Comparison of diesel particle volume distributions from EDS and MDTS measurement systems at 100% of full engine load (Engine mode 3).

In general, the particle volume concentrations obtained from the EDS measurement are usually higher than the MDTS measurement system for different engine loads as shown in Figs. 6.2, 6.4 and 6.6. However, the deviations of particle volume concentrations are less apparent from the two measurement systems when the results are presented in particle volume concentrations in nuclei mode. This is because the particle volume concentration in the accumulation mode has a higher order of magnitude than that in the nuclei mode.

It should be noted that the EDS system measures a higher particle number and volume concentrations than the MDTS system in nuclei mode particle. This is because the EDS measurement system has a heated primary diluter that can minimise the vapour pressure of volatile components and avoid the formation of nucleated particles during the dilution process. In contrast, the MDTS measurement system uses the compressed air as the dilution air at about 23°C. When the hot exhaust samples are diluted inside the mini-dilution tunnel, the saturation vapour pressure is reduced with the decreasing temperature, whereas the partial vapour pressure remains constant. The saturation vapour pressure ratio becomes greater than 1.0, hence the mixture of diluted exhaust samples changes to the supersaturation condition. The formation of nucleated particles will occur once the supersaturation mixture is formed. Hence, the MDTS measurement system obtains a larger amount

of nucleation particles than the EDS measurement system but the experimental results are contrary to expectations. The confusion caused by this result might be due to the existence of supersaturation mixture in the MDTS measurement system. Supersaturation mixture could also result in the condensation of vapour molecule on the surface of particles. This process will cause the size of the nucleation particles to grow and subsequently change to the accumulation particles. Hence, the MDTS measurement system would obtain a lesser amount of nucleation particles than the EDS measurement system. In fact, the EDS measurement system prevents the diluted exhaust samples from changing to a supersaturation mixture during the primary heated dilution air process. It also eliminates the condensation of the vapour molecules on the surface of the particles and avoids the growth of nucleation particles during the secondary dilution process at room temperature.

For accumulation mode particles larger than 100 nm in diameter, the results indicate that the particle number concentration measured from the EDS system are lower than those from the MDTS system for the three designated engine load modes, as shown in Figures 6.1, 6.3 and 6.5. The MDTS system always measures a higher particle number concentration in the range of 70 to 90 nm, whereas the EDS system measures the peak value of particle number concentration in the range of the nuclei mode. On the other hand, the particle volume distribution has a similar trend as the

particle number distribution in different engine load modes as shown in Figures 6.2, 6.4 and 6.6. The MDTS system measures higher accumulated particle volume concentrations than the EDS system. The peak particle volume concentrations from the MDTS and EDS measurement systems normally occur at the particle diameter around 100-150 nm and 80-90 nm, respectively for the three different engine load modes. More than 80% of the total particle volume concentrations come from the accumulation mode particle. It is also noted that a turning point occurs when the particle size is larger than 400 nm for the three different engine load modes. Beyond this turning point, the EDS measurement system obtains a higher volume concentration than the MDTS measurement system for the three designated engine load modes. This reveals that larger particles would be deposited on the wall of the mini-dilution tunnel during the particle transmission, hence causing the large reduction of volume concentration.

6.2.2 Comparison of CMD, total particle number and volume concentrations between the MDTS and EDS measurement systems

To investigate the characteristics of exhaust particle emissions from two different measurement systems, the results should include both the nature of the particles, the total number concentration and the total volume concentration of the particles emitted. Most exhaust particle distributions have a unimodal and lognormal distribution, so the particle CMD has been used to represent the particle size and trend for the particle size distribution [104]. The CMD, total number concentration and total volume concentration of particles emitted from the exhaust particle emissions for different engine conditions are presented in Table 6.1. The CMD measured from the MDTS measurement system grows from 67 to 91 nm when the engine load is increased from 10% to 100% of full load, whereas the EDS system measures a lower particle CMD which increases from 47 to 56 nm, accomplished with an increase in the engine load. Hence, the particle CMD measured from both measurement systems show an increase in the particle size with increasing engine load. The results have good agreement with the findings obtained from Patschull and Roth [105], who also found a remarkable growth of particle mean diameter with increasing engine load for a two-stroke engine. In addition, it also shows that it would increase the amount of total particle number and volume concentrations with increasing engine load from both measurement systems.

A comparison of the results of the particle CMD, total particle number and volume concentration of the MDTS measurement system and the EDS measurement system shows that the former is always larger than the latter system in all three engine modes. The difference in particle CMD is about 20 nm at low engine load condition, but becomes more noticeable to about 35 nm at high engine load condition. This implies that the MDTS measurement system would cause the exhaust particles to form larger particles; these findings are in good agreement with the results obtained from Maricq et al. [48]. At low and medium engine load conditions, the MDTS system measures almost higher in the total number concentration of particles than the results measured from the EDS system. The total number concentrations of particles, however, measured from both measurement systems have almost the same order of magnitude at high engine load condition. In general, the total particle volume concentration obtained from the MDTS measurement system is always higher than that from the EDS measurement system as shown in Table 6.1. As the engine load increases, the effect of sampling dilution becomes apparent, and the difference between these two measurement systems becomes more pronounced. The total particle volume concentration obtained from the MDTS measurement system is increased substantially at 50% load and decreased on further increasing the

load, whereas the total particle volume concentration obtained from the EDS measurement system is increased gradually at high engine loads.

Engine load (%)	Count median diameter (nm)		Total number concentration of particles (#/cm^3)		Total volume concentration of particles (nm^3/cm^3)	
	MDTS system	EDS system	MDTS system	EDS system	MDTS system	EDS system
10	67.3±1.5	46.8±1.0	$6.22x10^6$	$4.73x10^6$	$7.41x10^{11}$	$7.11x10^{11}$
50	75.7±1.2	50.9±0.6	$9.24x10^6$	$5.58x10^6$	$4.16x10^{12}$	$1.24x10^{12}$
100	90.7±2.1	55.7±2.7	$7.46x10^6$	$7.37x10^6$	$5.49x10^{12}$	$2.39x10^{12}$

Table 6.1 Comparison of the exhaust particle number size and volume distributions with dilution factor correction from the MDTS and EDS measurement systems for different engine load conditions at a maximum torque of constant speed.

Based on the above results, it can be observed that the MDTS system always measures a higher total number and volume concentrations of particles, and a larger CMD than the EDS system. This leads to the occurrence of particle transformations (i.e. nucleation, condensation and/or coagulation) taking place inside the mini-dilution tunnel, thus causing the change of particle concentration and distribution. However, the results show that the nucleation of particles will increase the number of particles in nuclei mode, and the condensation of vapour molecules on the surface of particles will also increase the particle volume concentration in the MDTS measurement system. On the other hand, the coagulation of particles that occurs in the MDTS measurement system is negligible because the residence time is

about 1.2 seconds and the particle number concentration does not exceed 1 x 10^7. In general, the total particle number concentrations in the MDTS measurement system should be lower than in the EDS measurement system, and the total particle volume concentrations should be almost the same for both measurement systems if coagulation takes place. However, the results show higher total particle number and volume concentrations measured from the MDTS system than from the EDS system. This might reveal that the nucleation and condensation processes are taken place in order to obtain higher particle number and volume concentrations.

6.2.3 Evaluation of the performance of MDTS and EDS measurement systems

For a stable and reliable exhaust particle emission measurement system, it should be possible to avoid the transformations of particles and the distortion of the particle number and volume distribution. The present results show that the EDS measurement system is capable of preventing the nucleation of particles and the condensation of vapour molecules when the exhaust samples are diluted. This is because the collected exhaust samples are transferred and diluted with heated air inside the primary diluter. In general, the saturation vapour pressure of a substance is a function of temperature. Hence, the vapour pressure of volatile components for exhaust samples is decreased during the heated dilution. This allows secondary

dilution at room temperature without causing any condensation of the volatile components. Therefore, the particle size is not increased by the condensation of the vapour molecules. In addition, the temperature drop of the exhaust samples is very small in the primary dilution process because the dilution air is heated up to the exhaust temperature at each designated engine load mode. This can prevent the nucleation of particles and the condensation of vapour molecules from the secondary dilution.

On the other hand, the exhaust samples are diluted at room temperature inside the MDTS measurement system. A significant temperature drop would occur during the dilution process, and the supersaturation mixture would be produced. It would cause the occurrence of particle nucleation and condensation. Consequently, the MDTS measurement system might enhance the particle transformation process because the particle distribution is shifted to larger particle sizes (i.e. particle CMD), and the total number and volume concentrations of particles become higher when they are compared with the results of the EDS measurement system. Recently, Ristovski et al. [104] have reported that if the particle concentration is sufficiently high, such as at a high engine load, then coagulation growth will occur, especially in smaller particulates. A reduction of particle number concentration accompanied with an increase in particle size would be observed. However, if both the measured

particle size and the number concentration are increased, then it is most likely that the coagulation, together with the homogenous nucleation of the metallic ash particle, will take place simultaneously. In order to infer the effect of coagulation on the particle concentration in the MDTS measurement system, a simple coagulation calculation is made. According to the description of Hinds [83], the diluted exhaust samples can be considered a polydisperse mixture. The average coagulation coefficient, $\overline{K}$, for the polydisperse mixture can be determined as follows:

$$\overline{K} = \frac{2kT}{3\mu}\left[1 + e^{\ln^2 \sigma_g} + \left(\frac{2.49\lambda}{CMD}\right)\left(e^{0.5\ln^2 \sigma_g} + e^{2.5\ln^2 \sigma_g}\right)\right] \tag{6.1}$$

$$N(t) = \frac{N_0}{1 + N_0 \overline{K} t} \tag{6.2}$$

where k is the Boltzmann constant, 1.38×10^{-16} dyn·cm/K; T is the temperature of the diluted exhaust, K; μ is the viscosity of air, 1.8×10^{-4} dyn·s/cm^2 at 293 K; λ is the gas mean free path, 0.066 μm; σ_g is the geometric standard deviation; N(t) is the number of particles at the residence time, t; N_o is the initial number of particles; t is the residence time, second.

For the MDTS measurement system, the total particle number concentrations varies from 8.8×10^5 to 1.3×10^6 and the residence time is within 1.2 seconds in all designated engine load conditions. Table 6.2 shows that the effect of coagulation on the total number particle concentration is negligible. The maximum reduction in the total particle number concentration is 0.15% at the engine load modes 1 and 2. This is because the particle number concentration is not very high and the residence time is short in the mini-dilution tunnel. The particles lack sufficient time to coagulate, so the coagulation is not the major factor to affect the particle number and volume concentrations. Recently, Wei et al. [49] have also found that the coagulation of particles does not play a major role in the transfer line of a dilution tunnel, but rather the residence time is one of the critical factors directly influencing the particle number concentration.

Engine load (%)	Residence time (s), t	Actual total number particle concentration (cm^{-3})	Coagulation effect on total particle number concentration after residence time, t (cm^{-3})	% change on total particle number concentration
10	1.2	$8.886\text{x}10^5$	$8.873\text{x}10^5$	-0.15
50	1.2	$1.320\text{x}10^6$	$1.318\text{x}10^6$	-0.15
100	1.1	$1.066\text{x}10^6$	$1.065\text{x}10^6$	-0.09

Table 6.2 Effect of the coagulation on the actual total number particle concentration without dilution factor correction for the MDTS measurement system.

Based on the results of the particle number and volume distributions as shown in Figures 6.1 to 6.6, it shows that the MDTS measurement system is likely to shift the entire particle number and volume distributions to a larger particle diameter range for different engine loads at a maximum torque of constant speed. It also measures a lower particle volume concentration in nuclei mode but a higher particle volume concentration in accumulation mode than the EDS measurement system. In addition, the MDTS measurement system increases the particle size (i.e. particle CMD), total number and the volume concentrations of particles in all engine load modes are observed. It is believed that the nucleation of particles and the condensation of vapour molecules take place simultaneously. These transformation processes would cause the deviation of particle size distribution, CMD, total number and volume concentrations of the particles from their actual magnitude. When the hot exhaust samples were diluted with the air at a room temperature of 23°C, a highly saturated mixture was formed due to the drastic temperature drop from about 130°C to 40°C. The nucleation of particles would take place and most of the SOF would then nucleate into the nuclei particles. These SOF were in the gaseous phase in the exhaust tailpipe, but would undergo the gas to particle conversion through homogenous nucleation during the dilution process. Once the stable particle was formed, the vapour molecules condensed on the surface of particles and cause the

growth in particle size. Hence, a higher particle number and volume concentration in accumulation mode were found in the MDTS measurement system than in the EDS measurement system. Maricq et al. [48] also found that a higher particle number concentration in accumulation mode was obtained using the mini-dilution tunnel measurement than the ejector diluter measurement system. Their findings agree with the present results. They concluded that the higher accumulation mode particle from the mini-dilution tunnel is due to the desorption and/or pyrolysis of organic materials, either hydrocarbons deposits on the walls of steel transfer hose or the silicone rubber, by hot exhaust gases, and their subsequent nucleation in the dilution tunnel. However, it is revealed that the higher accumulation mode particle from the mini-dilution tunnel is mainly caused by the particle transformations such as nucleation and condensation in the present study, as shown in Figures 6.1, 6.3 & 6.5. According to the findings of the present study and Maricq et al. [48], it can be concluded that the particle transformation would occur inside the mini-dilution tunnel and limit the ability to present the accurate particle distribution.

6.3 Performance of DOC on the Diesel Exhaust Particle Emission

6.3.1 Characteristics of two fresh DOCs for different engine load conditions

The initial characteristic of the DOC in particle emission for different engine conditions was investigated. Two brand-new DOCs (i.e. zeolite-based and platinum-based) were installed in an engine dynamometer test bed and tested under several prescribed testing conditions (i.e. 10%, 50%, and 100% of full engine load at maximum torque speed). The EDS particle system and scanning mobility particle sizer (TSI, SMPS Model No. 3934) were used to measure the particle number concentration. The operations of the SMPS and ejector dilutor were depicted in Chapter 4.

The effect of the two brand-new DOCs on particle number concentration when engine condition was operated from 10% to 100% of full engine load is shown in Figures 6.7 to 6.9. The exhaust gas temperature at the inlet of the DOC was also reported in these figures. From these figures, it obviously shows that the application of the DOC is capable of substantially abate the particle number concentration, especially in particle diameter of 30-100 nm. The results also show that the DOC-Type B always has a better reduction on particle emission than DOC-Type A. The differences of particle reduction between catalyst A and B are more significant

at the low engine load condition but it becomes smaller when the engine load increases from 50% to 100% of full load.

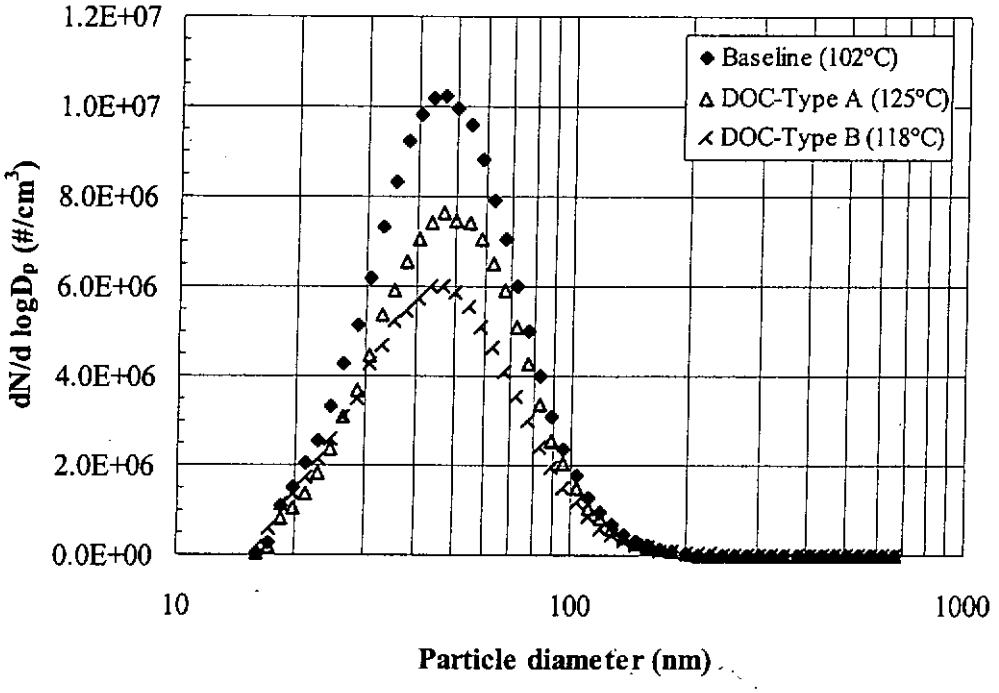

Figure 6.7 Effect of fresh DOCs on the exhaust particle concentration at 10% of full engine load (Engine mode 1).

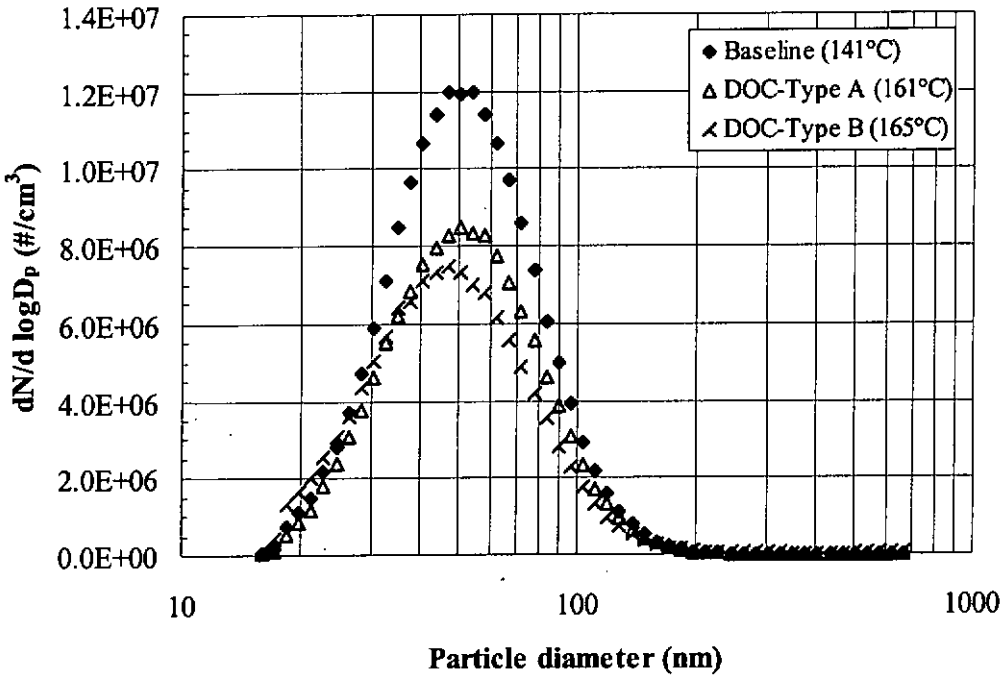

Figure 6.8 Effect of fresh DOCs on the exhaust particle concentration at 50% of full engine load (Engine mode 2).

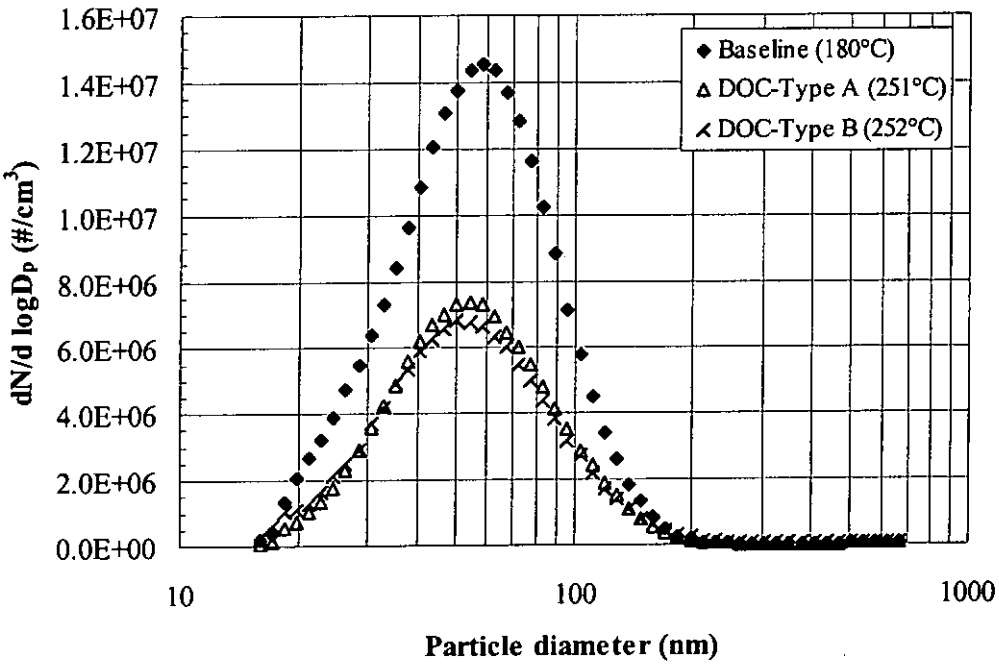

Figure 6.9 Effect of fresh DOCs on the exhaust particle concentration at 100% of full engine load (Engine mode 3).

The exhaust gas temperatures at the inlet of the DOC for the two catalysts were about 120°C as shown in Figure 6.7. The differences in the particle reduction between the two catalysts are more noticeable under the low engine load condition. The results show that DOC-Type B has a higher reduction in particle emission than DOC-Type A even though the inlet gas temperatures are similar to each other. In contrast, when the inlet exhaust gas temperatures for both catalysts are approximately identical at the high engine load condition as shown in Figure 6.9. The reduction in particle emission of these two DOCs is almost the same.

On the other hand, the discrepancy performance in particle emission under the low temperature condition can be ascribed to the coating materials and catalyst configurations. Zeolite and platinum are the common coating materials for use in the catalyst but they have inherent difference in light-off temperatures. The light-off temperature is the temperature at which 50% reduction of exhaust gaseous emission can be achieved. The differences in light-off temperatures cause the catalysts to have the effect particle emission, especially in low exhaust gas temperature. Consequently, the engine exhaust gas temperature is a critical parameter which affects the performance of the catalyst.

As shown in Figure 6.10, Zelenka et al. [106] presented a diagram showing a number of parameters affecting the performance of diesel oxidation catalyst and reported that exhaust gas temperature is one of the most crucial parameters influencing catalyst performance.

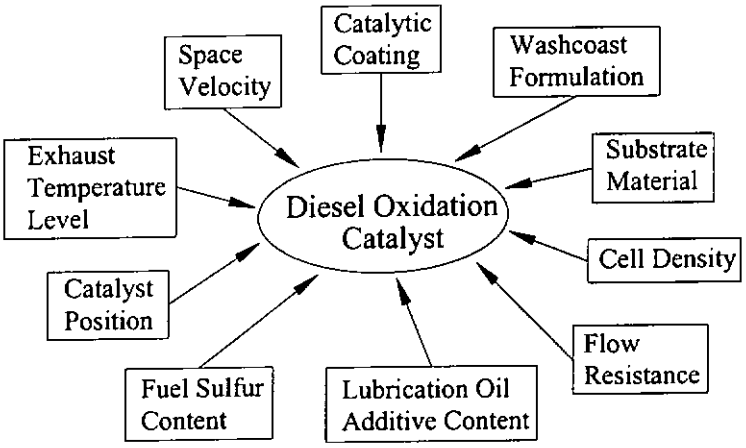

Figure 6.10 Parameters affecting the performance of DOC [106].

Table 6.3 summarises the effect of diesel oxidation catalysts on different particle size ranges. The data presented in this table are the average change in that particle size range. The result shows that the DOC-Type A and B have competence to curtail the nuclei mode particles. The reduction rate of nuclei mode particle varies from 17% to 50% for the engine which runs from 10% to 100% of full load at maximum torque speed. Indeed, when the engine condition is operated from 10% to 100% of full load, the exhaust gas temperature also increase significantly. Hence, the

exhaust gas temperature directly affects the reduction rate of particle emission. The higher the exhaust gas temperature, the higher reduction rate of particle emission is obtained.

		Change of particle concentration (%)		
		Nuclei mode particle	Accumulation mode particle	
Engine condition	DOC-Type	10-50 (nm)	50-100 (nm)	>100 (nm)
10 % of full engine load 2200rpm	A	-17	-17	1.3
	B	-19	-40	2.0
50 % of full engine load 2200rpm	A	-27	-26	3.6
	B	-29	-41	5.1
100 % of full engine load 2200rpm	A	-50	-51	4.4
	B	-45	-55	6.6

Table 6.3 Summary of the two DOCs effect on the particle emission for different engine load conditions.

In principle, the DOC could affect the particle emission in three ways: oxidation of particle, deposition and SO_2 to SO_3 conversion. The reaction of SO_2 and SO_3 to sulfate (SO_4) is dependent on the exhaust temperature level and the fuel sulphur content. The reaction would begin at the exhaust temperature above 400°C [107]. In the present study, the maximum exhaust temperature only reaches to around 250°C. With this temperature, it is believed that the formation of sulfate would not be

triggered to begin so the effect of SO_2 conversion on particle emission can be neglected. The reason why the DOC can abate the nuclei mode particle which is attributed to the catalyst which oxidises considerable amount of SOF to H_2O and CO_2 during the engine exhaust gas passing through the monolith substrate. In addition, Klein et al. [108] depicted that the catalyst caused the reduction in particle number concentration and it can be traced back to deposition mechanisms. Gravitational settling, Brownian diffusion, thermosphoresis, inertial impaction and interception are also considered possible deposition mechanisms for the particle deposition. Johnson et al. [91] also reported that there are some percentage reductions in the particle number concentration after the application of catalyst which is due to the deposition of particle. After the experiment was completed, the surface of the catalyst substrate was visibly covered by a layer of carbon particle, as shown in Figures 6.11a & 6.11b. The deposition of particle on the catalyst surface definitely exists and affects the particle emission. However, it is impossible to determine the size of particles that deposit on the catalyst surface with the naked eye. Thus, an investigation on deposition mechanisms was carried out to ascertain which particle size could deposit most and least on the catalyst surface.

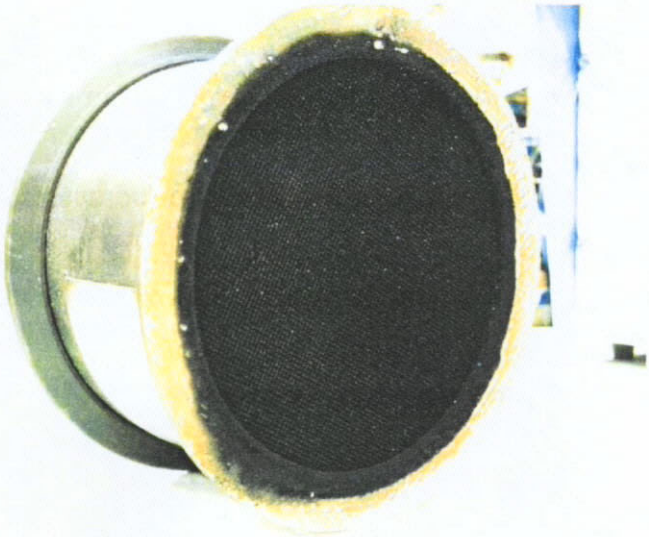

Figure 6.11a The front end of the DOC (Type A-Zeolite based catalyst).

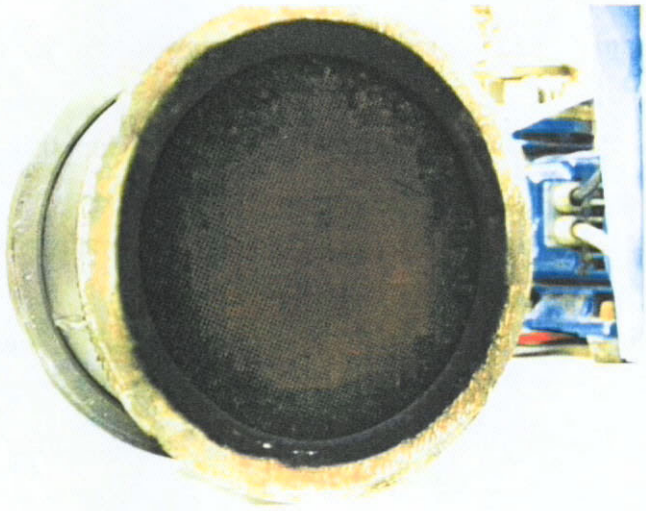

Figure 6.11b The rear end of the DOC (Type A-Zeolite based catalyst).

In Table 6.3, the results of the accumulation mode particle show a dilemma situation on the effect of the DOC on particle emission. For the particle size range of 50-100 nm, there is a reduction in particle number concentration for the three designated engine load conditions. This trend is similar to the result in nuclei mode

particle. The reason for this abatement can also be ascribed to the oxidisation of SOFs and deposition of particles. However, the result also reveals that there is a slight increase in particle number for the particles larger than 100 nm in diameter. The increase rate is also related to the increasing engine load condition and exhaust gas temperature. As stated in the aforementioned explanation, there are two possible factors for the catalyst affecting the particle emission (i.e. oxidation and deposition). As regards the deposition of particles, this process is able to curtail particle number concentration, but the current result reveals an opposite scenario, increasing in particle number. Hence, it is believed that this process is not dominant in affecting these particles (D_p > 100 nm). The only possible way to change these particle emissions remains the oxidation of the particles because this process may have a drawback on particle emission. Figure 6.12 shows a schematic diagram of a typical diesel particle and vapour phase compounds [109]. It unveils that the solid carbonaceous particle is wrapped by a layer of adsorbed hydrocarbons and SOF. The sulfate (SO_4) and hydrocarbons particle are adsorbed on the outer surface of the layer. The original size of the solid carbonaceous particle ranges from 0.01 to 0.08 μm diameter, but it agglomerates to form the accumulation mode particle (50-1000 nm) with the adsorbed hydrocarbons and SOF. As these large diesel particles flow through the catalyst substrate, the catalyst will oxidise the adsorbed SOF and HC to

make the size of particles become smaller and so the number of small particles will be increased. In addition, the result also shows that the increasing rate of the large accumulation mode particle becomes faster as the engine condition changes from 10% to 100% of full engine load. The higher exhaust temperature will also promote more oxidation of the organic compounds, making more particles alter to smaller size as described by Andrews et al. [110].

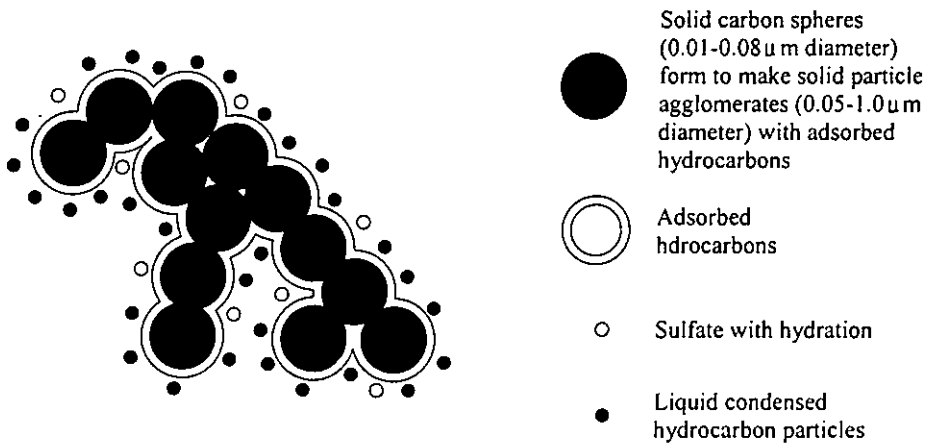

Figure 6.12 Schematic diagram of a typical diesel particle and vapour phase compounds [109].

From the above results, it can be concluded that a fresh catalyst can substantially reduce the number of nuclei mode particle but it will slightly increase the number of accumulation mode particles. The results are well-agreed with the previous study performed by Hammerle et al. [111], but they did not provide a detail explanation for this phenomenon. In the present study, this phenomenon can be well explained by using the oxidation and deposition processes of particles within DOC.

6.3.2 Total particle number and mass concentrations of fresh DOCs for different engine load conditions

The other essential parameters used to assess the performance of fresh DOCs are the total particle number and mass concentration. A count median diameter (CMD) is also presented to ascertain the overall particle size trend. The total particle number concentration is simply calculated by adding the particle number in each particle diameter together to obtain a total value. The total particle mass concentration is found by assuming that the particles are spherical, although it is well known that the diesel particles are long-branched fractal-like agglomerates [40,112]. Particle density is assumed to be 0.749 to 0.570 g/cm^3 at 125 to 250°C. By using the Equation 6.1, the mass concentration for individual particle diameter can be obtained. These individual values are then added together to determine the total mass concentration as follows.

$$m_T = \frac{\pi}{6}\rho\sum_{d=15}^{670} N_d D_d^3 \qquad (6.3)$$

where m_T is the total particle mass concentration, mg/m^3, N_d and D_d are the number of particle, #/cm^3 and particle size at particular particle diameter, d ranging from 15 to 670 nm, respectively.

The results of total particle number and mass concentrations, as well as the CMD for different engine load conditions are summarised in Table 6.4. These results are based on the particle ranging from 15 to 670 nm in diameter. The results of the catalysts and baseline reveal a significant difference in all designated engine conditions. In the 10% of full engine load condition, both oxidation catalysts are able to reduce about 15% of the total particle number from baseline value. The reduction rates for 50% and 100% of full engine load conditions are 28% and 49%, respectively. The reduction rate becomes higher with the increasing engine load and exhaust gas temperature. As regard the mass concentration, the results show that the total mass concentrations for all testing conditions are reduced significantly by the oxidation catalyst. The reduction rate ranges from 24% to 75%, depending on the exhaust gas temperature. The higher the exhaust gas temperature at the catalyst inlet, the higher the reduction rate is obtained. This trend makes an agreement with the result of total particle number concentration. On the other hand, the value of CMD always remains in the nuclei mode particle region for all testing conditions. It grows with the increasing engine load and intends to become smaller as the oxidation catalyst is installed. The alteration level of CMD is not pronounced. The performance of oxidation catalyst only reduces the size of CMD by 1-3 nm diameters comparing with its baseline value.

		Engine load condition		
		10%	50%	100%
Total particle mass concentration (#/cm^3)	Baseline	4.73×10^6	5.58×10^6	7.37×10^6
	DOC-Type A	1.21×10^6	4.24×10^6	3.80×10^6
	DOC-Type B	1.24×10^6	3.81×10^6	3.67×10^6
Total particle mass concentration (mg/m^3)	Baseline	1.16	4.21	8.75
	DOC-Type A	0.88	1.40	2.14
	DOC-Type B	0.69	1.32	2.26
CMD (nm)	Baseline	46.73	50.80	55.71
	DOC-Type A	49.20	51.48	54.82
	DOC-Type B	45.41	47.02	53.51

Table 6.4 Summary of the CMD, total particle number and mass concentrations for different DOC and engine load conditions.

As discussed in the previous Section 6.3.1, the reduction in particle number concentration can be ascribed to the deposition of particle on the catalyst substrate surface and the oxidation of the nuclei mode SOF particle. Regarding the reduction in mass concentration, it is mainly caused by the oxidation of the catalyst which reduces the particle number. Another reason is due to the fact that oxidation catalyst oxidises the organic fraction from the total particulate matter and thereby the total mass concentration of particle becomes smaller. From the previous investigation, Klein et al. [108] explained that the reason of oxidation is due to the HC (SOF) being oxidised by the catalyst. They conceived three possible mechanisms for this oxidation. Firstly, the HC molecules adsorbed at particulates are directly oxidised at the particulate surface. Secondly, the adsorbed HC molecules on the particulate

surface are in adsorption equilibrium with HC in gas phase. Gas phase of HC molecules are oxidised by the catalyst. More and more HC molecules desorb from the particulate surface and are subsequently oxidised in the gas phase. Thirdly, the HC molecules are in gas phase before the oxidation catalyst and do not adsorb on the particulates surface. These gas phase HC molecules are directly oxidised by the catalyst. On the other hand, a detailed interpretation for the reduction in particle mass was described by Barris [94]. He presented a schematic diagram as shown in Figure 6.13, to explain the physical activities taking place in the catalyst channels and on the particles. The carbonaceous particle physically adsorbs the vapour phase hydrocarbons onto its surface from a surrounding boundary layer. The depletion of this boundary layer creates a diffusion gradient, drawing more hydrocarbons molecules towards the particle. The adsorbed hydrocarbons (mostly from incompletely oxidised fuel), along with the collected lubricating oil droplets, form the organic fraction of the particulate matter. Meanwhile, the wash-coated channels walls are also adsorbing the reactive species (both hydrocarbons molecules and oil droplets). A diffusion boundary layer near the channel wall surfaces, depleted of the reactive species, gives rise to another diffusion gradient. Thus, a mass transport exists both towards the carbonaceous particles and the wash-coated walls. The adsorbed hydrocarbons wrapped on the carbonaceous particles are adsorbed on the

wash-coated walls and oxidised to CO_2 and H_2O during the subsequent oxidation reaction. Hence, the particle mass concentration will be reduced since the catalyst enhances the oxidation process of the organic fraction and adsorbed hydrocarbons. The reduction in particle mass is linked to a shift in particle size distribution towards smaller size particle because of less adsorbed hydrocarbons on the particle surface. Consequently, the experimental results of CMD tend to be smaller as the oxidation catalyst is retrofitted.

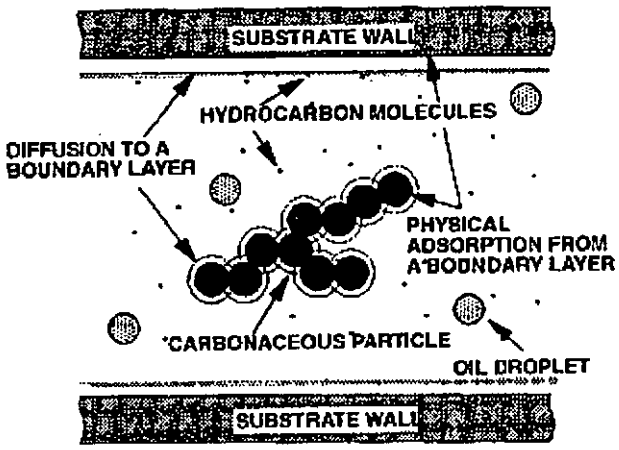

Figure 6.13 Adsorption and diffusion in the catalyst channel [94].

6.3.3 Operation time effect of DOC on the particle emission

The previous Section 6.3.2 has depicted that a fresh diesel oxidation catalyst accompanied by ultra low sulphur diesel fuel will have a high competence to reduce the particle emission in terms of the number and mass concentration. However, these

findings might be in contradiction with the previous investigations. It is because some literatures have pointed out that the application of diesel oxidation catalyst will not alter the particle size distribution and number concentration [113-115]. On the other hand, the other literatures have reported that oxidation catalyst has a negative effect on particle emission (i.e. more particles are emitted) [40,69]. These findings seem to contradict with the present results but it is not the fact indeed. Basically, their studies have not provided any detailed information about the condition of the catalyst or how long is the catalyst being used before running the tests. Since the operation time of the oxidation catalyst will influence the performance in the particle emission, if the catalyst has been used for a certain time, particulate matter will deposit on the catalyst surface. Most of the deposited particles blow-outs take place under low and medium speed driving conditions [110]. It will cause more particles to be generated and bring an adverse effect to DOC. These studies cannot provide detailed analysis on the characteristics of the oxidation catalyst in reducing the particle emission. The present investigation intends to provide detailed information on why the results contradict with the previous studies. Hence, the performance of DOC on particle emission against the operation time will be investigated. Since similar performances of catalyst A and B on the particle emission are obtained, only the catalyst A will be further investigated in the present study to avoid duplication.

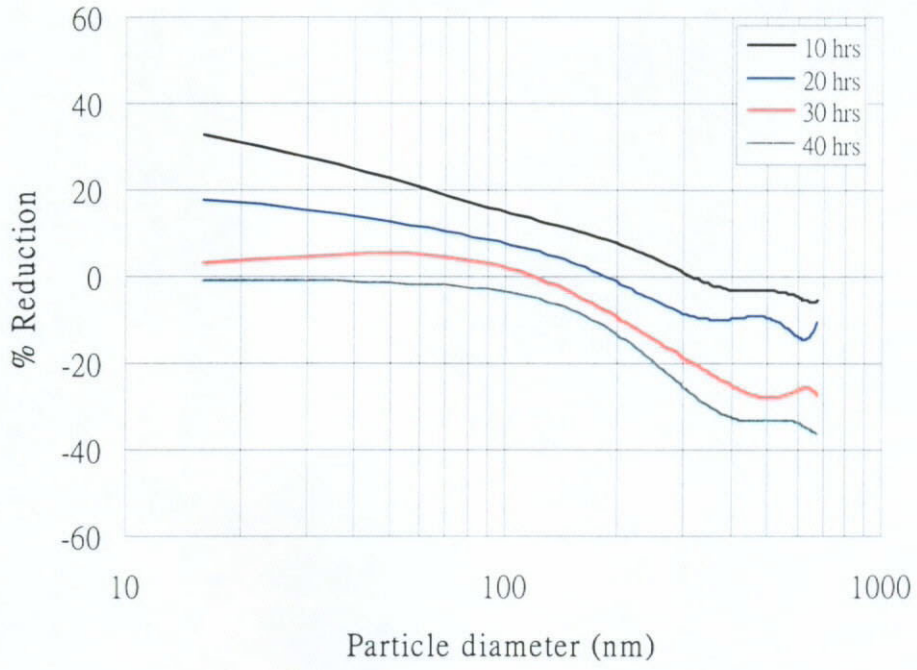

Figure 6.14 Reduction characteristics of the DOC on the particle emission against the operation time at 10% of full engine load (Engine mode 1).

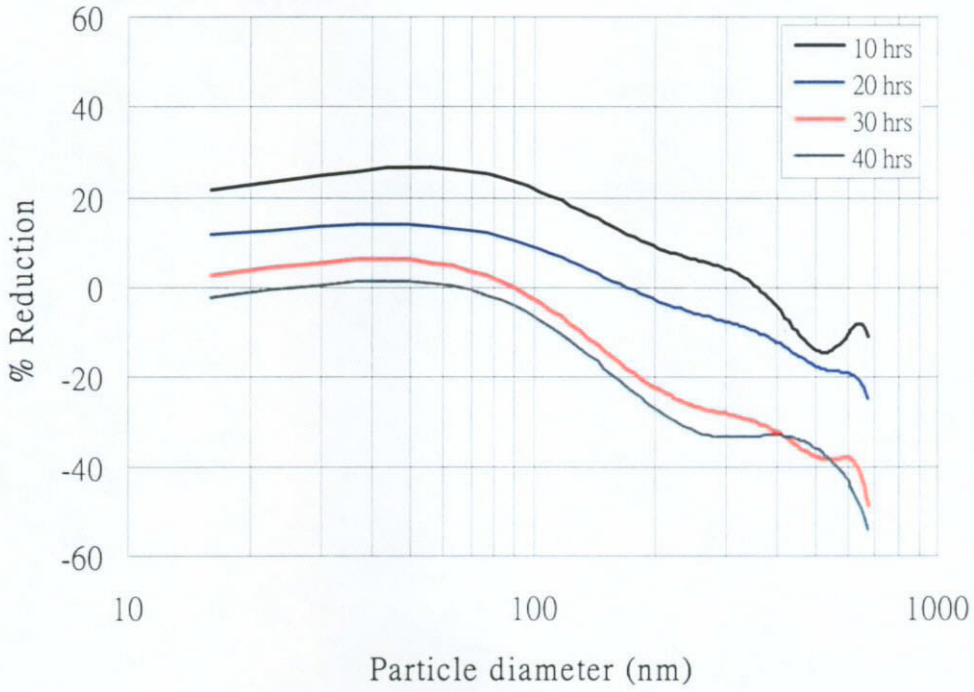

Figure 6.15 Reduction characteristics of the DOC on the particle emission against the operation time at 50% of full engine load (Engine mode 2).

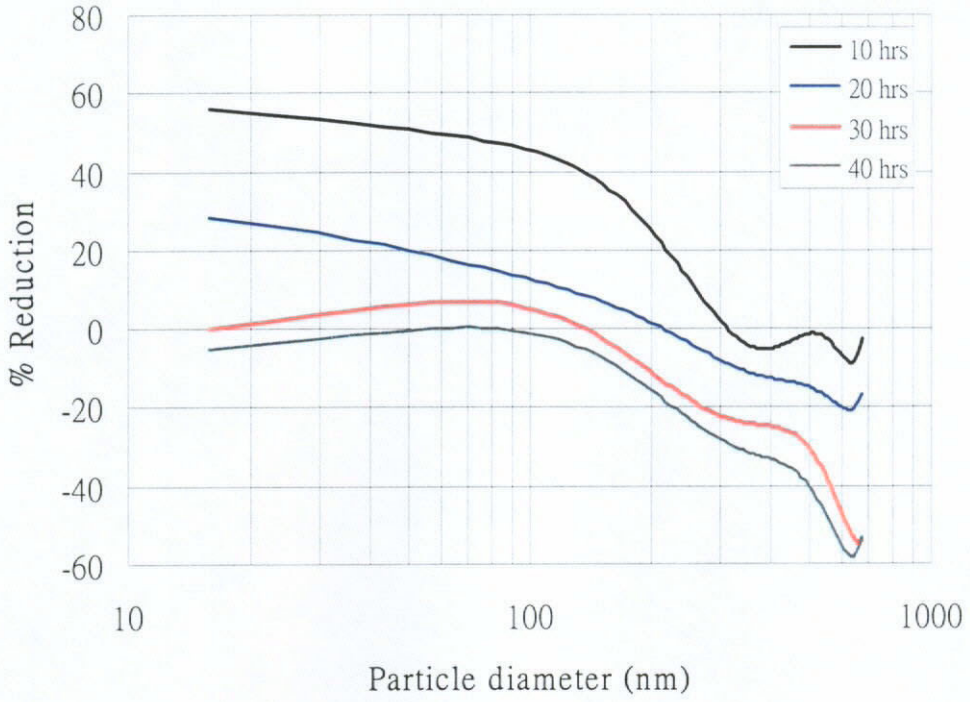

Figure 6.16 Reduction characteristics of the DOC on the particle emission against the operation time at 100% of full engine load (Engine mode 3).

The reduction characteristics of the DOC on the particle emission in the first 40 operation hours under the 10%, 50% and 100% of full engine load are presented in Figures 6.14, 6.15 and 6.16, respectively. The results obviously show that the reduction of nuclei mode particles in the first 10 hours operation is the highest as compared with other operation hours. In the 100% of full engine load condition as shown in Figure 6.16, the highest reduction of nuclei mode particle reaches 57%, whereas the other engine load conditions still have about 20-30% reduction. This reduction rate tends to decrease drastically as the particle size becomes larger. In the first 30 hours operation time, the diesel oxidation catalyst can still reduce the nuclei mode particle for different engine load conditions; however, the reduction

performance gradually decreases with the increasing in operation hour. Until over 30 hours operation, the diesel oxidation catalyst no longer abate the nuclei mode particle. Adversely, it tends to make more nuclei mode particles, especially in 100% of full engine load condition. For the accumulation mode particle, the oxidation catalyst mainly reduces the particle number in the size of 50-300 nm diameter in the first 10 hours operation time. The reduction rate can be kept to about 20%. It commences, however, to decrease as the particle size becomes larger. As the particle size is larger than 300 nm, there is an adverse effect on the particle emission. The negative effect is not serious at this operation time. However, along with the operation time becomes longer, this negative effect grows from 5% in the first 10 hours operation to about 40% after the 40 hours operation. The oxidation catalyst is likely to exacerbate the generation of the particle and lead to more nuclei and accumulation mode particles in the exhaust plume. From Figure 6.16, the advent of the negative reduction in the first 10 hours operation is located at the particle size about 300 nm. In the 40 hours operation, the negative reduction is shifted to the particle diameter of 80 nm. It tends to appear in smaller particle as the operation hour is increased.

From these experimental results, it unveils that the oxidation catalyst is able to curtail the exhaust particle number in the early operation period of the catalyst.

However, as the oxidation catalyst is used for more than 30 hours, there is an adverse effect on the particle number concentration in the exhaust plume. If the present oxidation catalyst serves around 40 hours, it will increase the number of particle for all sizes of particles. The performance of DOC is dependent on the operation time of the catalyst and might vary from the initial DOC condition. The interpretation for this phenomenon can attribute to the combined effects of deposition and oxidation inside the catalyst channel. For the first 10 hours operation, the oxidation catalyst can be treated as a fresh catalyst. Its surface provides a spate of space to the particle deposition. As the exhaust gas passes through the substrate channel, the nuclei and accumulation mode particles would deposit on the surface by a series of deposition mechanisms, such as adsorption, thermosphersis, diffusion and impaction deposition. As the DOC operation hours becomes longer, more and more particle would deposit on the substrate and this will increasingly reduce the space for the particles deposition. Eventually, the whole catalyst substrate will be saturated with the exhaust particles and causes the increase in back pressure. Figure 6.17 presents the change of back pressure against to the operation hours under individual testing condition. The result shows that the back pressure increases gradually as the operation time becomes longer. This is because the catalyst substrate is covered by more and more particles, and the space for the exhaust gas passing through the substrate channel of catalyst

becomes less and less. The pressure drop difference between these two studied DOCs is quite large. It is because the geometric arrangement of these two DOCs is totally different. In fact, the length of the substrate material in the Pt-based catalyst is much longer than that in zeolite-based catalyst, as shown in Appendix D. Hence, it causes a higher pressure drop for the DOC (Type B: platinum-based catalyst) than the DOC (Type A: zeolite-based catalyst).

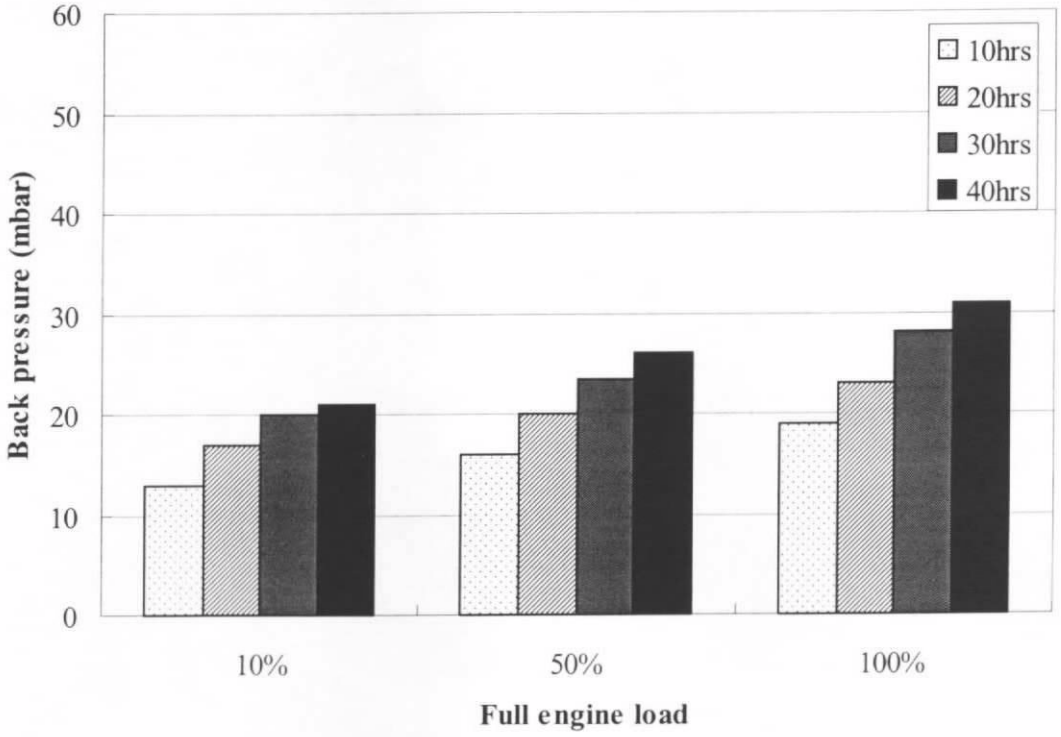

Figure 6.17 The deviation of back pressure at the inlet of DOC versus the operation time for different engine load conditions.

As the subsequent exhaust gas flows through the substrate channel, there is lack of space for the particle to deposit, so the exhaust particle number in the catalyst inlet and outlet should remain nearly the same. The result reveals that, however, there

is a slight increase in particle number of nuclei mode particle at 40 hours operation. It is because some of the deposited particles are blown out from the catalyst. From the present results, it is believed that the reduction of the nuclei mode particle is dominated by the effect of deposition rather than the oxidation. It is because the oxidation should cause a reduction in particle number but the results show an increase in particle number. Hence, the oxidation should not be the dominant process affecting the nuclei mode particle.

In regard to the accumulation mode particle, the deposition of particle is the major process taking place inside the catalyst channel at the initial operation time because the space is still available for the particle to deposit. The oxidation of particle is also carried out simultaneously but the effect is not significant at this stage. As the operation time of catalyst is increased, the effect of the deposition of particles becomes weaker, whereas the effect of the oxidation becomes more pronounced. The oxidation of particle has a drawback that is the catalyst oxidises the adsorbed HC from the particle surface, mainly coarse particle (D_p > 1000 nm). The size of the particle would become smaller. It causes more formation of the smaller size particles and the number of smaller particle increased. Hence, the effects of the deposition becomes weaker and the oxidation becomes more significant as the operation time of catalyst is longer.

6.3.4 Fast engine acceleration response of a used DOC on the particle emission

Concerning the vehicle traffic condition in Hong Kong, many traffic congestions occur in the urban transport area daily. The vehicles always experience a long period of idle condition and fast engine acceleration, alternatively. The reduction in particle emission of the DOC becomes not effective after certain operation hours (i.e. 30 hours) and it is almost impossible to remove the catalyst from the vehicle at this early time. Most of the time, the diesel vehicle would use a DOC with the saturated particle condition. Thus, the particle emission characteristics of the used DOC for the fast engine acceleration condition becomes the crucial one because this driving condition always appears in the real world driving in Hong Kong and other major urban cities.

The testing procedures for fast engine acceleration were given in section 4.6.2. This used DOC was the one which had been operated for 40 hours as mentioned in Section 6.3.3. The total number of particle concentration and the exhaust gas temperature at the inlet and outlet of a used DOC are presented in Figures 6.18 and 6.19. The result shows that the DOC increases the total number of particle concentration in the whole testing cycle, except at the beginning stage of the testing (0-800 seconds). The total particle number at the outlet of the DOC is lower than that at the inlet of DOC in the first 800 seconds. However, this phenomenon changes after

the first 800 seconds and the outlet value of DOC commences to be higher than the inlet value of DOC. This tendency is kept in the entire testing. As the engine speed and load are increased simultaneously (1000-2800 seconds), the total particle number differences between the inlet and outlet of DOC become significant. The number of particles emitted from the DOC becomes higher and increases by 26% in this operation condition. Even when the engine runs at the steady-state condition (100% load at 2200 rpm), the particle emission at the outlet of DOC is still higher than its inlet position. For the subsequent operation of deceleration (from 100% of engine load at 2200 rpm to idle condition) and hot idle condition, this scenario still maintains.

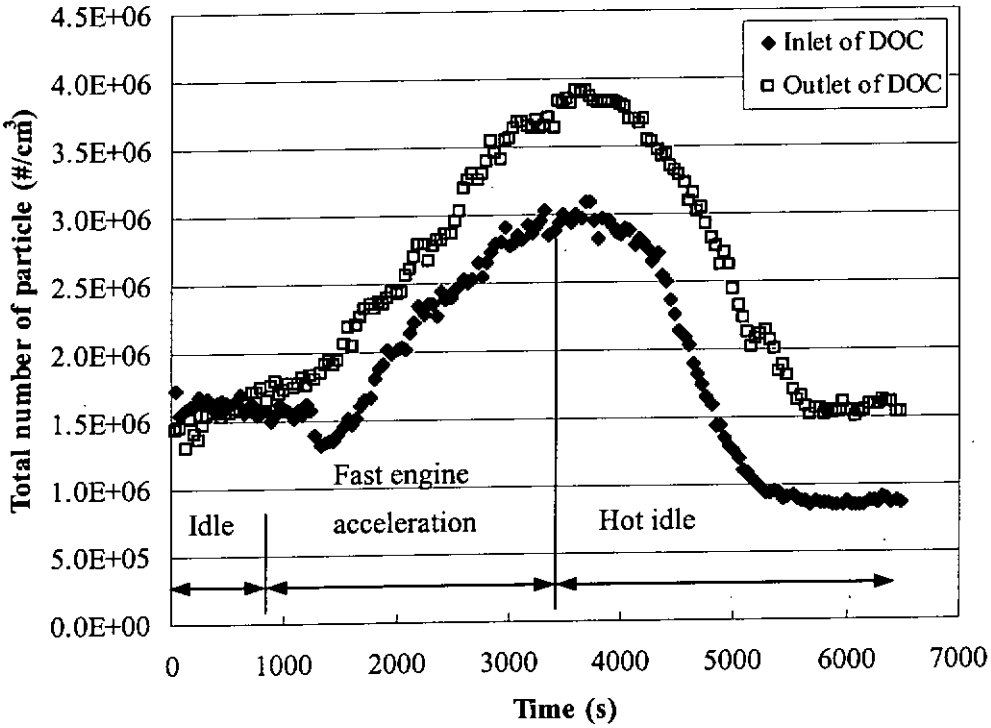

Figure 6.18 The total number of particle concentration of a used DOC between the inlet and outlet for the fast engine acceleration and idle conditions.

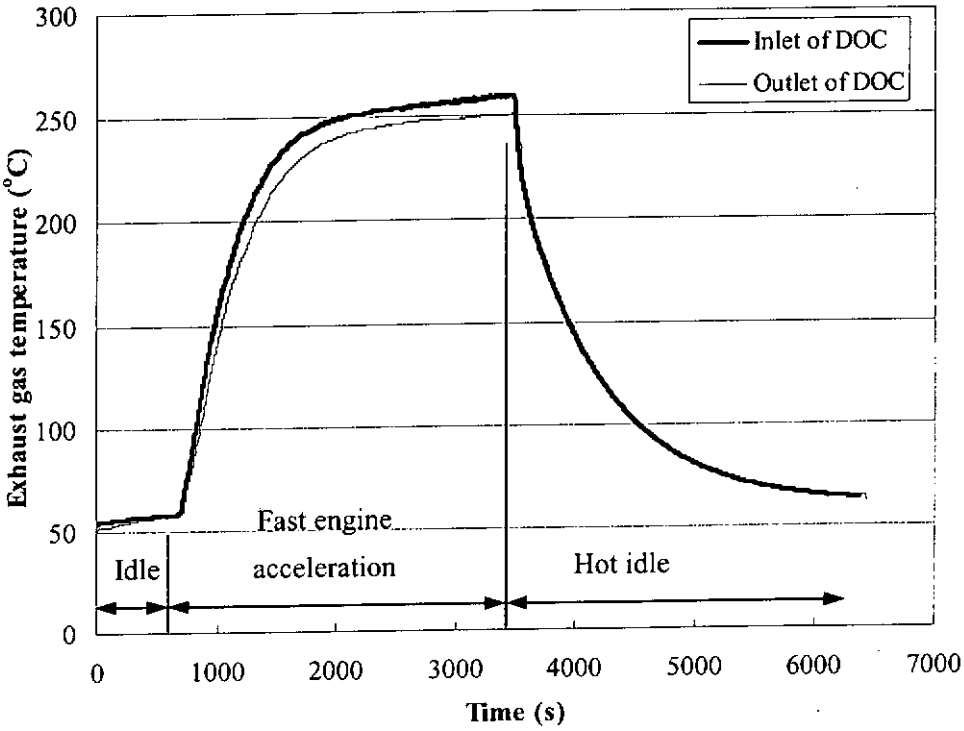

Figure 6.19 Exhaust gas temperature against operation time at the inlet and outlet of a used DOC for the fast engine acceleration and idle conditions.

This phenomena can be explained by the exhaust gas temperature against time at the inlet and outlet of DOC as shown in Figure 6.19. At the first 800 seconds operation, the engine was run at the idle engine condition and the exhaust gas temperature at the outlet of DOC is slightly lower than the inlet position. When the exhaust gas flows through the catalyst, there is a heat loss to warm up the catalyst monolith. So, this causes a decrease in exhaust gas temperature at the outlet of DOC. This temperature gradient causes a few particles deposit on the catalyst substrate by the effect of thermophoresis deposition [83], so the total particle number has a slight decrease. However, as the temperature difference between the inlet and outlet of DOC becomes smaller or even identical, the effect of thermophoresis deposition is less significant. This phenomenon can be observed after the 800 seconds operation. The total particle number at the outlet of a used DOC will be higher than the inlet position. In the operation period of 1000 to 2000 seconds, the increase in total particle number can be attributed to the particle blow-out process. It is because the engine is accelerated in this period and the velocity of exhaust gas passing through the catalyst channel is also increased. This would make it easier to blow the particles away from the surface of substrate and the oxidation process will not be activated effectively by such low exhaust gas temperature (i.e. $T_g \approx 100$ °C). However, as the exhaust gas temperature is increasing, the oxidation process of particle becomes

more active. The catalyst oxidises the adsorbed HC (i.e. SOF) on the particle surface and causes more smaller particles to be emitted. Hence, the particle number difference between the inlet and outlet of a used DOC at 100% of steady-state full engine load operation condition is more observable than that in the acceleration period (i.e. 1000-2800 seconds). Similarly, as the engine condition changes from 100% of full engine load to idle condition at the period of 3700 to 5600 seconds, the effect of the oxidation process becomes smaller along with the decreasing exhaust gas temperature. Even the particle oxidation process becomes less significant, the particle blow out process still exists inside the DOC. So, the total particle concentration at DOC outlet is still higher than DOC inlet.

Based on these experimental results, it is found that if the catalysts are saturated with the exhaust particle, the total particle number at the outlet of DOC will become higher as the vehicle is under the fast engine acceleration or even deceleration condition. In real world driving condition, the driver has always experienced the fast engine acceleration and deceleration modes on the road. This phenomenon has an adverse effect on the exhaust particle emission from the diesel vehicle.

6.3.5 Removal particle deposition efficiency inside a fresh DOC

The removal deposition efficiency of diesel particle inside a fresh DOC was determined in Chapter 5. The calculated overall removal efficiencies of solid particle by the catalyst for different engine conditions are presented in Figure 6.20. The results have combined the effect of the deposition mechanisms of gravitational settling, Brownian diffusion, thermophoresis, electrostatic deposition and inertial impaction. It should be noted that the calculated efficiencies are only presented for particle size in the range of 15 nm to 670 nm based on the present experimental particle results.

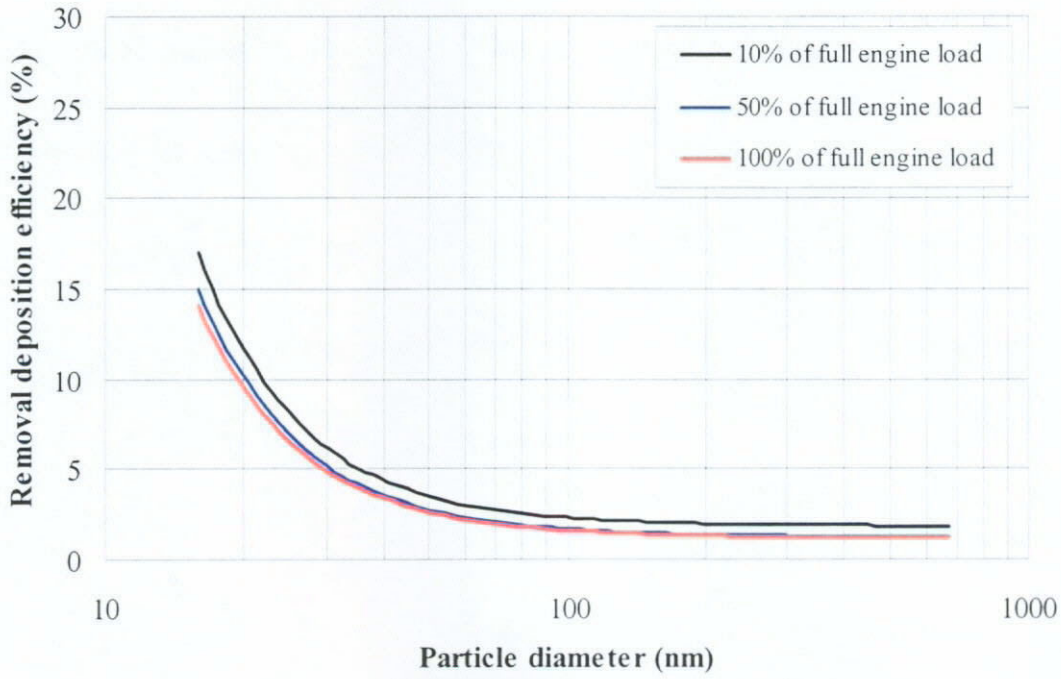

Figure 6.20 Calculated overall removal deposition efficiencies of solid particle of a fresh DOC for different engine load conditions.

In the gravitational settling calculation, the terminal velocities of the nanoparticles are considerably small because the particle sizes are extremely small. The terminal settling velocity for the particle size of 15 nm is about 7.3×10^{-9} m/s, whereas the larger particle of 670 nm also has 1.3×10^{-5} m/s. These small numbers of terminal settling velocities cause deposition efficiencies in the present particle size range less than 0.01%. Furthermore, the diffusion coefficients for the nanoparticles are also very small and have a range of 5.0×10^{-8} to 2.7×10^{-10} m^2/s in the present particle range. These low diffusion coefficients reduce the average mass transfer coefficient and cause the deposition efficiencies to become very low. The Brownian deposition efficiency only has a value of less than 0.01%. For the inertial impaction, the calculated Stokes numbers for the present particle size range are smaller than 0.25 because the particle sizes are extremely small. These nanoparticles are able to follow the streamline to prevent impacting on the substrate surface. Consequently, the inertial impaction for the particle deposition on the catalyst substrate can also be neglected. From the above results, it is found that the particle removal deposition efficiency of the gravitational settling, Brownian diffusion and inertial impaction mechanisms is relatively small, and hence the effects of these mechanisms on the particle deposition inside the DOC can be neglected.

In the calculation of thermophoresis, even testing conditions are steady-state, there are still temperature difference between the inlet and outlet of the catalyst. The temperature difference between the catalyst inlet and outlet of DOC under the 10%, 50% and 100% of full engine load conditions were 20°C, 14°C and 15°C, respectively. Because of these temperature gradients, the deposition efficiency due to thermophoresis contributes 1-2% of total particle deposition efficiency in the present particle size range. On the other hand, the results in Figure 6.20 show that there is significant removal deposition efficiency in the nuclei mode particle. The removal deposition efficiency decreases from the maximum value of 18% at 15 nm diameter to the minimum value of 2% at 680 nm diameter. This particle removal deposition efficiency can be attributed to the electrostatic deposition which occurs when the exhaust particle is flowing through the catalyst substrate. It is because the nuclei mode particles have higher electrical mobility, Z, than the accumulation mode particles [83], so the nuclei mode particle is charged more easily and a higher removal efficiency is obtained in this particle mode. It leads to the thermophoresis and electrostatic deposition dominating the diesel particle deposition on catalyst surface.

After investigating the removal deposition efficiency of the nanoparticles on the catalyst substrate, it was found that only 2-18% reduction of the nuclei and

accumulation mode particle number concentration can ascribe to this phenomenon. The remaining reduction efficiency is due to the oxidation of the catalyst. From the result of Table 6.3, Catalyst-B can reduce 19%, 29% and 45% of nuclei mode particle under the 10%, 50% and 100% of full engine load condition, respectively. Among these percentage reductions, about 15% of reduction is due to the particle deposition and the rest of 4%, 14% and 30% of reduction under 10%, 50% and 100% of full engine load condition was attributed to the oxidation process.

6.4 Performance of DOC on the Diesel Exhaust Gaseous Emissions

6.4.1 Gaseous emissions reduction for different engine load conditions

The effect of diesel oxidation catalyst on the exhaust gaseous emissions is also an indication of the intrinsic characteristic of the catalyst. The results of the exhaust gaseous emissions with or without installing the DOC were measured by a series of instruments which are described in Chapter 4. The measured data in volume basis were then converted into a mass emission rate. The mass emission rate and volume concentration of CO, HC and NOx with and without the installation of DOC for different engine load conditions are presented in Figures 6.21 to 6.26. The exhaust gas temperature at the inlet of DOC is a critical factor affecting the oxidation of the catalyst as shown in these figures. In the present study, the exhaust gas

temperature at the DOC inlet (Ti) ranges from 125°C to 250°C, depending on the engine condition.

CO emission

In Figure 6.21, the result shows that the emission of CO without installing used DOCs is decreased as the engine load is increased. The reason for this phenomenon can be attributed to the low exhaust gas temperature at the low engine load condition. CO is one of the compounds formed during the intermediate combustion stages of hydrocarbons fuels, as combustion proceeds to completion, the oxidation of CO to CO_2 occurs through recombination reactions between CO and the different oxidants. If these recombination reactions are incomplete due to the lack of oxidants or due to the low gas temperatures, CO will be left without oxidation. At low engine load, the gas temperature inside the engine combustion chamber is relatively low and very little oxidation reaction takes place under such short residence time of the combustion. The CO emission is higher in this circumstance. An increase in engine load results in lower CO emission because of the increased gas temperature and elimination reaction of CO formation [116]. Hence, the CO emission decreases gradually with an increase in engine load.

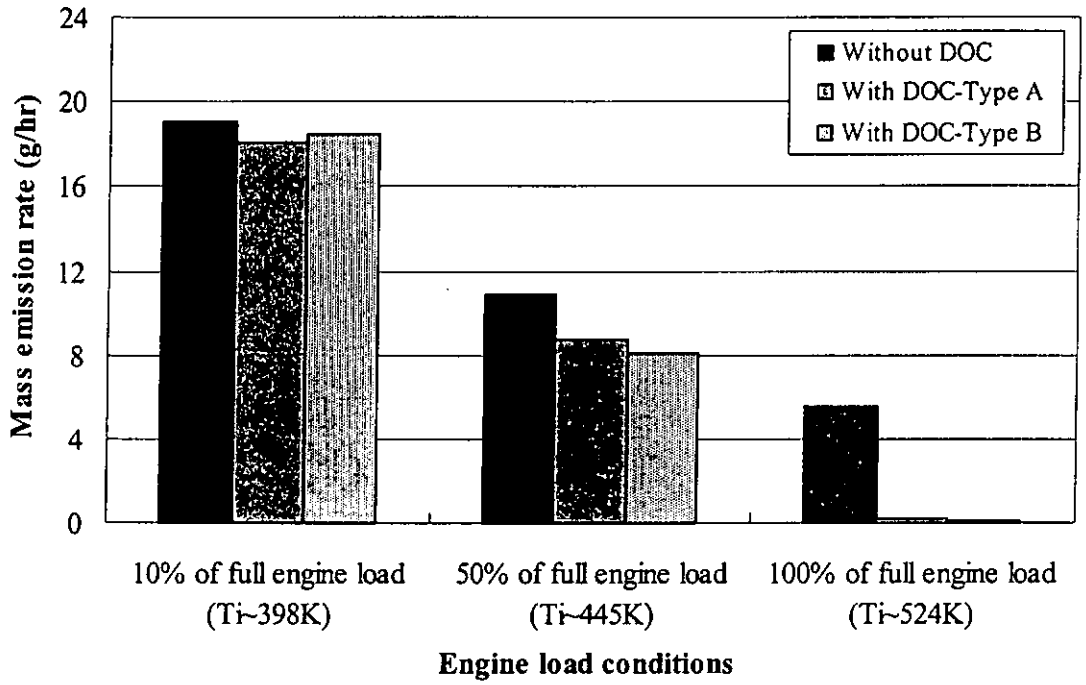

Figure 6.21 Comparison of mass emission rate of CO with and without the installation of used DOCs for different engine load conditions.

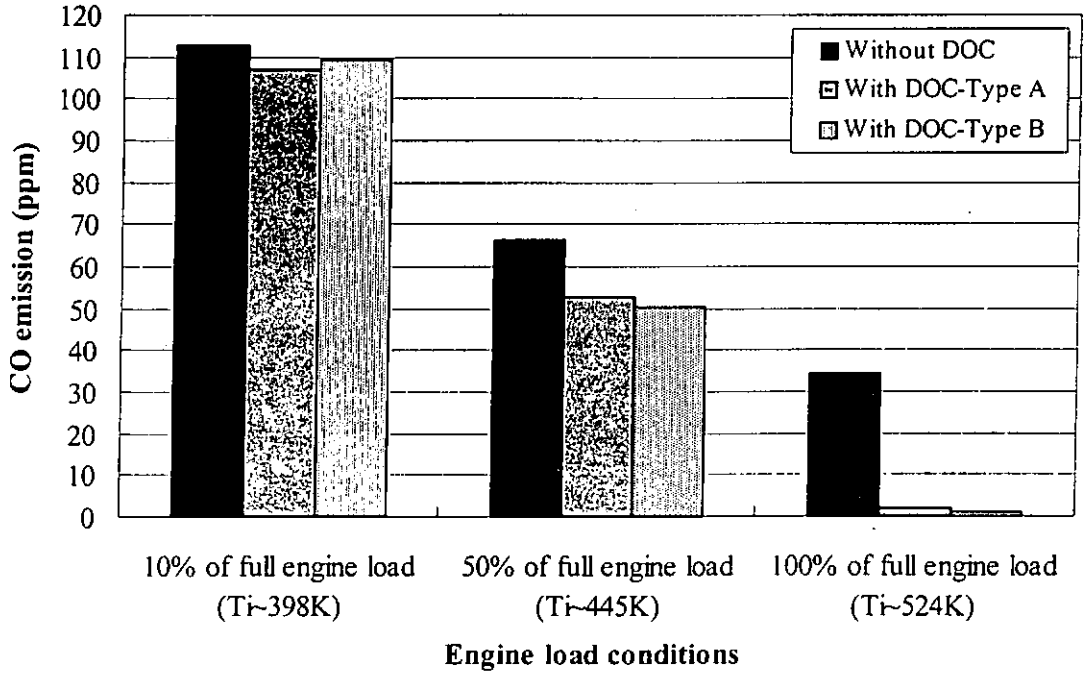

Figure 6.22 Comparison of volume concentration of CO with and without the installation of used DOCs for different engine load conditions.

The reduction rates for the DOC-Type A and B oxidising the CO are also lower at the low engine load condition. It is because the low exhaust gas temperature (i.e. 125°C) cannot activate the oxidation process of the DOC. When the exhaust gas temperature increases gradually, the oxidation process will be triggered to oxidise the CO to CO_2. This chemical reaction can be expressed by Equation 6.4. The reaction rate is highly dependent on the gas temperature. Once the engine is operated at 100% of full engine load at maximum torque speed of 2200 rpm and the exhaust gas temperature reaches 250°C, the oxidation process will become faster. The DOC can reduce the exhaust CO emission up to 97% for catalyst A and 98% for catalyst B.

$$CO + \frac{1}{2}O_2 \rightarrow CO_2 \qquad (6.4)$$

HC emission

The results of HC emission also demonstrate that the highest emission level was found at the low engine load condition as shown in Figure 6.23 and 6.24. The value of HC emission decreases slightly at the 50 % of full engine load but it increases again at the 100% of full engine load. It is the fact that the diesel fuel does not reach the wall of the engine combustion chamber and the fuel concentration in the core is small at the low engine load condition. Under these conditions, the HC emission originates mainly from the downstream edge of the fuel spray. The increase

in the local temperature, due to subsequent combustion of the rest of the fuel spray, is very small, and the oxidation reaction rate is also very slow. Thus, HC emission has the highest value at the low engine load condition. At 50% of full engine load, the fuel supplied to the engine is increased. This causes an increase in fuel-air ratio and more fuel is deposited on the walls and produces higher concentration in the core of fuel spray. The HC emission formed in these region increases; however, there is sufficient oxygen in the mixture so that, with increased temperature, the oxidation reaction is promoted and the HC emission is reduced. At 100% of full engine load, the fuel supplied to the engine is further increased. An increase in fuel-air ratio results in the formation of more HC molecules in the core of fuel spray and near the walls of the engine combustion chamber. The oxidation reaction is also limited due to the lack of oxygen, in spite of very high temperature reached [116]. Thus, this explains the reason for the HC emission increases at the full engine load condition.

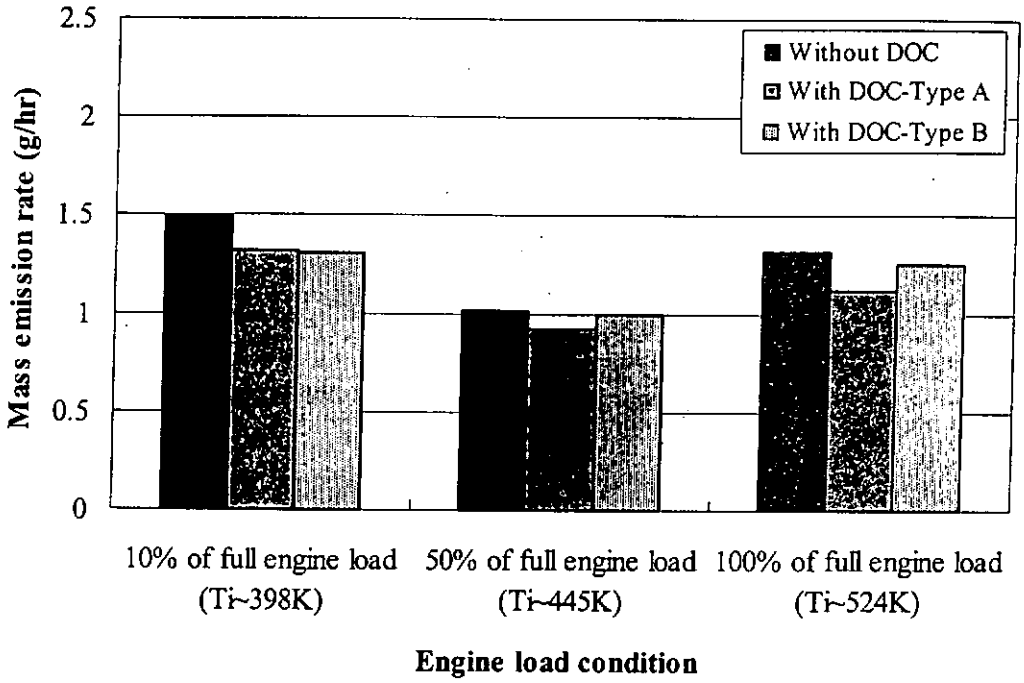

Figure 6.23 Comparison of mass emission rate of HC with and without the installation of used DOCs for different engine load conditions.

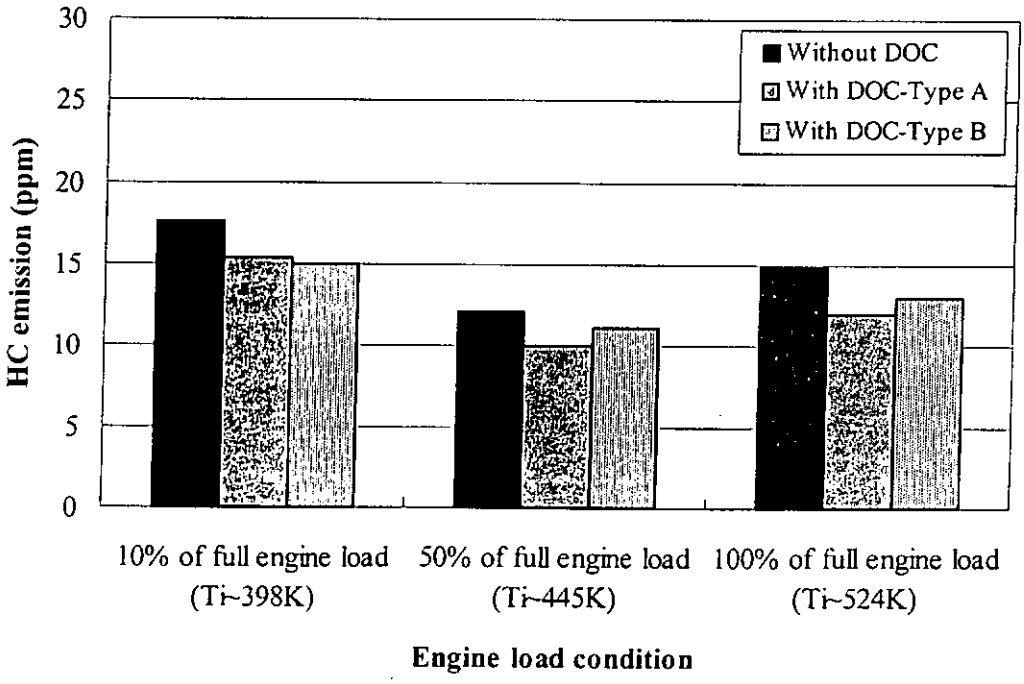

Figure 6.24 Comparison of volume concentration of HC with and without the installation of used DOCs for different engine load conditions.

In regard to the performance of DOC on the HC emission, the reduction rate is comparatively low as compared with the CO reduction even at the full engine load condition. The highest reduction occurs at the 100% of full engine load and the reduction rates of catalyst A and B are 14% and 4%, respectively. The catalyst A has a higher reduction than catalyst B because the zeolite-based catalyst has a higher ability to remove HC emission than Pt-based [117]. The reaction between the catalyst and HC gas molecules can be expressed by Equation 6.5. The catalyst oxidises the HC to H_2O and CO_2. The chemical reaction is also temperature dependent. It means that the oxidation process becomes faster as the exhaust gas temperature is higher. Thus, the reduction rate is more significant at 100% of full engine load condition than at 10% of full engine load condition. However, this reduction rate is still considered as a low reduction level. A substantial reduction in HC emission occurs when the exhaust gas temperature is greater than 250°C [85]. In fact, it is the highest temperature threshold in this present study. Consequently, the present result cannot reveal a significant reduction in HC emission.

$$C_yH_n + \left(1+\frac{n}{4}\right)O_2 \xrightarrow{RHC} yCO_2 + \frac{n}{2}H_2O \qquad (6.5)$$

NOx emission

The NOx emission is obviously increased with the increase in engine load and exhaust gas temperature as shown in Figure 6.25 and 6.26. At low engine load condition, the combustion gas temperature is lower. This leads to the slower reaction between the N_2 and O_2 and so the NOx emission is also lower. As the engine load is increased to the engine full load condition, the combustion gas temperature is, therefore, increased and it causes more N_2 gas to react with O_2 gas to form the NOx.

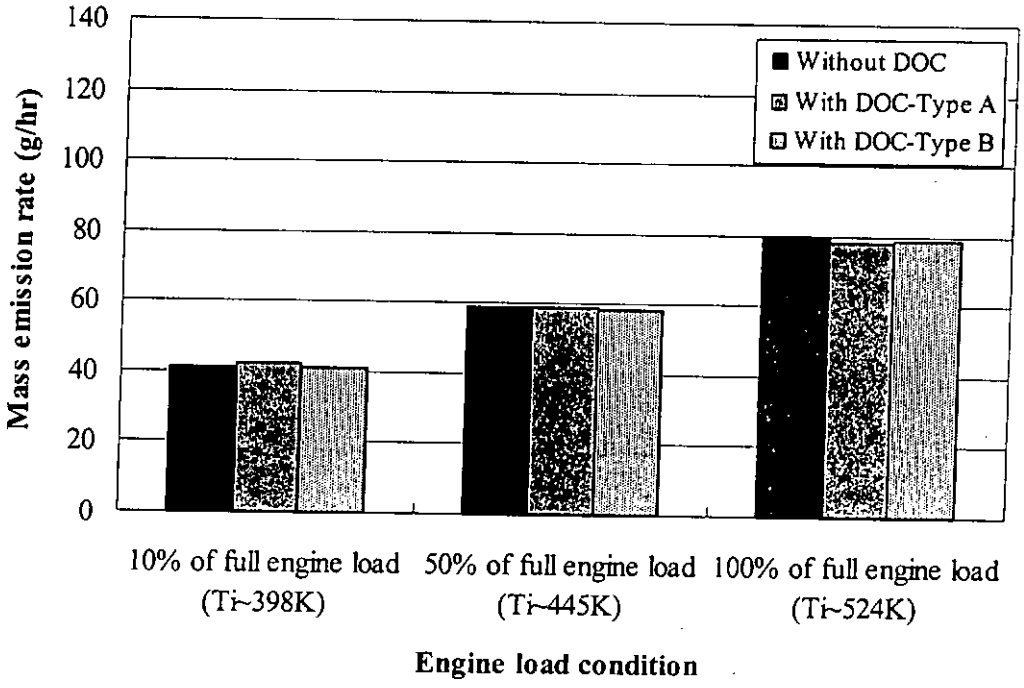

Figure 6.25 Comparison of mass emission rate of NOx with and without the installation of a used DOC for different engine load conditions.

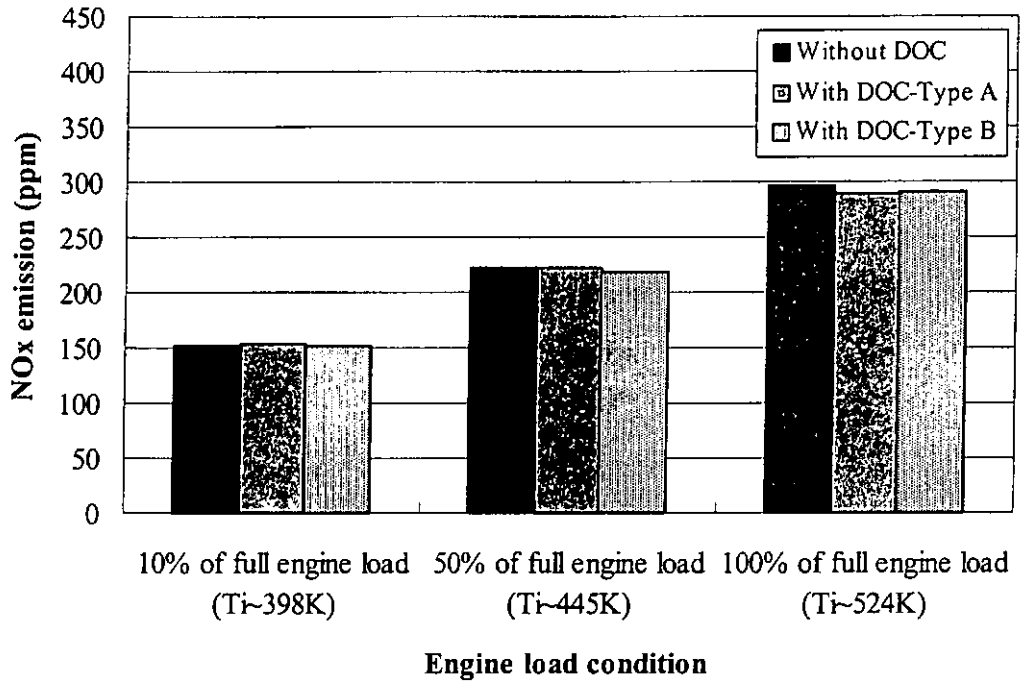

Figure 6.26 Comparison of volume concentration of NOx with and without the installation of a used DOC for different engine load conditions.

Indeed, the present DOC does not have the capability of reduction in the NOx emission as shown in Figure 6.25 and 6.26. Both catalysts only affect the NOx emission slightly under different engine load conditions. These results form a consensus to the previous investigation by Brown et al. [118]. It is because the oxidation catalyst is designed for reducing the CO, HC and smoke level, rather than abating the NOx emission. The present study shows that the DOC does not have an adverse effect on the NOx emission. Hence, the NOx emission will not be considered in the subsequent tests.

6.4.2 Fast engine acceleration response of a used DOC on gaseous emissions

Due to the fact that the fast engine acceleration mode is always experienced by the driver in the Hong Kong driving conditions, the performance of the oxidation catalyst for the fast engine acceleration condition is considerably important for the urban air quality. Both DOCs have the same tendency of reducing gaseous emissions, only the results of catalyst A are presented in the present study.

Exhaust gas temperature distribution at the inlet and outlet of DOC

The exhaust gas temperature distributions at the inlet and outlet of a used DOC are presented in Figure 6.27. The result shows that the exhaust gas temperature is quite steady at the first 400 seconds steady-state idle condition but the inlet and outlet of DOC still have a temperature difference between. This is caused by the heat loss which warms up the catalyst substrate; therefore, a lower exhaust gas temperature would be detected at the outlet of DOC. After the 400 seconds testing, the engine is subjected to a fast engine acceleration to 100% load and 2200 rpm, so its exhaust gas temperature increases substantially. The engine would be operated in this condition for 1400 seconds and the exhaust gas temperature rises gradually to a maximum value of 235°C. The engine load is removed at 1800 seconds and the exhaust gas temperature before DOC commences to drop evidently, whereas the outlet temperature decreases slowly. The outlet temperature is higher than the inlet

temperature in the period of 1800 to 3000 seconds because of the time lag of the exhaust temperature. When the engine load is removed, the inlet temperature of DOC would decrease immediately. However, the catalyst substrate is still hot. Heat would be transferred from the catalyst substrate to the exhaust gas passing through it. After this period, this phenomenon would reverse and be similar to the first 400 seconds due to the substrate becoming cold.

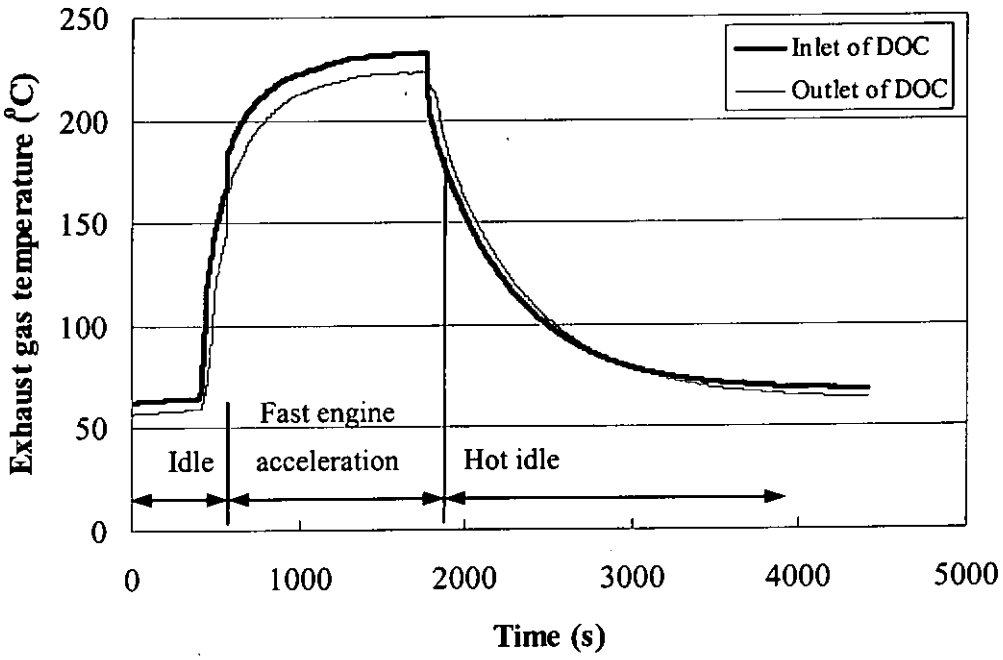

Figure 6.27 Exhaust gas temperature against operation time at the inlet and outlet of a used DOC for the fast engine acceleration and idle conditions.

CO and HC emissions

The response of CO and HC emissions at the inlet and outlet of a used DOC for the fast engine acceleration mode are presented in Figures 6.28 and 6.29,

respectively. The results show that a fast engine acceleration mode would cause the CO and HC emissions to increase drastically in a short period. The sudden increase in these emissions is due to a considerable amount of fuel which is suddenly supplied to the engine combustion chamber. At that time, the air supply cannot adjust immediately to an adequate fuel-air ratio. This causes more incomplete combustion sprays inside the engine chamber and more gaseous pollutant would be formed. During this fast engine acceleration mode, the exhaust gas temperature increases from 80°C in accordance with Figure 6.28. Although such temperature (i.e. 80°C) is not high enough to activate effectively the DOC to oxidise the gaseous emissions, it still has a slight enhancement on the oxidation process. As a result, it shows that the CO concentration at the outlet of a used DOC is lower than the inlet of a used DOC for the operation time is less than 650 seconds, as shown in Figure 6.28. Until the exhaust gaseous temperature rises above 150°C at 650 seconds of the fast engine acceleration condition, the DOC starts to enhance the oxidation process effectively. From the Figure 6.28, it completely oxidises the CO emission at 1000 seconds at which the exhaust gas temperature is about 220°C and reduces a certain level of HC emission. In the fast engine acceleration mode, the catalyst is not ready to perform effectively during the oxidation process in the first 200 seconds, but it reaches its maximum gas emission reduction at about 550 seconds. The reason for this

phenomenon can also attribute to the hot exhaust gas temperature which heats up the catalyst substrate and activates the oxidation process. From the results, it was found that the oxidation process of the catalyst is not only affected by the cold start of the vehicle, but also the initial stage of a fast engine acceleration mode would influence the performance of the DOC even when it has been operated for a long period of idle condition.

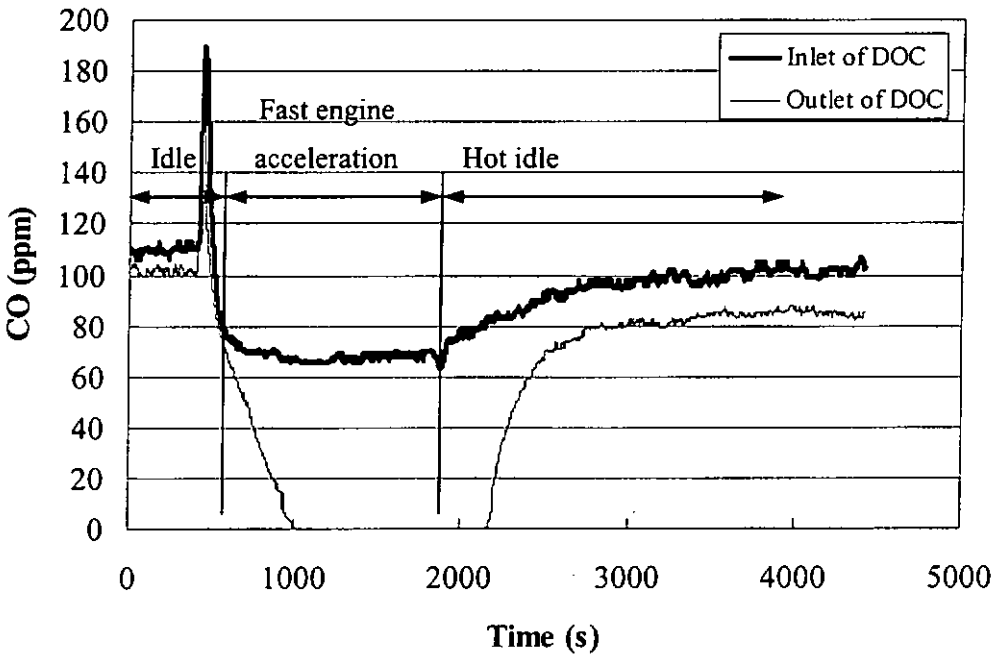

Figure 6.28 CO emission against the operation time of a used DOC for the fast engine acceleration and idle conditions.

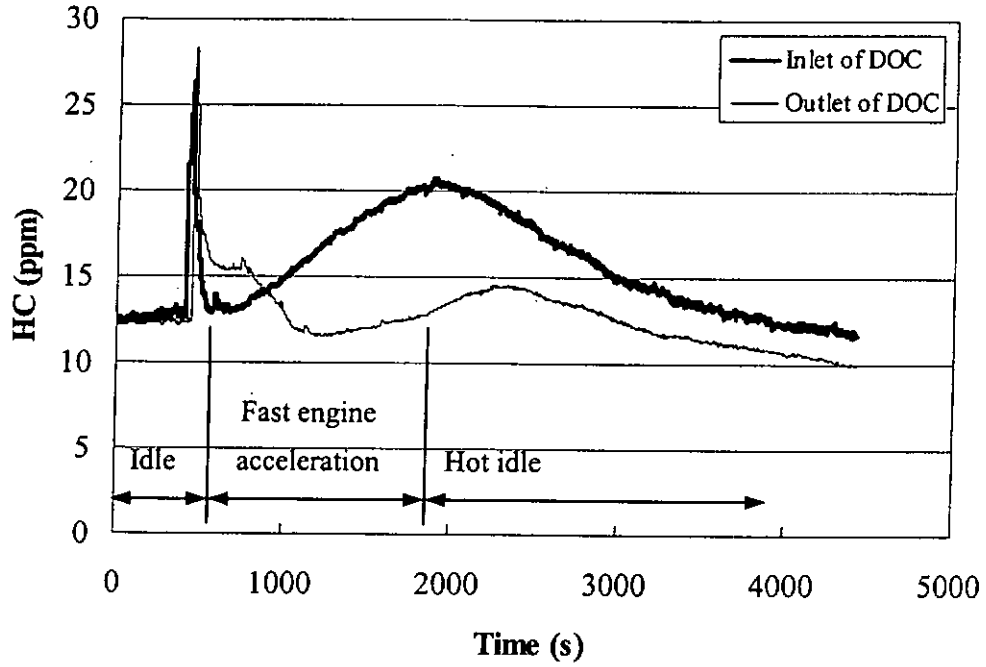

Figure 6.29 HC emission against the operation time of a used DOC for the fast engine acceleration and idle conditions.

6.4.3 Chemical kinetic analysis on the reduction rate of gaseous emissions along the exhaust gas temperature

The experimental reduction rate of gaseous emissions of the oxidation catalyst varies with the exhaust gas temperature as illustrated in Figure 6.30. It clearly shows that the reduction rate of gaseous emissions increases with the increasing exhaust gas temperature. The results can also be explained by the chemical kinetic analysis on the reaction rate against temperature as shown in Figure 6.31. From the chemical kinetic analysis, it is found that the increase in gaseous temperature would promote the reaction rate of $CO \rightarrow CO_2$ (RCO) and $HC \rightarrow H_2O+CO_2$ (RHC), simultaneously. From the experimental results, the CO

emission can be fully oxidised when the exhaust gas temperature is over 170°C, whereas the HC emission only has about 38% maximum reduction rate at the highest temperature. So, the performance of the DOC in reducing the CO emission is much better than the HC emission. This phenomenon also unveils in the results of the chemical kinetic analysis.

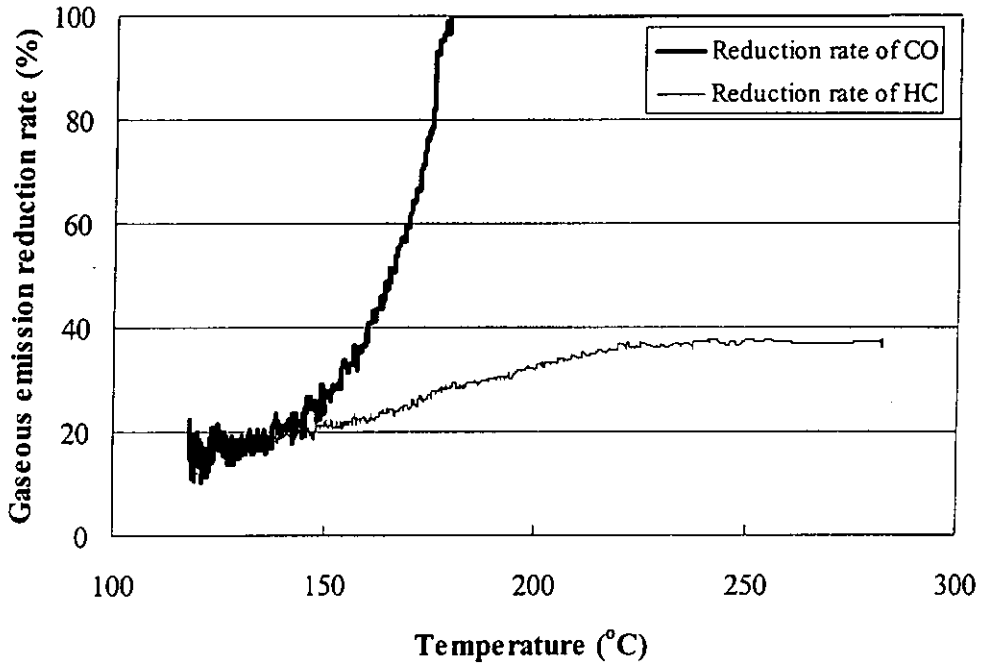

Figure 6.30 The reduction rate of CO and HC emissions along the exhaust gas temperature.

In Figure 6.31, it shows that the reaction rate of CO (RCO) is much higher than HC (RHC) in any exhaust gas temperatures. It is also observed that the reduction rate of the oxidation process is not only dependent on the gas temperature, but also the activation energy (E_a) which is another crucial parameter affecting the

chemical reduction rate. The activation energy for HC (i.e. $E_{a,HC}$ = 121 kJ/mol) oxidation process is higher than the CO oxidation process (i.e. $E_{a,CO}$ = 104 kJ/mol). This implies that the HC gas requires a higher energy to activate the oxidation process than the CO gas. Hence, during the same exhaust gas temperature, the chemical reaction rate of CO oxidation process is faster than the HC oxidation process.

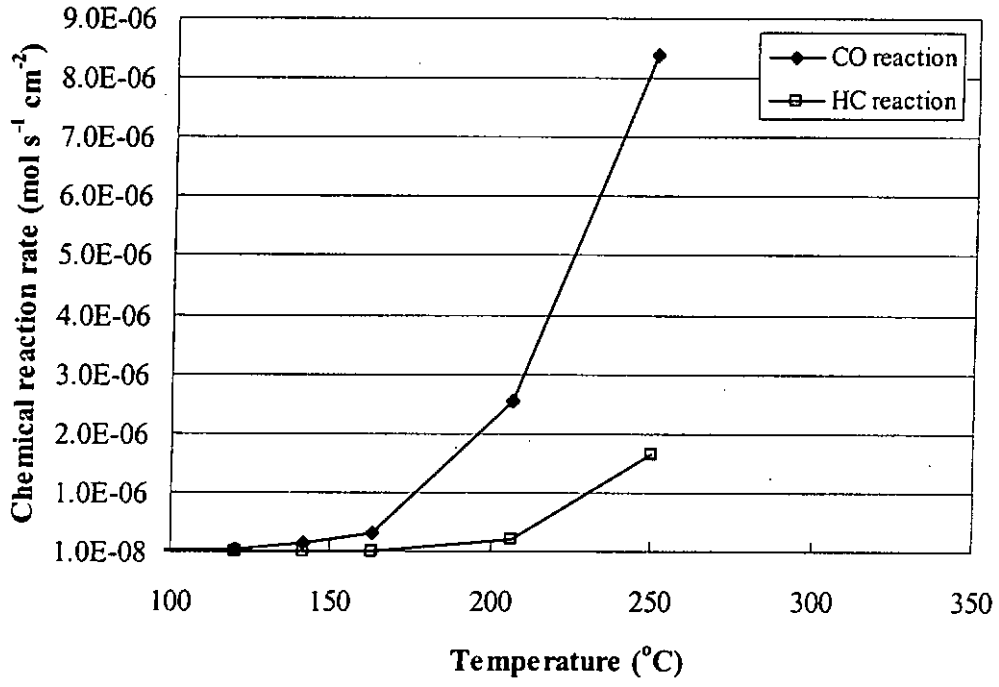

Figure 6.31 The chemical reaction rate of CO and HC emissions along the exhaust gas temperature.

From the present results, the light-off temperature for CO emission is about 170°C. This light-off temperature is an acceptable value and benefit in most of Hong Kong traffic conditions because the diesel vehicles have not ever been driven in

maximum power in the urban carriageway of Hong Kong. It leads to the exhaust gas temperature always remaining at the low exhaust gas level. Based on our on-road light-duty vehicle study on the performance of DOC in Hong Kong in Chapter 3, it shows that at more than 90% of the total travel time, the exhaust gas temperature is higher than 175°C. This illustrates that the DOC is always able to oxidise the gaseous emissions under the Hong Kong driving conditions.

Chapter 7 Conclusions and Recommendations for Future Work

7.1 Conclusions

The combined effects of diesel oxidation catalyst (DOC) and ultra low sulphur diesel (ULSD) fuel on the characteristics of diesel exhaust gaseous and particle emissions under a diesel engine dynamometer test bed using a steady-state mode cycle of the standard Economic Commission for Europe Regulation 49 test modes for different engine loads and idle to fast engine acceleration conditions have been investigated by using the developed gaseous emissions measurement system in accordance with the SAE standard and the EDS particle emission measurement system. In the absence of a standard diesel exhaust particle sampling measurement system to characterise the particle number and size distributions for different engine loads conditions (from 10% to 100% of full engine load at maximum torque speed), a mini-dilution tunnel sampling (MDTS) and an ejector diluter sampling (EDS) measurement systems have been established and studied. The particle number and volume concentrations, and the particle count median diameter (CMD) measured from these two developed systems have been evaluated to ascertain the most reliable diesel exhaust particle sampling measurement system that can minimise particle transformations (i.e. nucleation, condensation and coagulation) which take place

during dilution process affecting the exhaust particle number and size distributions during the dilution process.

The experimental results show that the EDS system measures a higher nuclei mode particle number concentration than the MDTS system for the three designated engine load modes: 10%, 50% and 100% of full engine load by a factor of about 2, 3 and 25, respectively. In contrast, it obtains a lower accumulation mode particle than the MDTS system. The measured results also show that the MDTS system shifts the particle CMD from below 50 nm (i.e. nuclei mode particle) to a larger particle diameter about 60 to 90 nm (i.e. accumulation mode particle), in addition to showing the particle number and volume distributions for all engine load conditions. It is mainly because the mini-dilution tunnel leads to particle transformation of nucleation and condensation simultaneously when the exhaust particle emissions are cooled and diluted. The MDTS measurement system uses compressed air at 23°C for the diluent. It causes two major particle transformations and affects the exhaust particle number and size distributions during the dilution process. Firstly, the compressed air causes the exhaust particles to become a supersaturation mixture. The condensation of vapour molecules will then take place and cause the nuclei mode particles to grow up to become the accumulation mode particles. Secondly, the compressed air also causes particle nucleation during the dilution process, leading the MDTS system to measure

two times higher of the total particle number concentration than the EDS measurement system. These two disadvantages will definitely affect the accuracy of exhaust particle measurements and cause deviation of the particle number and size distribution from the actual condition. However, the effect of coagulation on the total number particle concentration is shown to be negligible due to the short residence time (i.e. 1.2 seconds). It only causes 0.15% of reduction in the total number particle concentration.

On the other hand, the EDS measurement system can minimise the particle transformations taking place on the diesel exhaust particle number and size distribution during the heated dilution process. It has the advantage of reducing the vapour pressure of volatile components in the exhaust samples during the dilution process, and it can prevent the exhaust samples to become a supersaturation mixture and the advent of particle nucleation and condensation during the dilution process. The residence time for the EDS measurement system is found to be only 0.1 second. Hence, the coagulation effect on the total number particle concentration is less than 0.1% and it can be neglected. It is shown that the EDS measurement system can minimise the particle transformations taking place and provide more reliable exhaust particle number and size distributions than MTDS measurement system.

For a fresh catalyst of DOC, no matter what type, it can substantially reduce the nuclei mode particle number concentration from 17% to 50% and slightly increase the accumulation mode particle concentration from 1% to 7% when the diesel engine load increases from 10% to 100% of full engine load at the maximum torque speed. It also shows that the fresh catalyst can reduce 15% to 49% of the total particle number concentration and 24% to 75% of the total particle mass concentration when the diesel engine load increases from 10% to 100% of full engine load at maximum torque speed. However, the alteration level of particle CMD is not pronounced as it only reduces the particle CMD from 1 to 3 nm for different engine load conditions. The significant reduction of nuclei mode particle concentration is mainly due to the oxidation process taking place in the catalyst. When the diesel exhaust gas passes through the monolith substrate of DOC, the catalyst will oxidise a considerable amount of SOF (i.e. nuclei mode particle) to H_2O and CO_2, hence it leads to 14% to 35% reduction in the nuclei mode particle concentration. The remaining 3% to 15% reduction in nuclei mode particle number concentration comes from the dominant particle thermophoresis and electrostatic deposition mechanism inside the catalyst.

Between the nucleation and accumulation particle modes, it is shown that the used catalyst increases 60% of the particle number concentration in accumulation

particle mode (i.e. 650 nm) after 30 operation hours. It is because the oxidation process of catalyst removes the soluble organic fraction (SOF) from the surface of coarse particles and causes a considerable amount of smaller particles to be formed. In addition, the total particle number concentration is increased when the blow out of the deposited particles from the surface of catalyst substrate is taking place. It is also found that the advent of the negative reduction (or increasing) of particle number concentration in the first 10 operation hours of DOC is located at the particle diameter range of about 300 nm. However, the negative reduction is shifted to the particle diameter range of 80 nm after 40 operation hours. The negative reduction tends to appear in smaller particles when the operation period is longer. In the fast engine acceleration condition, the results show that the used DOC increases the total particle number concentration during the acceleration period. It is because the accelerated engine produces a higher velocity of exhaust gas which passes through the catalyst channel. Hence, it is easier to blow the particles away from the surface of catalyst substrate and increases the total particle number concentration.

In the aspect of diesel exhaust gaseous emissions, it is found that the installation of a used DOC can reduce the gaseous emissions from 10% to 97% for CO emission and 4% to 14% for HC, but increase the exhaust gas temperature from 125°C to 250°C when the diesel engine load increases from 10% to 100% of full

engine load at maximum torque speed. The lower reduction rate in HC emission can be ascribed to the fact that the required activation energy for the oxidation process of HC is higher than the oxidation of CO. In general, the reduction rate of gaseous emissions increases with increasing exhaust gas temperature. However, there is no reduction effect on the NOx emission with installing the DOC. In the fast engine acceleration test, it is shown that there is no significant reduction of gaseous emissions in CO and HC at the initial stage until the oxidation process of catalyst takes place at about 200 seconds.

7.2 Recommendations for Future Work

In the present study, the established diesel exhaust gaseous and particle emissions measurement systems have shown to provide a very reliable and repeatable exhaust particle number concentration and size distribution, and gaseous emission results from the diesel engine dynamometer test bed. The developed measurement systems can be used directly to characterise the real-time gaseous and particle emissions from a vehicle under different driving cycles on the chassis dynamometer or the advanced aftertreatment device such as the selective catalytic reduction (SCR) and continuous regeneration trap (CRT) due to the evolution of low vehicle emission standard control.

If the road vibration problem on the measurement systems can be solved, then these developed systems can be fitted into the on-road vehicle, then the real-time exhaust gaseous and particle emissions for the driving cycle in Hong Kong can be extracted directly from the exhaust tailpipe of vehicle. Those emission data will be highly valuable for providing the insight of real-world vehicle emissions and establishing the dispersion of gaseous and particulate emissions from a moving vehicle in Hong Kong condition.

On the other hand, the result of DOC investigation on particle emission shows that the zeolite-based catalyst might perform better than the Pt-based catalyst when the size of the particle was smaller, as shown in Figures 6.7, 6.8 and 6.9. It has not been fully investigated in the present study. Hence, it is worth further investigating whether the zeolite-based catalyst has a higher ability to reduce the smaller particle than Pt-based catalyst.

References

1. Hong Kong Government, "White Paper: Pollution in Hong Kong- A Time to Act". (1989).

2. Stoke, M. Opening Remarks, *Proceedings of Diesel Vehicle Exhaust Treatment Technology and Motorcycle Emission Workshop 1999*, The Hong Kong Polytechnic University, Hong Kong. 11-12 Jan., (1999).

3. The Chief Executive, the Honorable Tung C.H. of HKSAR, "The 1999 Policy Address". Hong Kong, pt.99 (1999).

4. Sydbom, A., Blomberg, A., Parnia, S., Stenfors, N., Sandström, T. and Dahlén, S-E. "Health effects of diesel exhaust emissions". *European Respiratory Journal*, Vol. 17, pp.733-746 (2001).

5. Walsh, M.P. "Pollution from diesel vehicles worldwide survey on retrofit catalyst technology". *HKEPD-Consultancy report*, pp.4 (1999).

6. Scheepers, P.T.J. and Bos, R.P. "Combustion of diesel fuel from a toxicological perspective I. Origin of incomplete combustion products". *International Archives of Occupational and Environmental Health*, Vol. 64, pp.149-161 (1992).

7. Greenwood, S. J., Coxon, J. E., Biddulph, T. and Bennett, J. "An investigation to determine the exhaust particulate size distributions for diesel, petrol, and compressed natural gas fuelled vehicles". *Society of Automotive Engineers (SAE)* 961085 (1996).

8. Yoshino, S. and Sagai, M. "Enhancement of collagen-induced arthritis in mice by diesel exhaust particles". *The Journal of Pharmacology and Experimental Therapeutics*, Vol. 290, pp.524-529 (1999).

9. Schwartz, J., Dockery, D.W. and Neas, L.M. "Is daily mortality associated specifically with fine particles?". *Journal of the Air & Waste Management Association*, Vol.46, pp.927-939 (1996).

10. Donaldson, K., Li, X. Y. and MacNee, W. "Ultrafine (nanometre) particle mediated lung injury". *Journal of Aerosol Science*, Vol.29, pp.553-560 (1998).

11. EU Directive 94/12/EC of the European Parliament and the Council relating to measures to be taken against air pollution by emissions from motor vehicles and amending Directive 70/220/EEC. *Official Journal of the European Communities*. No. L100 (1994).

12. Stone, V. and Donaldson, K., "Small particles- big problems". T*he Aerosol Society newsletter* No.33, Sept., (1998).

13. Harrison, R. M., Jones, M. and Collins, G. "Measurement of the physical properties of particles in the urban atmosphere". *Atmospheric Environment,* Vol. 33, pp.309-321 (1999).

14. Joumard, R. and Perrin, M. L. "Measurement of particle and gaseous pollution of the atmosphere due to buses". *The Science of the Total Environment,* Vol. 76, pp.55-62 (1988).

15. Kittelson, D., Johnson, J., Watts, W., Wei, Q., Drayton, M., Paulsen, D. and Bukowiecki, N. "Diesel aerosol sampling in the atmosphere". *Society of Automotive Engineers Technical Paper,* 2000-01-2212 (2000).

16. Whitby, K. T., Clark, W. E., Marple, V. A., Sverdrup, G. M., Sem, G. J., Willeke, K., Liu, B. Y. H. and Pui, D. Y. H. "Characterization of California Aerosols-I. Size Distribution of Freeway Aerosol". *Atmospheric Environment*, Vol. 9, pp. 463-482 (1975).

17. Brain, J.D. and Valberg, P.A. "Deposition of aerosol in the respiratory tract". *American Review of Respiratory Disease*, Vol. 120, pp.1325-1373 (1979).

18. Sequeira, R. and Lai, K. H. "The Effect of Meteorological Parameters and Aerosol Constituents on Visibility in Urban Hong Kong". *Atmospheric Environment*, Vol. 32, pp. 2865-2871 (1998).

19. Hung, W.T., Cheung, C.S., Yau, D., Hung, A., Tsang, M., Ha, K. and Mok, W.C. "Diesel vehicles emission control and its emissions benefits in Hong Kong". *Society of Automotive Engineers (SAE)*, 2001-01-0188 (2001).

20. Mooney, J.J. "Diesel engine emissions control requires low sulfur diesel fuel". *Society of Automotive Engineers (SAE),* 2000-01-1434, (2000).

21. Walsh, M.P. "The need for and benefits of low sulfur fuel". *Society of Automotive Engineers (SAE),* 2000-01-1433, (2000).

22. Clean Air Act, 42 U.S.C. s/s 7401 et seq. (1970) amended 1977, US EPA (1990). www.epa.gov/region5/defs/html/caa.htm.

23. The Air Quality (England) Regulations 2000. Statutory Instruments No. 928. Department for Environment, Food and Rural Affairs (2000). www.defra.gov.uk/environment/ airquality/airqual/index.htm.

24. Kruger, M., Luders, H., Luers, B., Kaufmann, R. Koch, W. and Kauffeldt, T. "Influence of exhaust gas aftertreatment on particulate characteristics of vehicle diesel engine". *Motortechnische Zeitschrift*, Vol. 58, (1997).

25. Wong C.P., Chan T.L., Leung C.W. and Cheung C.S., "Performance of Diesel Oxidation Catalyst for a Light Duty Vehicle under Hong Kong Driving Conditions", *Proc. of 6th Int. Conf. on Urban Transport and the Environment for 21st Century*, July 26-28, 2000, Cambridge, UK, pp.393-401 (2000).

26. Stone, R. *Introduction to internal combustion engines.* Third Ed., Macmillan Press Ltd., London (1999).

27. Meguerdicchian, M. and Waston, N. "Predication of mixture formation and heat release in diesel engines". *Society of Automotive Engineers (SAE)*, 780225 (1978).

28. Patterson, D.J. and Henein, N.A. *Emissions from combustion engines and their control.* Ann Arbor Science Publishers, Inc. Michigan (1972).

29. Greeves, G., Khan, I.M., Wang, C.H.T. and Fenna, I. "Origins of hydrocarbon emissions from diesel engines". *Society of Automotive Engineers (SAE),* 770259 (1977).

30. Glassman, I. *Combustion.* Third Ed., Academis Press Inc. USA (1996).

31. Nightingale, D. "A fundamental investigation into the problem of NO formation in diesel engines". *Society of Automotive Engineers (SAE)*, 750848 (1975).

32. Broome, D. and Khan, I.M. "The mechanism of soot release from combustion of hydrocarbon fuels with particular reference to the diesel engine". *Proceeding of Institute of Mechanical Engineers*, Paper C140/71 (1971).

33. Khan, I.M. "Formation and combustion of carbon in a diesel engine". *Proceeding of Institute of Mechanical Engineers*, Vol.184, Pt.3J (1969/70).

34. Stanmore, B.R., Brilhac, J.F. and Gilot, P. "The oxidation of soot: a review of experiments, mechanisms and models". *Carbon*, Vol. 39, pp.2247-2268 (2001).

35. Code of Federal Regulations 40-Protection of Environment, *Chapter I Environmental Protection Agency*, 86.110-90 (1990).

36. *SAE Handbook* Recommended Practice. "Constant Volume Sampler System for Exhaust Emission Measurement". Section 13. Emissions SAE J1094a, (1978).

37. Kittelson, D.B., Engine and nanoparticles: a review. *Journal of Aerosol Science.* Vol. 29, pp.575-588 (1998).

38. Tanaka, S. and Shimizu, T. "A study of composition and size distribution of particulate matter from DI diesel engine". *Society of Automotive Engineers (SAE)*, 1999-01-3487 (1999).

39. Hall, D. E., Stradling, R. J., Zemroch, P. J., Rickeard, D. J., Mann, N., Heinze, P., Martini, G., Hagemann, R., Rantanen, L. and Szendefi, J. "Measurement of the number and size distribution of particle emissions from heavy duty engines". *Society of Automotive Engineers (SAE)*, 2000-01-2000 (2000).

40. Luders, H., Kruger, M., Stommel, P. and Luers, B. "The role of sampling conditions in particle size distribution measurements". *Society of Automotive Engineers (SAE)*, 981374 (1998).

41. *SAE Handbook*- Information Report. "Determination of Sulfur Compounds in Automotive Exhaust". SAE J1280 JAN80 (1980).

42. Suzuki, J., Yamazaki, H., Yoshida, Y. and Hori, M. "Development of dilution mini-tunnel and its availability for measuring diesel exhaust particulate matter", *Society of Automotive Engineers (SAE)*, 851547 (1985).

43. Hirakouchi, N., Fukano, I. and Shoji, T. "Measurement of diesel exhaust emissions with mini-dilution tunnel". *Society of Automotive Engineers (SAE)*, 890181 (1989).

44. Hirakouchi, N., Fukano, I. and Nagano, H. "Measurement of unregulated exhaust emissions from heavy duty diesel engines with mini-dilution tunnel". *Society of Automotive Engineers (SAE)*, 900643 (1990).

45. Hood, J.F. and Silvis, W.M. "Predicting and preventing water condensation in sampled vehicle exhaust for optimal CVS dilution". *Society of Automotive Engineers (SAE)*, 980404 (1998).

46. Abdul-Khalek, I. S., Kittelson, D. B., Graskow, B. R., Wei, Q. and Brear, F. "Diesel exhaust particle size: measurement issues and trends". *Society of Automotive Engineers (SAE)*, 980525 (1998).

47. Pagan, J. "Study of particle size distribution emitted by a diesel engine". *Society of Automotive Engineers (SAE)*, 1999-01-1141 (1999).

48. Maricq, M. M., Chase, R. E., Podsiadlik, D. H. and Vogt, R. "Vehicle exhaust particle size distributions: A comparison of tailpipe and dilution tunnel measurements". *Society of Automotive Engineers (SAE)*, 1999-01-1461 (1999).

49. Wei, Q., Kittelson, D.B. and Watts, W.F. "Single-stage dilution tunnel performance". *Society of Automotive Engineers (SAE)*, 2001-01-0201 (2001).

50. Khair, M., Lemaire, J. and Fischer, S. "Achieving heavy-duty diesel NOx/PM levels below the EPA 2002 standards – an integrated solution". *Society of Automotive Engineers (SAE)*, 2000-01-0187 (2000).

51. Johnson, T.V. "Diesel emission control in review". *Society of Automotive Engineers (SAE)*, 2000-01-0184 (2000).

52. Degobert, P. *Automobiles and Pollution.* Warrendale, Pa., Society of Automotive Engineers (1995).

53. Heck, R.M., Farrauto, R.J. and Gulati, S.T., *Catalytic Air Pollution Control: Commercial Technology*. Second edition, John Wiley & Sons, Inc., New York, (2002).

54. Mogi, H., Tajima, K., Hosoya, M. and Shimoda, M. "The reduction of diesel engine emissions by using the oxidation catalysts on Japan diesel 13 mode cycle". *Society of Automotive Engineers (SAE)*, 1999-01-0471 (1999).

55. Voss, K., Adomaitis, J., Feldwisch, R., Borg, C.M., Karlsson, E. and Josefsson, B. "Performance of diesel oxidation catalysts for European bus applications". *Society of Automotive Engineers (SAE)*, 950155 (1995).

56. Brown, K.F. and Rideout, G. "Urban driving cycle results of retrofitted diesel oxidation catalysts on heavy duty vehicles". *Society of Automotive Engineers (SAE)*, 960134 (1996).

57. Tamanouchi, M., Morihisa, H., Araki, H. and Yamada, S. "Effects of fuel properties and oxidation catalyst on exhaust emissions for heavy duty diesel engines and diesel passenger cars". *Society of Automotive Engineers (SAE)*, 980530 (1998).

58. Hosoya, M. and Shimoda, M. "The application of diesel oxidation catalysts to heavy duty diesel engine in Japan". *Applied Catalysis B: Environmental*, Vol. 10, pp. 83-97 (1996).

59. Ferion, J., Oberdorster, G., and Penney, D.P. "Pulmonary retention of ultrafine and fine particles in rats". *American Journal of Respiratory Cell Molecular Biology*, Vol. 6, pp535-542 (1992).

60. Seaton, A., MacNee, W., Donaldson, K. and Godden, D. "Particulate air pollution and acute health effects". *The Lancet*, Vol. 345, pp.176-178 (1985).

61. Baumgard, K.J. and Johnson, J.H. "The effect of low sulfur fuel and a ceramic particle filter on diesel exhaust particle size distributions". *Society of Automotive Engineers (SAE) Transactions 101*, pp.691-699 (1992).

62. Ulfvarson, U. "Diesel-exhaust tests should be revised with respect to health-indicators". *Society of Automotive Engineers (SAE)*, 2000-01-0235 (2000).

63. Watson, A.Y., Bates, R.R., and Kennedy, D. (Editors), "Air Pollution, the Automobile and Public Health". National Academic Press (1988).

64. Rickeard, D.J., Bateman, J.R., Kwon, Y.K., McAughey, J.J. and Dickens, C.J. "Exhaust Particulate Size Distribution: Vehicle and Fuel Influences in Light Duty Vehicles". *Society of Automotive Engineers (SAE)*, 961980 (1996).

65. Cooper, B.J. and Roth, S.A. "Flow-through catalysts for diesel engine emissions control". *Platinum Metals Revision*, Vol. 35, pt. 4, pp.178-187 (1991).

66. Fukano, I., Sugawara, K., SaSaki, K., Honjou, T. and Hatano, S. "A diesel oxidation catalyst for exhaust emissions reduction". *Society of Automotive Engineers (SAE)*, 932958 (1993).

67. Ueno, H., Furutani, T., Nagami, T., Aono, N., Goshima, H. and Kasahara, K. "Development of catalyst for diesel engine". *Society of Automotive Engineers (SAE)*, 980195 (1998).

68. Horiuchi, M., Saito, K. and Ichihara, S. "The effect of flow-through type oxidation catalysts on the particulate reduction of 1990s diesel engines". *Society of Automotive Engineers (SAE)*, 900600 (1990).

69. Mayer, A., Matter, U., Scheidegger, Czerwinski, J., Wyser, M., Kieser, D. and Weidhofer "VERT: diesel nano-particulate emissions: properties and reduction strategies". *Society of Automotive Engineers (SAE)*, 980539 (1998).

70. Maricq, M. M., Chase, R. E., Xu, N. and Laing, P.M. "The effects of the catalytic converter and fuel sulfur level on motor vehicle particulate matter emissions: Light duty diesel vehicles". *Environmental Science & Technology*, Vol. 36, pp.283-289 (2002).

71. Blackwood, A., Tidmarsh, D. and Willcock, M. "The effect of an oxidation catalyst on cold start diesel emissions in the first 120 seconds of running". *Society of Automotive Engineers (SAE)*, 980193 (1998).

72. Zhao, H., Cheung, C.S. and Hung, W.T. "Investigation of motor vehicle on-road exhaust emissions behavior". *Journal of Combustion Science and Technology*, Vol. 5, pt.1, pp. 100-107 (1999).

73. German, J. "Observations concerning current motor vehicle emissions". *Society of Automotive Engineers (SAE)*, 950812 (1995).

74. Hakim, K.A.A., Youssef, M.M., EI-Tawwab, A. and Hassan, M.A. "Vehicle performance and exhaust emission on road". *Society of Automotive Engineers (SAE)*, 99087 (1999).

75. Sioutas, C., Abt, E., Wolfson, J.M. and Koutrakis, P. "Evaluation of the measurement performance of the scanning mobility particle sizer and aerodynamic particle sizer". *Aerosol Science and Technology*, Vol. 30, pp. 84-92 (1999).

76. Bielaczyc, P., Merkisz, J. and Pielecha, J. "Exhaust Emissions from diesel engine during cold start in low temperature condition". *World Automotive Congress*, FISITA, F20000H213, Seoul (2000).

77. Bielaczyc, P., Merkisz, J. and Pielecha, J. "Investigation of exhaust emissions from DI diesel engine during cold and warm start". *Society of Automotive Engineers (SAE)*, 2001-01-1260 (2001).

78. Hotta, Y., Nakakita, K., Inayoshi, M., Ogawa, T., Sato, T. and Yamada, M. "Combustion improvement for reducing exhaust emissions in IDI diesel engine" *Society of Automotive Engineers (SAE)*, 980503 (1998).

79. CONCAWE, "Motor vehicle emission regulations and fuel specifications-Part 2: Detailed information and historic review (1970-1996)". *Report No. 6/97, CONCAWE, Brussels.* (1997).

80. *SAE Handbook*- Recommended Practice. "Measurement of carbon dioxide, carbon monoxide, and oxides of nitrogen in diesel exhaust". Section 13. Emissions, SAE J177, pp13.01-13.05 (1995).

81. Biswas, P. "Measurement of high-concentration and high-temperature aerosols". In Willeke, K. and Baron, P. A., eds., *Aerosol Measurement: Principles, Techniques, and Applications*, Van Nostrand Reinhold, New York, pp.705-720 (1993).

82. Maricq, M. M., Chase R. E., Podsiadlik, D. H., Siegl, W. O. and Kaiser, E. W. "The effect of dimethoxy methane additive on diesel vehicle particulate emissions". *Society of Automotive Engineers (SAE)*, 982572 (1998).

83. Hinds, W. C. *Aerosol Technology: Properties, Behavior and Measurement of Airborne Particles*. Second Ed., John Wiley & Sons, Inc. (1999).

84. Chan, T.L., Dong, G., Cheung, C.S., Leung, C.W., Wong, C.P. and Hung, W.T. "Monte Carlo simulation of nitrogen oxides dispersion from a vehicular exhaust plume and its sensitivity studies". *Atmospheric Environment*, Vol.35, pp.6117-6127 (2001).

85. Kanesaki, N., Sekiya, Y., Shinzawa, M. and Aoyama, S. "Diesel particulate reduction by a catalytic converter". *JSAR Review*, Vol. 14 No.1 pp.49-51 9300800 (1993).

86. Code of Federal Regulations 40-Protection of Environment Chapter I Environmental Protection Agency, 86.345-79 pp.568-571 (1998).

87. Kayes D. and Hochgreb S., Investigation of the dilution process for measurement of particulate matter from spark-ignition engines, *Society of Automotive Engineers (SAE)*, 982601 (1998).

88. An American National Standard, Measurement Uncertainty, ANSI/ASME PTC 19.1 (1985).

89. Graskow B. R., Kittelson D. B., Ahmadi M. R. and Morris J. E., "Characterization of exhaust particulate emissions from a spark ignition engine, *Society of Automotive Engineers (SAE)*, 980528 (1998).

90. TSI Incorporated, Model 3934 SMPS (Scanning Mobility Particle Sizer) Instruction Manual, (1996).

91. Johnson, J.E. and Kittelson, D.B. "Deposition, diffusion and adsorption in the diesel oxidation catalyst". *Applied Catalysis B: Environmental*, Vol. 10, pp.117-137 (1996).

92. Johnson, J.E. and Kittelson, D.B. "Physical factors affecting hydrocarbon oxidation in a diesel oxidation catalyst". *Society of Automotive Engineers (SAE)*, 941771 (1994).

93. Weltens, H., Bressler, H., Terres, F., Neumaier, H. and Rammoser, D. "Optimisation of catalytic converter gas flow distribution by CFD prediction". *Society of Automotive Engineers (SAE)*, 930780 (1993).

94. Barris, M.A. "Development of diesel exhaust catalytic converter mufflers". *Society of Automotive Engineers (SAE)*, 920369 (1992).

95. Shah, R.K. and London, A.L. "Laminar flow forced convection in ducts". In Irvine, T.F. and Hartnett, J.P., eds., *Supplement to Advances in Heat Transfer*, Academic Press, pp.196-222 (1978).

96. Talbot, L., Cheng, R.K., Schefer, R.W. and Willis, D.R. "Thermophoresis of particles in a heated boundary layer". *Journal of Fluid Mechanics*, Vol.101, part 4, pp.737-758 (1980).

97. Kittelson, D.B., Pui, D.Y.H. and Moon, K.C. "Electrostatic collection of diesel particles". *Society of Automotive Engineers (SAE)*, 860009 (1986).

98. Kittelson, D.B., Reinertsen, J. and Michalski, J. "Further studies of electrostatic collection and agglomeration of diesel particles". *Society of Automotive Engineers (SAE)*, 910329 (1991).

99. Liu, B.Y.H. and Pui, D.Y.H., Rubow, K.L. and Szymanski, W.W. "Electrostatic effects in aerosol sampling and filtration". *The Annals of Occupational Hygiene*, Vol.29, No.2, pp.251-269 (1985).

100. Liu, B.Y.H. and Pui, D.Y.H. "Equilibrium bipolar charge distribution of aerosols". *Journal of Colloid and Interface Science*, Vol.49, pp.305-312 (1974).

101. Liu, B.Y.H. and Pui, D.Y.H. "Electrical neutralisation of aerosols". *Journal of Aerosol Science*, Vol.5, pp.465-472 (1974).

102. Logan, S.R. *Fundamentals of Chemical Kinetics*. Longman Group Limited, England (1996).

103. Cundari, D. and Nuti, M. "A one-dimensional model for monolithic converter: numerical simulation and experimental verification of conversion and thermal responses for two-stroke engine". *Society of Automotive Engineers (SAE)*, 910668 (1991).

104. Ristovski, Z. D., Morawska, L., Hitchins, J., Thomas, S., Greenaway, C. and Gilbert, D. "Particle emissions from compressed natural gas engines". *Journal of Aerosol Science*, Vol.31, pp.403-413 (2000).

105. Patschull, J. and Roth, P. "Measurement and reduction of particles emitted from a two-stroke engine". *Journal of Aerosol Science*, Vol.26, pp.979-987 (1995).

106. Zelenka, P., Kriegler, W., Herzog, P.L. and Cartellieri, W.P. "Ways toward the clean heavy-duty diesel". *Society of Automotive Engineers (SAE)*, 900602 (1990).

107. Engler, B.H., Koberstein, E., Lox, E. and Ostgthe, K. "Diesel emission control with newly developed catalysts". *IMechE AUTOTECH 89 Congress*, Birmingham, England, November 1989 (1989).

108. Klein H., Lox E., Kreuzer T., Kawanami M., Ried T. and Bachmann K., "Diesel particulate emissions of passenger cars – new insights into structural changes during the process of exhaust aftertreatment using diesel oxidation catalysts", *Society of Automotive Engineers (SAE)*, 980196 (1998).

109. Johnson, J.H., Bagley, S.T., Gratz, L.D. and Leddy, D.G. "A review of diesel particulate control technology and emissions effects-1992 horning memorial award lecture". *Society of Automotive Engineers (SAE)*, 940233 (1994).

110. Andrews, G.E., Xu, J. and Sale, T. "Influence of catalyst and exhaust system on particulate deposition and release from an IDI diesel passenger car under real world driving". *Society of Automotive Engineers (SAE)*, 2002-01-1006 (2002).

111. Hammerle, R.H., Ketcher, D., Horrocks, R.W., Lepperhoff, G., Hüthwohl, G. and Lüers, B. "Emissions from diesel vehicles with and without lean NOx and oxidation catalysts and particulate traps". *Society of Automotive Engineers (SAE)*, 952391 (1995).

112. Brasil, A.M., Farias, T.L. and Carvalho, M.G. "A recipe for image characterization of fractal-like aggregates". *Journal of Aerosol Science*, Vol.30, No.10, pp.1379-1389 (1999).

113. Baumgard, K.J. and Johnson, J.H. "The effect of fuel and engine design on diesel exhaust particle size distributions". *Society of Automotive Engineers (SAE)*, 960131 (1996).

114. Lepperhoff, G. "Influences on the particle size distribution of diesel particulate emissions". *Topics in Catalysis*, Vol.16/17, pp.249-254 (2001).

115. Standt, U.D. and König, A. "Performance of Zeolite-based diesel catalysts". *Society of Automotive Engineers (SAE)*, 950749 (1995).

116. Henein, N.A. "Analysis of pollutant formation and control and fuel economy in diesel engines". In Chigier, N.A., eds., *Energy and Combustion Science* Pergamon Press, U.S.A., pp.283-325 (1979).

117. Toussimis, G., Lois, E. and Lüders, H. "Influence of exhaust aftertreatment devices on heavy-duty diesel engine's particulate emissions". *Journal of Propulsion and Power*, Vol.16, No.4, pp.636-640 (2000).

118. Brown, K.F., Rideout, G.R. and Turner, J.E. "Urban driving cycle results of retrofitted diesel oxidation catalysts on heavy duty vehicles: one year later". *Society of Automotive Engineers (SAE)*, 970186 (1997).

Appendices

Appendix A

A1 Specifications of the tested direct injection (DI) diesel engine

Model	Nissan TD23
Engine Type	Diesel
No. of cylinders	4
Bore x stroke (mm)	89 x 92
Compression ratio	21.9
Displacement (c.c.)	2289
Rated power	65 hp at 4300 rpm
Maximum torque	147 N at 2200 rpm

Table A1 Specifications of the tested direct injection (DI) diesel engine.

A2 Specifications of ultra low sulphur diesel (ULSD) fuel

Parameter	Specification
Sulphur (% wt.)	0.005
Cetane number	51.0
Cetane index	51.0
Viscosity 40 °C ($mm^2 s^{-1}$)	2 – 4.5
Distillation: IBP (°C) 95% volume (°C, max.) % recovered at 250 °C (%vol., max.)	 345 65
Density at 15 °C (kg $litre^{-1}$)	0.835

Table A2 Properties of the ULSD fuel.

Appendix B Operation principles and specifications of particle instruments

Operation principle:

The model 3934 scanning mobility particle sizer (SMPS) from TSI Inc. is composed of the model 3071A electrostatic classifier and the model 3010 condensation particle counter (CPC) from TSI Inc. The electrostatic classifier consists of a neutralizer/charger, a mobility section, particle detection instrument, and a computerized control and data acquisition system. Particles coming from the diluted exhaust sample pass through a Differential Mobility Analyzer (DMA) first to determine the particle size. These particles are then detected by a Condensation Particle Counter (CPC) to count the particle concentration.

DMA is based on the movement of gas-borne particles carrying a known electric charge towards an electrode of opposite charge. A schematic diagram is shown in Figure B1. The sampling exhaust gas is flow through an impactor before entering into the particle sizer. Large particles in the sample stream are removed with 456 nm 50% cutoff impactor. The remaining particles are flow to an Boltzmann charge equilibrium by passing them through a ^{85}Kr bipolar charger and are injected along the outer periphery of a cylindrical cavity that fixes the differential mobility analyser. A voltage applied between the outer wall and the central cylindrical

electrode induces a drift of the positively charged particles through the sheath flow and towards the central electrode. The electrode voltage is initially adjusted to a low positive potential; particles that have a narrow range of high electrical mobilities (smallest particles) enter the gap and are collected by the detector as a "monodisperse" aerosol. When the electrode voltage increases, the sizes of particles exiting the electrostatic classifier also increase, since the electrical mobility of the particles that enter the gap at the base of the electrode decreases. Particles carrying the correct charge to mobility ratio and leave through an aperture at the downstream end of DMA. Then, particles are transferred to a model 3010A Condensation Particle Counter (CPC) for countering the number of particles.

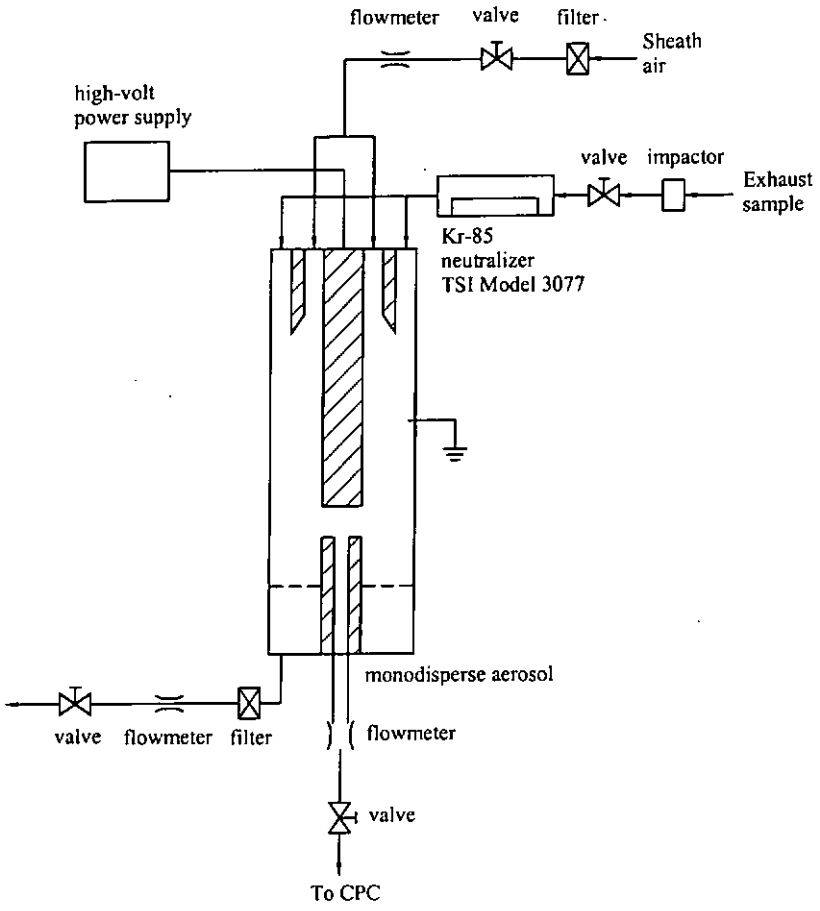

Figure B1 Schematic diagram of a differential mobility analyser (DMA).

The CPC is used to measure the total particle number concentration. A schematic diagram of the CPC measurement system is shown in Figure B2. It composes of a saturated tube, condenser, particle sensor, flowmeter and pump. The aerosol sample enters the CPC through the inlet and then it would be exposed to a heated alcohol reservoir where it becomes saturated. The sample then passes into a condenser tube which is maintained at a temperature well below the dew point of the alcohol-saturated aerosol, forcing the alcohol into a state of supersaturation.

The supersaturated alcohol would begin to condense on the particles, causing them to increase in size from the various original diameters to a relatively uniform final diameter of approximately 10-12 μm. Then, these large particle pass through an illuminated viewing volume. The light scattered by these particles when they pass through the viewing volume is measured by a photodetector and converted into a number concentration measurement. The CPC has a 50% detection efficiency at 10 nm and less then 5 second for 95% response to concentration step.

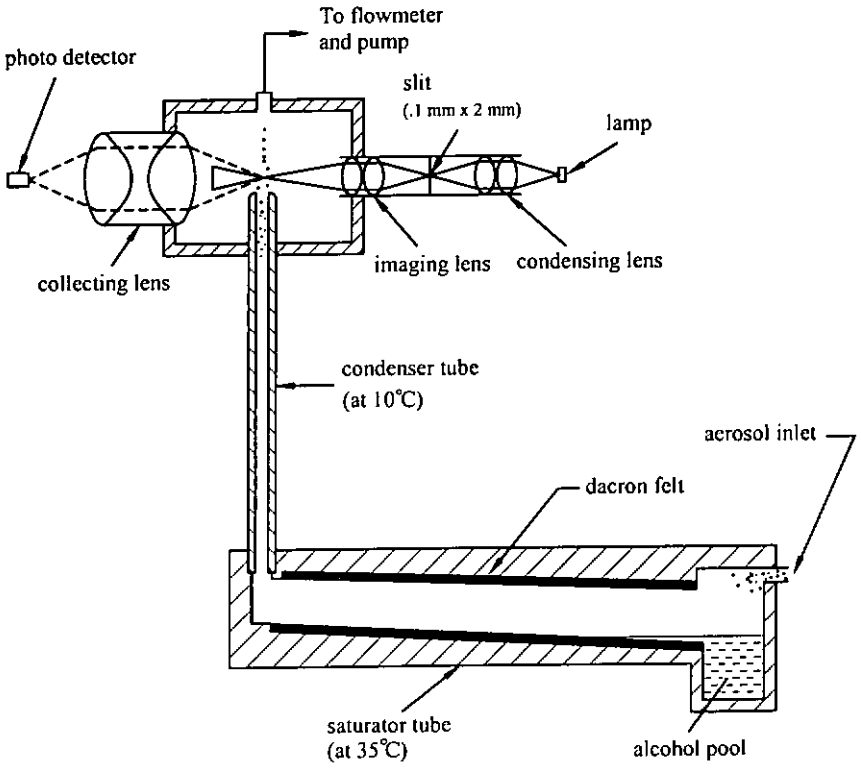

Figure B2 Schematic diagram of the condensation particle counter (CPC).

Specifications:

Scanning Mobility Particle Sizer (SMPS, TSI3934)

Concentration range:	1 particle cm^3 to 107 particle/cm^3
Particle diameter range:	10 to 1000 nm
Displayed resolution:	4, 8,16, 32 or 64 geometrically equal channels per decade
Inlet flowrate of the CPC:	1.0 lpm
Flowrate of the	
Electrostatic classifier:	Adjustable
Aerosol:	0.2 to 2.0 lpm
Sheath air:	10 times aerosol flow (nominal) 2-20 lpm
Measurement cycle time:	Total: 60 to 500 seconds, user selectable.
Up scan:	30 to 300 second
Down scan:	up scan + (2 × down scan) = 500 seconds or less
Sample averaging:	One sample can average 1 to 999 scans
Power requirement:	220 VAC, 50-60 Hz, single phase, Model 3071A EC 25W Model 3010S CPC 40W
Aerosol temperature range:	10-35°C

Aerosol pressure range:	1.0 ± 0.2 atmospheres. The electrostatic classifier must not be subjected to pressures above 5 psig

Condensation Particle Counter (CPC TSI 3010)

Sample flowrate:	1.0 lpm (0.035 cfm) ± 10%
Outlet (total) flowrate:	2.0 lpm (cfm)
Vacuum source:	450 mm (18in.) Hg minimum
Particle size range:	Minimum detectable particle: 50% of 0.01 μm particle Maximum detectable particle: >3 μm
Particle concentration range:	0.0001 to 10000 particles/cm^3 (3 to 2.8 × 10^8 particles/ft^3) with <10% coincidence at 10000 particles/cm^3
Background count:	<0.0001 particle/cm^3
Working fluid:	Reagent-grade n-butylalcohol
Reservoir capacity:	350 ml (7 day supply at 22°C)
Light source:	50 mW, 780 nm laser diode
Signal-to-noise ratio:	20:1 minimum
Digital output:	
Square pulse:	5 V, 500 ± 100 ns

16 bit analog output:	0-10 volt full scale (0-11 volt under HOST control)
Serial communications I/O:	Pinouts compatible with standard 9-pin IBM-AT style RS-232 cables and interfaces
Power:	220 VAC, 50-60 Hz, 25W
Size (LWH):	19 by 22 by 19 cm
Weight:	5.5 kg
Ambient temperature:	10 to 35 °C
Ambient humidity range:	0 to 90% RH

Appendix C Operation principles and specifications of gaseous instruments

Anapol gas analyser EU-200/4

Operation principle:

The analyser is equipped with a non-dispersive infra-red (NDIR) sensor to detect the amount of CO_2 and CO and an electrochemical cell to measure the concentration of O_2. The NDIR analyser measures the absorption at the required wavelength and compares the result to that given by calibration gases. It is a comparator not an absolute analyser and depends heavily on the quality of the pure gas blends. There is a wideband infra-red source inside the detector. The infra-red is split into two parallel beams which both pass through reflecting (gold plated) tubes internally and finally fall on either end of a differential gas detector. The detector consists of a sealed container with two calcium fluoride Infra-red transmitting windows. It is divided through the middle by a flexible diaphragm forming one plate of a condenser and is filled with the gas to be measured. When the two beams enter the detector the components at the specified gas wavelength, they are absorbed by the detector gas which heats and expands, but if the beams are equal there is no unbalance of the separating diaphragm. One beam acts as a reference and passes through a fixed path, the other passes through the analysis tube which contains the

unknown gas. Here the beam loses strength by its absorption by the specific component, and on passing through into its half of the detector develops less heat of absorption, thus allowing the diaphragm to bulge towards it and change the condenser capacity. The beams are chopped at from 6-10 Hz, giving the system an A.C. output.

The operation of an electrochemical cell is based on an oxidation-reduction reaction, which is specifically the characteristic of the gas to be measured. For the oxygen sensors, it comprises a diffusion barrier, a sensing electrode (cathode) made of noble metal such as gold or platinum, and a working electrode made of base metal such as lead or zinc immersed in a basic electrolyte (such as a solution of potassium hydroxide). Oxygen diffusing into the sensor is reduced to hydroxyl ions at the cathode:

$$O_2 + 2H_2O + 4e^- \longrightarrow OH^- \qquad (C.1)$$

Hydroxyl ions in turn oxidize the lead (or zinc) anode:

$$2Pb + 4OH^- \longrightarrow 2PbO + 2H_2O + 4e^- \qquad (C.2)$$

This yields an overall cell reaction of:

$$2Pb + O_2 \longrightarrow 2PbO \qquad (C.3)$$

Fuel cell oxygen sensors are current generators. The amount of current generated is proportional to the amount of oxygen consumed (Faraday's Law). Oxygen reading instruments simply monitor the current output of the sensor. The sensor would convert the current output into the digital reading which is shown on the panel of the Anapol gas analyser.

Specifications:

Measuring range: Gas compound related to dry gas

Gas	Range	Unit
O_2	0-20.9	% vol.
CO_2	0-20.0	% vol.
CO	0-15000	ppm/% vol.
CO low	0-1000	ppm
NO	0-5000	ppm
HC	0-60000	ppm
SO_2	0-10000	ppm
TG	0-800	°C
TA	0-80	°C
Soot	Filter paper method	

Calculated values: efficiency0-99.9

qA 0-99.9%

Lambda 1-∞ Brettschneider's rule

Lambda 1-∞ (excess air)

Temperature:

Temp.	Unit	Sensor	Total
0-100 °C	±1 °C	±2 °C	±3 °C
100-200 °C	±1 %	±2 °C	±3 °C
200-300 °C	±2 °C	±4 °C	±6 °C
300-800 °C	±3 °C	±6 °C	±9 °C
TG	±3 °C		

Resolution:

Gas	Resolution
O_2	0.1 % vol.
CO_2	0.01 % vol.
CO	10/1 ppm 0.1%
CO low	0.5 ppm
NO	1 ppm
HC	1 ppm
SO_2	1 ppm
TG	1 °C
TA	1 °C

Calibration: 60 second on fresh air

Printer: needle printer, 24 signs per line

Working temperature: 5-24°C

Sensors:

Gas	Method
O_2	Electrochemical cell
CO_2	NDIR
CO	NDIR
HC	NDIR
CO/H2	Electrochemical cell (no cross effect with hydrogen)
NO	Electrochemical cell
SO_2	Electrochemical cell
TG	Thermocouple NiCr/Ni
TA	Semi-conductor detector

California Analytical Instrument (CAI) HFID HC analyser (Model 300)

Operation principle:

The Model 300 HFID uses the flame Ionization Detection method to determine the total hydrocarbon concentration within a gaseous sample. It contains an internal heated sample pump and an adjustable temperature heated oven. All components in contact with the sample are maintained at the oven set temperature-preventing condensation. A burner jet is used as an electrode and is connected to the negative side of a precision power supply. An additional electrode, known as the "collector," is connected to high impedance, low noise electronic amplifier. The two electrodes establish an electrostatic field. When a gaseous sample

is introduced to the burner, it is ionised in the flame and the electrostatic field causes a small current between by the precision electrometer amplifier and is directly proportional to the hydrogen concentration of the sample.

Specifications:

Resolution:	0.01 ppm carbon (lowest range)
Repeatability:	Better than ±0.5% of full scale
Linearity:	Better than 1% of full scale
O_2 effect:	Less than 2% of full scale
CH_4 effect:	Less than 1.3 times Propane
Response time:	90%of full scale in 1.5 seconds
Sample flow rate:	With Pump 3.0 liter/min ± 1.5 liter/min
Internal sample filter:	0.1 micron replaceable filter provided
Noise:	Less than ±0.5% of full scale
Zero & span drift:	Les than 1% of full scale per 24 hours
Flow control:	Electronic proportional pressure controller
Fuel requirement:	40% H2/60% He (100cc/min) or 100% H2
	(300cc/min) fuel inlet pressure 25 psig
Air requirement:	Less than 1 ppm carbon purified or synthetic air
	(200cc/min) air inlet pressure 25 psig

Display:	3-1/2 Digit panel meter
Diagnostics:	31/2 Digit panel meter with 8 position switch
	• Collector voltage • +15VDC
	• Fuel pressure • Burner temperature
	• Air pressure • Oven temperature
	• Sample pressure • Catalyst temperature
Analog output:	0-10 VDC & 4-20mA DC/0-20mA DC
Fuel/air control:	Forward pressure regulator
Ignition:	Momentary push-button with flame-on indicator
Ambient temperature:	5-45°C
Warm-up time:	1 hour
Fitting:	1/4" tube
Power requirements:	115/230 (±10%) VAC @50/60 Hz, 750 watts
Relative humidity:	Less than 90% RH non-condensing

***California Analytical Instrument (CAI)* NO/NOx Analyser (Model 400)**

Operation principle:

The NO/NOx gas analyser utilizes the principle of chemiluminescent for analysing the NO or Noxconcentration within the gaseous sample. In the NO mode, the method is based upon the chemiluminescent reaction between ozone and nitric oxide (NO) yielding nitrogen dioxide (NO_2) and oxygen. Approximately 10% of the NO_2 produced from this reaction is in an electronically excited state. The transition form this state to a normal state produces red light which has an intensity proportional to the mass flow rate of NO_2 into the reaction chamber.

$$NO + O_3 \rightarrow NO_2^* + O_2 \qquad (4.4)$$

$$NO_2^* \rightarrow NO_2 + h\nu \qquad (4.5)$$

The red light is measured by means of a photodiode tube and associated amplification electronics. In the NOx mode, NO plus NO_2 is determined as above, however, the sample is first routed through the internal NO_2 to NO converter which converts the NO_2 in the sample to NO. The resultant reaction is then directly proportional to the total concentration of NOx. The important point is the entire sample, prior to the reaction chamber, must be maintained at a temperature above 60 °C.

Specifications:

Resolution:	0.1 ppm NO/NOx (or better)
Repeatability:	Better than 0.5% of full scale
Linearity:	Better than 1% of full scale
CO_2 effect:	Less than 1% with 10% CO_2
H_2O effect:	Less than 1% with 3% H_2O
Ozonizer:	Ultraviolet lamp
Response time:	Adjustable from 1.5 to 10 seconds to 90% of full scale
Sample flow rate:	With Pump 3.0 liter/min ± 1.5 liter/min
Noise:	Less than 0.5% of full scale
Zero & span drift:	Les than 1% of full scale per 24 hours
Flow control:	Electronic proportional pressure controller
Air or O_2 requirement:	Dry air less than 1 ppm NOx at 210 cc/min @ 25psig
Display:	4-1/2 Digit panel meter
Diagnostics:	31/2 Digit panel meter with 6 position switch
	• Converter temperature • Filter temperature
	• Pump temperature • Air pressure
	• Sample pressure • Oven temperature
Analog output:	0-10 VDC & 4-20mA DC/0-20mA DC

O_3 control:	Manual push button with automatic shutdown with loss of air or oxygen pressure
NO/NOx control:	Manual push button or remote
Ambient temperature:	5-45°C
Sample temperature:	0-65°C
Warm-up time:	1 hour
Fitting:	1/4" tube
Power requirements:	115/230 (±10%) VAC @50/60 Hz, 750 watts
Relative humidity:	Less than 90% RH non-condensing

Appendix D Specifications of diesel oxidation catalysts (DOCs)

DOC-Type A

Metal substrate:	Zeolite-based
Size:	113.5mm(diameter) × 78.8mm (length)
Cell density:	64 cells/cm^2
Wall thickness:	0.6 mm

DOC-Type B

Metal substrate:	Platinum-based
Size:	120mm(diameter) × 243mm (length)
Cell density:	64 cells/cm^2
Wall thickness:	0.5 mm